Universidade Federal de Minas Gerais
Instituto de Ciências Biológicas
Departamento de Fisiologia e Farmacologia

DANIEL DE CASTRO MEDEIROS

Resposta evocada por estimulação elétrica cerebral profunda como um marcador substituto de crise epiléptica induzida por infusão de pentilenotetrazol em ratos

Belo Horizonte

Março de 2014

DANIEL DE CASTRO MEDEIROS

Resposta evocada por estimulação elétrica cerebral profunda como um marcador substituto de crise epiléptica induzida por infusão de pentilenotetrazol em ratos

Tese apresentada ao Curso de Pós-graduação em Fisiologia e Farmacologia do Departamento de Fisiologia e Biofísica do Instituto de Ciências Biológicas da Universidade Federal de Minas Gerais para obtenção do título de doutor.

Área de concentração: Fisiologia.

Orientador: Prof. Dr. Márcio Flávio Dutra Moraes

Belo Horizonte

Março de 2014

043 Medeiros, Daniel de Castro.
Resposta evocada por estimulação elétrica cerebral profunda como um marcador substituto de crise epiléptica induzida por infusão de pentilenotetrazol em ratos [manuscrito] / Daniel de Castro Medeiros. – 2014.

128 f. : il. ; 29,5 cm.

Orientador: Márcio Flávio Dutra Moraes.

Tese (doutorado) – Universidade Federal de Minas Gerais, Departamento de Fisiologia e Biofísica

1. Epilepsia - Teses. 2. Crise epiléptica. 3. Eletroencefalografia – Teses. 4. Pentilenotetrazol. 5. Rato como animal de laboratório – Teses. 6. Fisiologia – Teses. I. Moraes, Márcio Flávio Dutra. II. Universidade Federal de Minas Gerais. Departamento de Fisiologia e Biofísica. III. Título.

CDU: 612

"RESPOSTA EVOCADA POR ESTIMULAÇÃO ELÉTRICA CEREBRAL PROFUNDA COMO UM MARCADOR SUBSTITUTO DE CRISE EPILÉPTICA INDUZIDA POR INFUSÃO DE PENTILENOTETRAZOL EM RATOS"

DANIEL DE CASTRO MEDEIROS

Tese de Doutorado defendida e aprovada, no dia **14 de abril de 2014**, pela Banca Examinadora constituída pelos seguintes professores:

PROF. DR. CHRISTOPHER KUSHMERICK
UNIVERSIDADE FEDERAL DE MINAS GERAIS

PROF. DR. DANILO BARBOSA MELGES
UNIVERSIDADE FEDERAL DE MINAS GERAIS

PROF. DR. JADERSON COSTA DACOSTA
PONTIFÍCIA UNIVERSIDADE CATÓLICA-RS

PROF. DR. NORBERTO GARCIA CAIRASCO
UNIVERSIDADE DE SÃO PAULO

PROF. DR. MÁRCIO FLÁVIO DUTRA MORAES
ICB/UNIVERSIDADE FEDERAL DE MINAS GERAIS
ORIENTADOR

Programa de Pós-Graduação em Ciências Biológicas - Fisiologia e Farmacologia
Instituto de Ciências Biológicas - Universidade Federal de Minas Gerais – UFMG
Belo Horizonte, 14 de abril de 2014

Universidade Federal de Minas Gerais
Instituto de Ciências Biológicas
Departamento de Fisiologia e Biofísica
Programa de Pós-Graduação em Ciências Biológicas: Fisiologia e Farmacologia

PÓS FISIOLOGIA E FARMACOLOGIA

ATA DA DEFESA DA TESE DE DOUTORADO Nº 215 DE DANIEL DE CASTRO MEDEIROS

Às 14:00 horas do dia 14 do mês de abril de 2014, na Sala Prof. Wilson Beraldo - Bloco A4 , departamento de Fisiologia e Biofísica, ICB-UFMG, realizou-se a sessão pública para a defesa da Tese de **Daniel de Castro Medeiros.** A presidência da sessão coube ao **Prof. Dr. Márcio Flávio Dutra Moraes,** orientador. Inicialmente, o presidente fez a apresentação da Comissão Examinadora assim constituída: **Prof. Dr. Christopher Kushmerick,** Universidade Federal de Minas Gerais, **Prof. Dr. Danilo Barbosa Melges,** Universidade Federal de Minas Gerais, **Prof. Dr. Jaderson Costa Dacosta,** Pontifícia Universidade Católica do Rio Grande do Sul, **Prof. Dr. Norberto Garcia Cairasco,** Universidade de São Paulo, e **Prof. Dr. Márcio Flávio Dutra Moraes,** Universidade Federal de Minas Gerais, orientador. Em seguida, o candidato fez a apresentação do trabalho que constitui sua **Tese de Doutorado**, intitulada: **"RESPOSTA EVOCADA POR ESTIMULAÇÃO ELÉTRICA CEREBRAL PROFUNDA COMO UM MARCADOR SUBSTITUTO DE CRISE EPILÉPTICA INDUZIDA POR INFUSÃO DE PENTILENOTETRAZOL EM RATOS".** Seguiu-se a arguição pelos examinadores e logo após, a Comissão reuniu-se, sem a presença do candidato e do público e decidiu considerar ..... a Tese de Doutorado. O resultado final foi comunicado publicamente ao candidato pelo presidente da Comissão. Nada mais havendo a tratar, o presidente encerrou a sessão e lavrou a presente ata que, depois de lida, se aprovada, será assinada pela Comissão Examinadora.

Belo Horizonte, 14 de abril de 2014.

Assinatura dos membros da banca examinadora:

Departamento de Fisiologia e Biofísica. Av Antonio Carlos, 6627 - ICB - UFMG. 31270-901, Belo Horizonte, MG, Brasil - Fone: (55-31) 3409-2923. FAX: (55-31) 3409-2924. E-mail: pgfisfar@icb.ufmg.br

Universidade Federal de Minas Gerais
Instituto de Ciências Biológicas
Departamento de Fisiologia e Biofísica
Programa de Pós-Graduação em Ciências Biológicas: Fisiologia e Farmacologia

TÍTULO:
"RESPOSTA EVOCADA POR ESTIMULAÇÃO ELÉTRICA CEREBRAL PROFUNDA COMO UM MARCADOR SUBSTITUTO DE CRISE EPILÉPTICA INDUZIDA POR INFUSÃO DE PENTILENOTETRAZOL EM RATOS"
ALUNO: DANIEL DE CASTRO MEDEIROS
ORIENTADOR: PROF. DR. MÁRCIO FLÁVIO DUTRA MORAES

PARECER:

Considerando a excelência da pesquisa desenvolvida, a potencial capacidade do candidato, a adequada apresentação pública de seus resultados e a extensa e significativa produção científica relacionada a sua tese, a Banca examinadora recomenda VOTO DE LOUVOR ao candidato Daniel de Castro Medeiros

AVALIAÇÃO FINAL:

DATA: **14 de abril de 2014**

ASSINATURA DA BANCA EXAMINADORA:

Departamento de Fisiologia e Biofísica. Av Antonio Carlos, 6627 - ICB - UFMG. 31270-901, Belo Horizonte, MG, Brasil - Fone: (55-31) 3409-2923. FAX: (55-31) 3409-2924. E-mail: pgfisfar@icb.ufmg.br

Este trabalho foi desenvolvido no Núcleo de Neurociências (Departamento de Fisiologia e Biofísica do Instituto de Ciências Biológicas da Universidade Federal de Minas Gerais), com o auxílio das seguintes agências de fomento:

- Conselho Nacional de Desenvolvimento Científico e Tecnológico – CNPq;

- Coordenação de Aperfeiçoamento de Pessoal de Nível Superior – CAPES;

- Fundação de Amparo à Pesquisa do Estado de Minas Gerais – FAPEMIG

Agradecimentos

Professor e mestre Márcio Flávio Dutra Moraes pela oportunidade ímpar de fazer ciência e tentar entender, por hipóteses falseáveis, segredos da natureza.

Minha esposa e companheira de vida, Tatiana Nader Lana, cujo apoio foi e é de suma importância em minha caminhada.

Meus pais, Rafael Egídio de Medeiros e Maria da Glória de Castro Medeiros, pelo apoio e amor incondicional fundamentais em todas as conquistas de minha vida.

Professora Dra. Grace Schenatto Pereira Moraes pelo carinho e motivação.

Professores do Núcleo de Neurociência, Dr. André Ricardo Massensini, Dra Juliana Tavares, Dr. Bruno Souza.

Amigo Flávio Afonso Gonsalves Mourão.

Companheiros de laboratório, Laio Paiva, Marina Pádua Reis, Gabriel Perfeito Castro, Ana Raquel Pereira Caixeta, Hyorrana Pereira, Pedro Lopes.

Todos os integrantes do Núcleo de Neurociência.

Pós-graduação de Fisiologia e Farmacologia do Instituto de Ciências Biológicas da Universidade Federal de Minas Gerais.

Resumo

Epilepsia é uma afecção neurológica que atinge em média de 1% da população mundial, sendo que 25% são resistentes ao tratamento medicamentoso. Um dos fatores mais incapacitantes dessa síndrome é a imprevisibilidade de ocorrência das crises epilépticas (CE). Há um grande interesse no desenvolvimento de dispositivos capazes de predizer a ocorrência de CE.

O objetivo deste trabalho foi utilizar a estimulação elétrica cerebral profunda (ES) como forma de sondagem dos estados da rede neural em um modelo de crise epiléptica por infusão intravenosa de pentilenotetrazol (PTZ).

Eletrodos bipolares foram cirurgicamente implantados na região do núcleo anterior do tálamo ou do complexo amigdaloide de ratos Wistar, assim como micro parafusos na região do cortex parietal para aquisição de EEG. Os animais foram divididos em três grupos: PTZ-noES (infusão de PTZ sem ES), ES-noPTZ (ES concomitante a infusão de salina i.v.) e PTZ+ES (simultaneamente infusão de PTZ e aplicação de ES).

A estimulação talâmica (0.5 Hz, 0.1 ms largura de pulso e 0,8 mA) em animais acordados concomitante à infusão de PTZ (grupo PTZ+ES) resultou em um aumento significativo da atividade cortical, 250ms após o ES, doze segundos antes da ocorrência da crise epiléptica, composto principalmente de frequências de 12 a 30Hz (banda beta). Quando ES (0.5 Hz, 0.1 ms largura de pulso e 0,6mA) foi aplicado no complexo amigdaloide de animais anestesiados juntamente com infusão de PTZ, um aumento significativo da energia do EEG peri estímulo (250ms após ES) foi detectado oitenta segundos antes da ocorrência da crise eletrográfica. Houve também, para ao grupo PTZ+ES, um aumento significativo da expressão de c-Fos em regiões como tálamo, hipotálamo e amigdala contralateral ao eletrodo, evidenciado pela marcação imuno-histoquímica de c-Fos.

Em contrapartida, ES (0.5 Hz, 0.1 ms largura de pulso e 0,8 mA) em complexo amigdaloide de animais acordados somente resultou em um aumento de atividade cortical precedente à crise epilética (doze segundos) se o ES foi temporalmente pareado com os disparos epileptiformes 24 horas antes.

Em nenhum dos protocolos a ES apresentou característica pró-convulsivas, sem qualquer alteração na latência ou duração das crises (quando se compara os grupos PTZ+ES e PTZ-noES) ou qualquer disparo epileptiforme para o grupo ES-noPTZ.

A estimulação elétrica apresenta-se como uma estratégia eficiente de sondagem do estado neural e, futuramente, pode ser usada como uma técnica de previsão de crise epiléptica.

Abstract

Epilepsy is a common neurological disease affecting 1% of world population, whose 25% has no seizure control by pharmacotherapy. The seizure unpredictability is one of the most disable features of this syndrome. Therefore, the designing of devices able to forecast a seizure occurrence is a paramount goal.

The aim of this work was to probe the neural system state by deep brain electrical stimulation (DBS) in a pentylenetetrazole (PTZ) seizure model.

Bipolar electrodes were surgically implanted in wistar rats anterior thalamus (ANT) or amygaloid complex (AMY) for electrical stimulation and two micro screws on parietal cortex for EEG acquisition. The animals were further divided in three groups: PTZ-noES (i.v. PTZ infusion without DBS), ES-noPTZ (DBS and saline infusion) and PTZ+ES (i.v. PTZ infusion and DBS).

ANT DBS on awake animals (0.5 Hz, 0.1ms pulse width, 0,8mA) simultaneously with PTZ infusion showed an increase of cortical activity (250ms after stimuli) twelve seconds prior seizure, mainly in beta band (12-30Hz).

DBS (0.5 Hz, 0.1ms pulse width, 0,6mA) applied on AMY of anesthetized animals, concomitantly with PTZ infusion, produced a detectable cortical evoked response 80s prior seizure onset and increase thalamus, hypothalamus, and amygdala (contralateral to electrode) cell activity by c-Fos immunohistochemistry labeling. Nevertheless, AMY DBS on awaked animals only increase cortical EEG activity prior seizure onset (12s) if the electrical stimuli were temporal paired with epileptic discharges 24 hours earlier.

DBS used in this study demonstrated no pro-convulsive effect due to any statistical alteration on seizure latency and duration (PTZ + ES compared with PTZ-noES) or any epileptic discharge presented by ES-noPTZ group.

The DBS presents as a reliable strategy to probe the neural system state and a possible tool to seizure prediction device.

Sumário

There is no terror in a bang, only in the anticipation of it.

Alfred Hitchcock

1.0 Revisão de Literatura

1.1 Epilepsia

Epilepsia e crises epilépticas têm sido documentadas desde os primórdios das civilizações. Acreditava-se que pessoas eram tomadas de possessão que as levavam à perda de si (consciência) e/ou às convulsões. Com a maior compressão da neurobiologia, explicações etéreas foram substituídas. Atualmente, a definição geral de epilepsia é de uma desordem do cérebro caracterizada por uma persistente predisposição para geração de crises epilépticas e por consequências neurobiológicas, cognitivas, psicológicas e sociais desta condição. A definição de epilepsia requer a ocorrência de ao menos uma crise epiléptica, definida como sinais e/ou sintomas transitórios decorrentes de um disparo sincrônico excessivo (hipersincronia (Penfield, Jasper *et al.*, 1954)) de populações de neurônios cerebrais (Fisher, Van Emde Boas *et al.*, 2005). Os sintomas dependem do local de origem destes disparos anormais e de seu padrão de propagação para áreas encefálicas circunvizinhas. As manifestações podem ser mínimas como rubor, sensação estranha ou pequena contração muscular (Gotman, 2011) ou até alterações drásticas de humor como agressividade e afetividade exacerbadas, contrações tônicas de membros superiores e inferiores (Engel, 1996). O disparo sincrônico de regiões cerebrais, sinal clássico da crise epiléptica, é detectado pelo eletroencefalograma (EEG) como oscilações de grande amplitude (30% maior que o basal) e que perduram por uma janela de tempo maior que 3 segundos (Gotman, 2011). A rica interconexão das células piramidais corticais (Johnston e Brown, 1984), a presença de junções comunicantes (Traub, Michelson-Law *et al.*, 2004) e, paradoxalmente, a atividade de células inibitórias (Cobb, Buhl *et al.*, 1995) favorecem a

hipersincronia. A contradição a respeito da atividade inibitória vem do fato que muitas escolas defendem que o excesso de sincronia está intimamente ligado ao aumento da excitabilidade (Scharfman, 2007), presente em tecidos cerebrais ictogênicos (Mcnamara, 1994; Lothman, Rempe *et al.*, 1995; Mangan, Rempe *et al.*, 1995; Bernard, Anderson *et al.*, 2004; Fritschy, 2008). De fato, simulações computacionais mostram que mudança no tônus excitatório sem compensação adequada de inibição, resulta em aumento da sincronia da rede neural (Kudela, Franaszczuk *et al.*, 2003). Sendo assim, os tratamentos farmacológicos vigentes agem, sobretudo, no aspecto da excitabilidade celular, visando diminuir a atividade do tecido neural (Rho e Sankar, 1999):

1) Barbitúrico fenobarbital aumenta ação do receptor para o neurotransmissor ácido gama-aminobutírico (GABA) ao prolongar a abertura dos canais de cloreto (Silva Brum e Elisabetsky, 2000)

2) Fenitoína atua de diversas formas e diminui a excitabilidade do neurônio, interferindo, sobretudo, no transporte de sódio através da membrana (Tunnicliff, 1996);

3) Carbamazepina diminui a condutância da membrana ao íon sódio e a neurotransmissão sináptica excitatória, antagonizando purinas, monoaminas, acetilcolina e receptor de glutamato NMDA (Yan, Mishra *et al.*, 1992; Kaneko, Okada *et al.*, 1993; Dailey, Reith *et al.*, 1997);

4) Ácido valpróico não tem seus mecanismos farmacológicos bem elucidados, mas, ao que parece, é capaz de elevar os níveis de GABA no sistema nervoso central (Davis, Peters *et al.*, 1994).

O tratamento medicamentoso é capaz de controlar as crises epilépticas em dois terços dos pacientes, sendo o tratamento cirúrgico a única opção para aqueles que não respondem ao tratamento convencional. Porém a cirurgia de ablação do foco ictogênico somente pode ser

realizada em 8 a 10% dos pacientes. Logo, para 25% dos pacientes, não há tratamento disponível (epilepsia refratária) (Mormann, Andrzejak *et al.*, 2007). Para esses pacientes a imprevisibilidade das crises é um dos maiores aspectos de morbidade dessa síndrome. Mesmo breves episódios de diminuição da consciência podem gerar danos físicos, especialmente quando a pessoa está dirigindo, nadando, escalando, e principalmente quando sozinho. Além disso, é frequente a existência de um intenso sentimento de desamparo que impacta negativamente a qualidade de vida diária do paciente (Carney, Myers *et al.*, 2011). Em um estudo sobre a visão de pacientes com epilepsia sobre possíveis sistemas de previsão de crise, em torno de 90% deles afirmaram que o desenvolvimento de tais sistemas é muito importante, sendo as razões para tal (Schulze-Bonhage, Sales *et al.*, 2010):

- Aumentar do sentimento de segurança, de opções de lazer e de trabalho.
- Diminuir a ansiedade gerada pela imprevisibilidade das crises recorrentes
- Desenvolver intervenções de supressão de crise mais acuradas

1.2 Previsão de crises convulsivas

A previsão de crise epiléptica consiste na identificação de um estado pré-ictal, período de tempo no qual há uma maior probabilidade de início das crises (Viglione e Walsh, 1975; Esteller, Echauz *et al.*, 2005). Porém, muito se questionava se esse período pre-ictal realmente existia, pois as crises epilépticas eram consideradas fenômenos abruptos, sem qualquer tipo de percussor. Mesmo sinais prodrômicos, considerados desde tempos antigos como sintomas predecessores de crise convulsiva, estão sendo agora avaliados como crises já instaladas, porém não convulsivas (Alving e Beniczky, 2013). Somente a partir da

década de 1990, alguns sinais clínicos como aumento do volume sanguíneo cerebral (Weinand, Carter *et al.*, 1997; Baumgartner, Serles *et al.*, 1998), viabilidade de oxigênio (Adelson, Nemoto *et al.*, 1999), frequência cardíaca (Delamont, Julu *et al.*, 1999; Kerem e Geva, 2005) que antecediam a crise epiléptica, começaram por corroborar para a existência de um estado pre-ictal.

O processo de instauração da crise epiléptica pode ser visto como um aumento do número de interações sincrônicas entre neurônios de uma determinada região cujas conexões com outras unidades se desdobram e espalham o padrão anormalmente sincrônico de disparo às regiões circunvizinhas. Sobre esse conceito, vários estudos têm sido realizados com o intuito de caracterizar esse comportamento neural pre-ictal por meio de técnicas matemático-computacionais capazes de extrair do EEG parâmetros descritivos da neurodinâmica cerebral (Mormann, Andrzejak *et al.*, 2007). Tais técnicas podem ser de divididas basicamente em: 1) técnicas univariáveis; 2) técnicas multivariáveis (Carney, Myers *et al.*, 2011). Apesar do grande avanço, esses métodos passivos de análise do EEG para previsão de crise ainda geram resultados falsos positivos e negativos (Andrzejak, Chicharro *et al.*, 2009), logo, distantes de alcançar uma aplicação clínica. Uma das razões para tal é a mudança rápida do padrão de disparo neural de um estado normal, fisiológico, para um estado de disparos epileptiformes, o que dificulta a analise passiva (Lopes Da Silva, Blanes *et al.*, 2003). Uma nova abordagem ao desafio de predição de crise epiléptica é o uso de estimulação elétrica profunda como forma de sondagem do sistema neural (Kalitzin, Velis *et al.*, 2010). A resposta neural perante o estímulo elétrico poderia ser usado para quantificar o tônus excitatório, onde uma grande resposta indica uma alta

excitabilidade (Freestone, Kuhlmann *et al.*, 2011); consequentemente, avaliar a probabilidade de ocorrência de um estado de anormal sincronia neural.

1.2.1 Técnicas univariáveis

Análise univariável é realizada sobre uma série temporal, definida como coleção de observações feitas sequencialmente ao longo do tempo. O eletroencefalograma é um exemplo de série temporal cujas informações sobre o início da observação e sua taxa de amostragem permite uma representação gráfica em função do tempo, ao longo do período de gravação. Análise univariável do EEG emprega somente um único ponto de aquisição de sinal.

1.2.1.1 Transformada de Fourier de curto tempo

A técnica consiste em aplicar a transformada de Fourier sobre intervalos iguais e sequenciais do EEG, com o intuito de decompor o sinal em seus diferentes componentes de frequência (Litt e Echauz, 2002) tendo como resultado final a densidade espectral (magnitude da energia para cada valor de frequência) para cada intervalo temporal. É o método mais usado para predição e detecção de crise epiléptica eletrográfica cujo racional parte da diferença entre a densidade espectral do período interictal e do ictal (Carney, Myers *et al.*, 2011).

1.2.1.2 Energia acumulada

Por esta técnica, a média da energia do sinal (V^2) é computada para cada segmento temporal do EEG (Litt, Esteller *et al.*, 2001; Harrison, Frei *et al.*, 2005).

1.2.2 Técnica multivariável

Análises multivariáveis de séries temporais consistem em mais de um ponto de registro sequencial ao longo do tempo. Essas análises são comumente usadas para se mensurar a interação entre diferentes componentes de um sistema, como por exemplo, o neural (Carney, Myers *et al.*, 2011). Apesar da possibilidade de múltiplos mecanismos para o início das crises epilépticas (Mormann, Andrzejak *et al.*, 2007), frequentemente há certo aumento de interação (sincronismo) entre diferentes regiões cerebrais antes da ocorrência dos disparos ictais (Carney, Myers *et al.*, 2011). Tal interação pode ser tanto linearmente mensurada entre dois ou mais canais de EEG como correlação cruzada e coerência, quanto não linearmente como sincronização em fase.

1.2.2.1 Correlação cruzada

Quando um sinal de EEG possui uma variação em amplitude que é similar à de outra região, mesmo com certo atraso temporal, diz-se que essas regiões estão correlacionadas. Logo, perante a correlação cruzada, a similaridade entre dois sinais é mensurada em função de um atraso temporal aplicado a um deles. Sendo os sinais normalizados, a correlação cruzada possui um valor máximo de um, que indica que os sinais possuem curso temporal similar e o valor mínimo de zero indicando não há similaridade entre os mesmos.

1.2.2.2 Coerência

A similaridade entre dois sinais pode ocorrer também em uma frequência (ou banda de frequência) específica, sendo então mensurada pela função de coerência. Por esta, a análise do espectro de frequência é realizada para cada sinal. As frequências que possuem densidades similares entre os dois sinais geram altos valores de coerência (próximos de um).

1.2.2.3 Sincronia em fase

Dois sinais podem estar sincronizados mesmo na ausência similaridade em amplitude (correlação e coerência). Tal sincronia pode se manifestar na fase de determinada frequência. Diz-se que duas ondas (por exemplo, uma determinada frequência de dois sinais) estão oscilando em fase quando suas cristas e vales estão coincidentes no tempo. Dada a característica aleatória do EEG, quando há uma sincronia em fase entre dois pontos de registro, é provável que essas regiões possuam atividades correlacionadas. Pode-se mensurar também a diferença de fase. No caso, as duas ondas não estão 100% coincidentes, havendo um atraso temporal entre elas. Se esse atraso for tamanho que a crista de uma onda ocorra no momento exato do vale de outra, indica que elas estão completamente fora de fase.

1.3 Estimulação elétrica

A estimulação elétrica de sistemas biológicos consiste em posicionar dois eletrodos, sendo um próximo da área de interesse (músculo, nervo ou mesmo estruturas do sistema nervoso central) e forçar a passagem de uma corrente elétrica entre eles. Alguns fatores influenciam na resposta biológica perante essa corrente, como distância entre os eletrodos (quanto maior a distância, maior a área afetada), a resistência elétrica tecidual (quanto maior a resistência, menor a corrente elétrica para uma dada diferença de potencial entre os eletrodos), forma da onda dos pulsos elétricos, bem como sua frequência. Mesmo frente a todos esses parâmetros, o intuito final da estimulação elétrica é causar uma perturbação no sistema biológico que o distancie do seu estado basal. Quando tal perturbação é realizada em estruturas cerebrais, pode modular a atividade tanto de neurônios excitatórios quanto de

inibitórios (Tehovnik, Tolias *et al.*, 2006), bem como influenciar na ação de astrócitos (Kuga, Sasaki *et al.*, 2011) e afetar até mesmo a dinâmica vascular (Canals, Beyerlein *et al.*, 2008)(Mesquita, Medeiros *et al.*, 2011). A consequência difusa da estimulação elétrica cerebral pode ser um dos fatores para o desconhecimento do seu mecanismo de ação. Apesar desse fato, as consequências de seu uso são benéficas como forma de tratamento de doenças motoras como tremor basal e Parkinson (tratamentos estes aprovados pelo *Food and Drug Administration* – FDA) bem como no estudo de outras patologias neurológicas (Wichmann e Delong, 2006), entre elas a epilepsia (Halpern, Samadani *et al.*, 2008).

1.3.1 Estimulação elétrica cerebral profunda nas epilepsias

No tratamento de uma doença catastrófica como epilepsia refratária ao tratamento medicamentoso, a investigação de novas metodologias terapêuticas é de suma importância. A estimulação elétrica (ES) profunda desponta como uma alternativa para esse cenário médico e renova o interesse tanto da pesquisa básica quanto da clínica para o entendimento e melhoria desta técnica. Recentemente, dados de testes amplos e randomizados demonstraram que DBS aplicado no núcleo anterior do tálamo (SANTE-*Stimulation of the Anterior Nucleus of Thalamus for Epilepsy*) (Fisher, Salanova *et al.*, 2010) ou estimulação elétrica de estruturas corticais (Morrell, 2011) reduz significativamente a frequência de ocorrência de crises (Fridley, Thomas *et al.*, 2012). De fato, o último recentemente recebeu a aprovação do FDA (*Food and Drug Admnistration*) para o tratamento de epilepsia refratária. A teoria vigente sobre a ação da DBS se assenta na mesma premissa de ação dos medicamentos, diminuir o tônus excitatório. A estimulação de alta frequência, intermitente ou contínua, agiria inibindo a estrutura alvo, mimetizando o efeito de uma cirurgia ablativa, retirando do sistema neural a área disfuncional (Gwinn e Spencer, 2004). Dados de

eletroencefalografia, magneto-ressonância funcional, microdialise e modelos computacionais sugerem que a estimulação em alta frequência causa um bloqueio da despolarização, inibição sináptica ou depressão sináptica que inativa a rede neural e a impede de comprometer a função cerebral fisiológica. Por outro lado, a estimulação em baixas frequências produziria uma ativação de estruturas cerebrais notoriamente inibitórias que restaurariam a função da rede neural por uma diminuição da excitabilidade (Gwinn e Spencer, 2004).

A estimulação elétrica cerebral profunda também vem sendo utilizada como forma de avaliação de circuitos epileptogênicos em humanos e como ferramenta de prognóstico de cirurgia de ressecção do foco ictogênico (Valentin, Alarcon, Honavar *et al.*, 2005). Pulsos de baixíssima frequência são aplicados em diversas regiões corticais no intuito de localizar uma resposta evocada prolongada, indicando assim uma área de alta excitabilidade neural, eletiva a foco da crise epiléptica (Valentin, Alarcon, Garcia-Seoane *et al.*, 2005).

Uma abordagem recente para o uso da estimulação elétrica cerebral profunda se mostra na forma de sondagem do estado de ativação do circuito neural. Por este, pulsos elétricos são usados como perturbações do sistema neural. A leitura do potencial de campo de diferentes redes neurais, bem como sua análise matemática (como energia, espectro de frequência etc) mediante tal perturbação pode revelar o nível de excitabilidade neural, bem como uma maior probabilidade de ocorrência de crise epiléptica (Kalitzin, Velis *et al.*, 2010). Em nosso trabalho, seguimos essa proposta, sendo todas as análises baseadas na sondagem do sistema neural perante estimulação elétrica profunda.

1.3 Modelos animais de crise convulsiva e epilepsia

Modelos experimentais que mimetizam tanto crises convulsivas quanto epilepsias têm contribuído enormemente para epileptologia. Esses modelos podem mimetizar um amplo espectro de características, tanto clínicas quanto anatomopatológicas em um ambiente controlado. Para o estudo do processo ictogênico, um modelo que seja altamente reprodutível durante as mudanças na atividade neural na transição do período pre-ictal para o ictal é de suma importância (Lopes Da Silva e Harding, 2011).

1.3.1 Modelo de indução de crise convulsiva por Pentilenotetrazol

O pentilenotetrazol (PTZ) é um antagonista gabaérgico, que infundido na cobaia aumenta o tônus excitatório ao ponto de evocar crises epilépticas (Loscher, Fassbender *et al.*, 1991). O modelo de PTZ para indução de crise convulsiva é largamente usado no *screening* de drogas anticonvulsivas por mimetizar crises mioclônicas generalizadas (Loscher, 2011). As crises mioclônicas ativam preferencialmente áreas límbicas como córtex periforme, complexo amigdaloide, hipocampo e tálamo (Eells, Clough *et al.*, 2004). A infusão gradativa de PTZ intravenosa em ratos proporciona um modelo altamente reprodutivo de transição do período pre-ictal para o ictal e ótimo candidato para o estudo de previsão de crise epiléptica.

1.4 Tálamo

O tálamo é uma estrutura bilateral que se assenta sobre o tronco-encefálico no centro do cérebro, formado por um conjunto de agrupamentos celulares (núcleos) que são classicamente nomeados de acordo com sua localização anatômica: medial, lateral, ventral,

anterior e posterior (Jankowski, Ronnqvist *et al.*, 2013). A maioria das informações que recebemos do mundo externo, ou interno, é baseada em mensagens que devem passar primeiramente pelo tálamo; com exceção do olfato, todos os sentidos enviam projeções para essa estrutura, antes de alcançar o córtex (Wiegell, Tuch *et al.*, 2003). Além de ser uma via de passagem, o tálamo também modula o fluxo de informação que alcança o córtex, demonstrando importante função no processamento sensorial, motor e de funções cognitivas (Morel, Magnin *et al.*, 1997). Por ser uma estrutura de confluência e redirecionamento de informação, o tálamo desenvolve importante papel na sincronia entre áreas cerebrais, principalmente o córtex, o que o leva tanto à gênese e manutenção de padrões sincrônicos fisiológicos (sono) quanto de patológicos, como disparos ictais (Steriade, 2005).

A crise de ausência, cujo sinal clássico é a abrupta diminuição da consciência, possui como característica eletroencefalográfica padrões oscilatórios do tipo ponta-onda, formados a partir do circuito tálamo-cortical. Estudos de Pierr Gloor e col. demonstraram que sem as interações entre o córtex e o tálamo, os disparos do tipo ponta-onda não aconteciam (Avoli e Gloor, 1982). Além da presença marcante na crise de ausência, o tálamo também modula as crises límbicas. Inibição do tálamo afeta profundamente a expressão comportamental de crise límbica (Cassidy e Gale, 1998) além de modificar a atividade ictal do hipocampo (Bertram, Zhang *et al.*, 2008).

Logo, por ser uma região centralizadora, com difuso poder modulatório, tanto cortical quanto sub-cortical, o tálamo se mostra como um ótimo candidato a estimulação elétrica

cerebral profunda, principalmente núcleos que possuem conexões tanto com o sistema límbico quanto com o córtex, como o núcleo anterior.

1.4.1 Núcleo anterior do tálamo

O núcleo anterior do tálamo (ANT) está interposto entre os corpos mamilares e o córtex cingulado (Van Groen, Kadish *et al.*, 1999). Esse núcleo medeia conexões entre estruturas corticais e sub-corticais, pois possui extensas ligações recíprocas com córtex frontal, córtex cingulado, corpos mamilares e formação hipocampal (Jankowski, Ronnqvist *et al.*, 2013). Logo, a ativação desta relativa pequena região talâmica, é possível influenciar extensas áreas límbicas quanto corticais (Takebayashi, Hashizume *et al.*, 2007). Além disso, está intimamente relacionado a funções de memória (Aggleton, O'mara *et al.*, 2010) e navegação (Jankowski, Ronnqvist *et al.*, 2013).

1.5 Complexo amigdaloide

A amigdala (AMG) é uma estrutura complexa que compreende diversos agrupamentos (núcleos e subnúcleos) celulares (Sah, Faber *et al.*, 2003). Em ratos, o complexo amigdaloide pode ser subdividido em três grandes núcleos: basolateral, cortical e o centro medial. As projeções aferentes e eferentes podem ser basicamente separadas em (Sah, Faber *et al.*, 2003):

- Conexões com estruturas corticais e talâmicas, relacionadas com informações sensoriais e memória.
- Conexões com hipotálamo e tronco cerebral, envolvidas com sistemas autonômicos e com respostas comportamentais inatas (Mcdonald, 1998).

O complexo Amigdalóide possui grande densidade de conexões recíprocas entre as regiões corticais, hipotalâmicas e tronco cerebrais. De forma geral, as projeções para regiões sensoriais corticais partem dos núcleos corticais e do complexo basolateral. O córtex perirrinal, juntamente com áreas do córtex frontal que projetam-se para a amígdala, recebem conexões recíprocas do núcleo basolateral e cortical (Pitkanen, Savander *et al.*, 1997; Sah, Faber *et al.*, 2003). Os núcleos corticais que recebem projeções olfatórias enviam projeções recíprocas de volta para o córtex olfatório. O complexo basolateral apresenta substanciais projeções recíprocas para os sistemas de memória no lobo temporal medial, como hipocampo e córtex perirrinal (Petrovich, Canteras *et al.*, 2001), além de projeções para o núcleo accumbens, caudado-putamem e núcleos da estria terminal(Mcdonald, 1991). Os núcleos centrais apresentam maciças conexões tanto para o hipotálamo quanto para núcleos da estria terminal (Dong, Petrovich *et al.*, 2001), núcleos do tronco cerebral, ponte e medula (Veening, Swanson *et al.*, 1984). As projeções para o tronco cerebral podem ser divididas de acordo com três principais alvos: 1) substância cinzenta periaquedutal, (capaz de gerar vocalização, sobressaltos, analgesia e alterações cardiovasculares) (Rizvi, Ennis *et al.*, 1991; Behbehani, 1995); 2) núcleo parabraquial (vias responsáveis pela dor) (Moga, Herbert *et al.*, 1990; Gauriau e Bernard, 2002); 3) núcleo do trato solitário e motor dorsal do vago (Van Der Kooy, Koda *et al.*, 1984).

Uma variedade de funções é atribuída ao complexo amigdaloide, como memória (Hamann, 2001; Mcgaugh, 2002; Pare, Collins *et al.*, 2002), atenção (Gallagher e Holland, 1994), emoção e significância emocional a estímulos sensórios (Aggleton e Mishkin, 1985; Rogan

e Ledoux, 1996; Ledoux, 2000; Adolphs, 2002; Ledoux, 2003) e percepção de movimentos corporais (Bonda, Petrides *et al.*, 1996).

2.0 Justificativa e Objetivos

2.1 Justificativa

O desenvolvimento de metodologias capazes de detectar alterações neurodinâmicas que precedem crises epilépticas é uma opção que aliviaria o fardo de pessoas com epilepsia, principalmente as de difícil tratamento convencional (farmacológico). Um sistema de alarme para crises poderia beneficiar o paciente levando-o a se esquivar com antecedência de situações de risco potencial. Um sistema de previsão poderia ainda ser acoplado a um de supressão de crise, criando assim um sistema fechado que mudaria as opções terapêuticas de profiláticas para uma que seria usada somente sob demanda (somente no período pre-ictal) o que minimizaria os efeitos colaterais de tais intervenções.

2.2 Objetivo geral

Sondar os circuitos neurais durante o processo ictogênico utilizando estimulação elétrica cerebral profunda de baixíssima frequência.

2.2.1 Objetivos específicos

- Realizar sondagem do estado neurodinâmico durante período ictogênico por DBS em animais anestesiados
- Verificar estruturas cerebrais requeridas pela estimulação elétrica cerebral profunda em animais anestesiados perante infusão de pentilenotetrazol utilizando-se técnica imunoistoquímica de marcação de C-fos
- Realizar sondagem do estado neurodinâmico durante período ictogênico por DBS no núcleo anterior do tálamo em animais acordados e movendo-se livremente.

- Realizar sondagem do estado neurodinâmico durante período ictogênico por DBS no complexo amigdalóide em animais acordados e movendo-se livremente.
- Proceder a análises matemático-computacionais do EEG dos grupos experimentais a fim de destacar um período pre-ictal
- Promover a sincronia entre áreas distantes pelo prévio pareamento entre a crise epiléptica com a estimulação elétrica.

3.0 Materiais e métodos

3.1 Materiais e métodos protocolo sondagem em animal anestesiado

3.1.1 Grupos experimentais

Foram utilizados 36 ratos wistar machos (300 – 320g) provenientes do CEBIO-ICB-UFMG *vivarium*. Os protocolos foram realizados sob a licença nº 150/06 aprovada pelo comitê de ética e experimentação animal (CETEA – UFMG). Os animais foram divididos em dois grupos principais: grupo EEG (n=18) e grupo c-Fos (n=18). Ambos então foram divididos em 3 sub-grupos: PTZ-noES (infusão de pentilenetetrazol), ES-noPTZ (estimulação elétrica) e PTZ+ES (estimulação elétrica concomitante com infusão de PTZ). O registro de eletroencefalograma, a infusão de PTZ e a estimulação elétrica iniciaram simultaneamente.

3.1.2 Cirurgia estereotáxica

Todos os animais foram anestesiados (uretana 140mg/ml; 10ml/kg, ip) e posicionados no estereotáxico para posicionamento de eletrodo bipolar no complexo amigdaloide (AP: -2,8 referencia no bregma, ML: -5,0, DV: -7,2) para a realização de estimulação elétrica e microparafusos em ambos os córtex parietais para a aquisição do EEG. Os eletrodos, bem como os parafusos, foram então soldados em um conector RJ11 (6 pinos) e fixado ao crânio com acrílico dental.

3.1.3 Infusão de pentilenotetrazol e estimulação elétrica cerebral profunda

Imediatamente após a cirurgia, a veia da cauda dos animais foi canulada para infusão de PTZ (40mg/ml) ou salina (grupo ES-noPTZ) a uma velocidade de 4mg/ml/min. A infusão de PTZ foi interrompida no início da apresentação da crise eletrográfica para os animais do

grupo EEG e metade da dose de PTZ necessária para evocar a crise convulsiva para os animais c-Fos (150g/KG ou 790± 30 segundos). Para os animais dos grupos ES-noPTZ e PTZ+ES a estimulação elétrica consistiu de pulsos quadráticos monofásicos (0,1ms largura de pulso e 0,6mA de intensidade) a uma frequência de 0,5Hz.

3.1.4 Aquisição de sinal EEG e preparação histoquímica

O sinal de EEG do córtex parietal foi amplificado (500 vezes), filtrado (passa alta de 1Hz e passa baixa de 500Hz), digitalizado a uma taxa de amostragem de 1KHz e então armazenado no disco rígido de um computador para análises posteriores. Em um segundo canal de registro, foi armazenado também o sinal de *trigger*, momento no qual ocorria a estimulação elétrica. A aquisição do EEG foi mantida por 1 minuto após a crise eletrográfica para os animais do grupo EEG e por 90 minutos após o fim da infusão de PTZ para o grupo C-fos, com o intuito de garantir ausência de crise epiléptica eletrográfica para este grupo. Imediatamente após a aquisição do EEG, os animais foram eutanasiados com overdose de uretana e encaminhados à perfusão cardíaca com 0,01M de PBS seguido de paraformaldeído a 4%. Os cérebros foram removidos e processados dependendo do grupo a que pertence: EEG (confirmação do posicionamento do eletrodo) e c-Fos para imunoistoquímica, seguindo o protocolo descrito em (Fonseca, Gusmao *et al.*, 2012).

3.1.5 Análise de c-Fos

As imagens de imunocoloração, obtidas a partir de fatias coronais dos cérebros dos aniamis (-2,5 até -3,2 com referencia no Bregma), foram adquiridas através do microscópio AxioImager M2 (Zeiss) com objetiva de 5 vezes. As fotomicrografias foram realizadas pela câmara digital AxioCam MRm (Zeiss) através do programa Carl Zeiss Axiovision 4.8

(1388x1420 pixels; 1.02µmx1.02µm tamanho do pixel) e armazenadas em formato TIFF no disco-rígido de um computador para posterior análise pelo programa ImageJ (http://rsbweb.nih.gov/ij/). Utilizou-se a ferramenta de limiar do ImageJ para criar uma máscara que separava as células marcadas da imagem de fundo (o mesmo limiar foi mantido para todas as imagens). O total de células, com diâmetro entre 5 e 100 µm, foram quantificadas e normalizadas pela área (mm^2) para cada região de interesse: Córtex parietal, complexo amigdaloide contra-lateral ao eletrodo, tálamo, e hipotálamo. Devido à alta intensidade de células presente no hipocampo, que acaba produzindo uma sobreposição, a análise desta região de interesse foi realizada através da densitometria ótica, onde o valor da escala de cinza do giro denteado foi normalizado pela escala de cinza de região de fundo sem corpos celulares (corpo caloso).

3.1.5 Atividade elétrica epileptiforme

A detecção dos disparos ictais típicos foi determinada pelo experimentador tomando-se como diretriz: disparos 30% maiores que a linha de base que perduraram por mais de 3 segundos. Foram quantificadas a duração da crise eletrográfica e a latência para início dos disparos ictais, sendo este o tempo quantificado entre o início da infusão de PTZ e o surgimento dos disparos epileptiformes. Foi calculado também o padrão de distribuição em frequência dos dois primeiros segundos dos disparos ictais para os grupos PTZ-noES e PTZ+ES utilizando um algoritmo do MATLAB® (*fast Fourier transform- FFT).*

3.1.6 Análise pré-ictal do EEG

3.1.6.1 Cálculo do período de oscilação basal do grupo PTZ-noES

O início dos disparos ictais foi determinado como sendo o tempo zero (T_{zero}) e todas as subsequentes análises foram realizadas nos 600 segundos anteriores (T_{zero}-600s até T_{zero}) utilizando algoritmos criados no programa MATLAB. Primeiramente foi determinado o intervalo médio entre os disparos do período pré-ictal, utilizando animais do grupo PTZ-noES. Para tal, um limiar de 75% da amplitude do último disparo antes da crise eletrográfica foi selecionado e um algoritmo foi desenvolvido para detectar todos os disparos que ultrapassassem esse limiar. O tempo no qual cada disparo pre-ictal ultrapassasse o limiar era então armazenado. Posteriormente, foi subtraído o tempo de ocorrência do disparo (N+1) pelo anterior N na janela de análise de -600s até Tzero e um histograma de 1 segundo de escala foi então produzido com esses valores. Baseado neste resultado, a frequência de 0,5Hz foi escolhida para a estimulação elétrica dos grupos ES-noPTZ e PTZ+ES.

3.1.6.2 Sincronização dos picos máximos a ES

Com o intuído de quantificar o grau de modulação da estimulação elétrica sobre a atividade pré-ictal, foi desenvolvido um algoritmo para determinar a sincronização dos picos máximos com um oscilador externo (estimulação elétrica). O EEG foi inicialmente segmentado em janelas de 2 segundos e o tempo no qual o maior valor de voltagem (pico máximo - TMP) ocorreu dentro desta janela, foi armazenado. Posteriormente, o tempo de ocorrência do máximo pico (N+1) foi subtraído pelo anterior N e um histograma cujo eixo das abscissas possui 9 valores, de -2 a 2 segundos, foi construído. É importante salientar que uma distribuição totalmente aleatória no tempo dos picos máximos gera uma dispersão

gaussiana dos dados. Para mostrar a gradual modulação do estímulo sobre os disparos pré-ictais, essa análise do EEG foi dividida em três períodos de 100 janelas de 2s: de -600s a -400s, -400s a -200s e -200s a T_{zero}.

3.1.6.3 Potencial evocado por estimulação elétrica profunda

O instante no qual a ES era fornecida ao animal foi armazenado juntamente e posteriormente usado para separar o sinal do córtex parietal (EEG) em janelas de 2 segundos (1500ms antes da estimulação elétrica e 500ms depois). Foi então criada uma sequência de 300 períodos, cobrindo os 600s de registro para a subsequente análise. Com o intuito de evidenciar efeito da estimulação elétrica sobre a atividade do córtex parietal, a energia do sinal 250 ms após ao estímulo foi normalizada pelo basal, assumida como a energia 250ms imediatamente anterior ao mesmo. A energia (V^2) nos 300 períodos de 2 segundos também foi calculada para todos os grupos e normalizada pela energia do período de -598 até -600s. Com o intuito de também evidenciar que a estimulação elétrica não alterou o número de ocorrência dos disparos pre-ictais, os 600 anteriores a crise foram divididos em janelas de 10s e o total de disparos em cada janela foi contabilizado. Para o encontro de tais disparos, seguiu-se a mesma metodologia do tópico 3.1.6.1.

3.1.6.4 Evolução de padrões de onda

Foi desenvolvido um algoritmo que reconhece e localiza um padrão de onda ao longo do período pré-ictal. O modelo padrão da onda a ser reconhecido foi escolhido arbitrariamente pelo experimentador em uma porção do EEG onde as ondas são claramente identificadas. Como a forma de onda pode alterar, mesmo que minimamente, devido à infusão de PTZ (aumentar em amplitude, por exemplo), esse algoritmo ajusta o formato da onda ao longo do tempo. O algoritmo consiste em inicialmente dividir o sinal de EEG em janelas de 20s.

Em cada janela, o padrão de onda escolhido é comparado a todas as ondas encontradas. As ondas similares ao padrão são selecionadas e a média das três melhores é armazenada como modelo para a janela de 20s subsequente. Para cada animal representativo, três diferentes ondas foram selecionadas e sua ocorrência disposta em uma janela de 2 segundos, tendo-se como referencia o instante no qual a estimulação elétrica era fornecida ao animal.

3.2 Materiais e métodos protocolo sondagem por estimulação elétrica no núcleo anterior do tálamo em animal acordado

3.2.1 Grupos experimentais

Foram utilizados 22 ratos wistar machos (300 – 320g) provenientes do CEBIO-ICB-UFMG *vivarium*. Os protocolos foram realizados sob a licença nº 150/06 aprovada pelo comitê de ética e experimentação animal (CETEA – UFMG). Os animais foram divididos em três grupos: PTZ-noES (infusão de pentilenetetrazol), ES-noPTZ (estimulação elétrica) e PTZ+ES (estimulação elétrica concomitante com infusão de PTZ).

3.2.2 Cirurgia estereotáxica

Todos os animais foram anestesiados com Ketamina e Xilasina (proporção, 1 de ketamina para 0,7 de xilasina, sendo as concentrações da solução estoque de 10g/100ml e 2g/100ml respectivamente; 0.10 mL/100 g de peso animal i.p.) e posicionados no estereotáxico. Foram implantados eletrodos bipolares no núcleo anterior do tálamo (AP: -1,4 referenciam no bregma, ML: -1,0, DV: -5,2) para a realização de estimulação elétrica e micro parafusos em ambos os córtex parietais para a aquisição do EEG. Os eletrodos, bem como os

parafusos foram então soldados em um conector RJ11 (6 pinos) e este fixado ao crânio com acrílico dental. Foi permitido um tempo de recuperação de 5 dias antes do experimento.

3.2.3 Infusão de pentilenotetrazol e estimulação elétrica cerebral profunda

Após o período de recuperação, a veia da cauda dos animais foi canulada para infusão de PTZ (10mg/ml) ou salina (grupo ES-noPTZ) a uma taxa de 2,5mg/ml/min. A infusão de PTZ foi interrompida quando o animal apresentou a crise mioclônica. Para os animais dos grupos ES-noPTZ e PTZ+ES a estimulação elétrica consistiu de pulsos quadráticos monofásicos (0,1ms largura de pulso e 0,8mA de intensidade) a uma frequência de 0,5Hz.

3.2.4 Aquisição de sinal EEG

O sinal de EEG do córtex parietal foi amplificado (500 vezes), filtrado (passa alta de 1Hz e passa baixa de 500Hz), digitalizado a uma taxa de amostragem de 1KHz e então armazenado no disco rígido de um computador para análises posteriores. Em um segundo canal de registro, foi armazenado também o momento no qual ocorria a estimulação elétrica.

3.2.5 Desenho experimental

O protocolo foi dividido em três períodos temporais sequencias distintos: período basal (120s de registro sem estimulação elétrica ou infusão de PTZ), período estimulação elétrica (120s de estimulação elétrica, conforme tópico 3.2.3) e período experimental que é dependente do grupo a que pertence o animal (PTZ-noES: infusão de PTZ até o animal alcançar a crise mioclonica; ES-noPTZ: 600s de estimulação; PTZ+ES: infusão de PTZ até o animal alcançar a crise mioclônica concomitante com ES desde o início da infusão, até o tempo de 120s após a crise convulsiva).

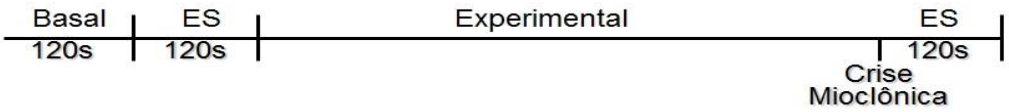

Figura 1: Esquemático do desenho experimental da sondagem de circuitos neurais por estimulação elétrica no ANT de ratos acordados. Os animais eram submetidos a três etapas sequenciais, sendo elas a basal (sem qualquer influencia de fármaco (PTZ) ou estimulação elétrica, período ES no qual todos os animais recebiam pulsos elétricos no ANT sem a influência do fármaco e período experimental que era dependente do grupo a que o animal pertencia (PTZ+ES, PTZ-noES, ES-noPTZ).

3.2.6 Atividade elétrica epileptiforme

A detecção dos disparos ictais típicos foi determinada pelo experimentador, tomando-se como diretriz: disparos 30% maiores que a linha de base que perduraram por mais de 3 segundos. Foram quantificadas a duração da crise eletrográfica e a latência para início dos disparos ictais, sendo o tempo quantificado entre o início da infusão de PTZ e o surgimento dos disparos epileptiformes.

3.2.7 Análise da atividade pre-ictal (120 segundos anteriores à crise epiléptica)

Uma janela temporal de dois minutos anteriores à crise epiléptica (-120 a Tzero) foi inicialmente selecionada para os grupos PTZ+ES e PTZ-noES. Foi então calculada a energia do sinal de EEG (V^2) para ambos os grupos ao longo desta janela. Com o intuito de realizar uma análise estatística, a média da energia dos dez segundos anteriores à crise (-10s até Tzero) foi comparada entre os grupos. Foi também realizada, para ambos os grupos, a transformada de Fourier de curto tempo para esta janela temporal de 120s, utilizando a função *spectrogram* do programa MATLAB (1s de janela amostral com sobreposição de 90%).

3.2.8 Resposta cortical perante estimulação elétrica profunda pré-crise epiléptica

Como foi armazenado o instante no qual a estimulação elétrica era fornecida ao animal, foi possível separar o sinal do córtex parietal em janelas de 2 segundos (500ms antes da estimulação elétrica e 1500ms depois). Para a análise subsequente, foi criada uma sequência de 120 janelas (cobrindo os 240 segundos de registro), sendo 60 janelas (de 0 a 120s) referentes ao início do período experimental e 60 referentes ao período anterior à crise epiléptica (-120 a Tzero). Com o intuito de evidenciar efeito da estimulação elétrica no ANT sobre a atividade do córtex parietal, foi calculada a energia (V^2) normalizada do EEG para essas janelas (energia 250 ms após o estímulo normalizada pela energia 250ms imediatamente anterior ao mesmo). O cálculo da energia normalizada para o grupo ES-noPTZ foi realizado no início do período experimental e no tempo de 480 a 600s. A energia normalizada foi também calculada 30segundos após a crise eletrográfica. A média da energia normalizada nos 10s (-10s até Tzero) anteriores aos disparos epileptiformes foram comparados à energia normalizada 30s após a crise convulsiva (25 a 34s após a crise convulsiva) para os grupos PTZ+ES e PTZ-noES.

3.2.9 Bandas de frequência que compõem o potencial evocado

Para a análise das bandas de frequências que compõem o potencial evocado pela estimulação elétrica, o sinal de EEG parietal foi filtrado em quatro bandas de frequências distintas: banda teta 4-8Hz, alfa 8-12Hz, beta 12-30Hz, e gama 30-100Hz. Posteriormente, o cálculo da energia normalizada (energia 250 ms após o estímulo normalizada pela energia 250ms imediatamente anterior ao mesmo) foi realizado para cada banda. A média da energia normalizada foi então calculada para os 10s anteriores (-10s até Tzero) à crise epiléptica para cada banda de frequência e então comparada entre os grupos

3.2.10 Análise espectral do potencial evocado e do disparo pre-ictal.

Para esta análise foi selecionada a janela de -4 a -2 segundos anteriores á crise epiléptica. Para cada animal do grupo PTZ+ES, foi selecionado o potencial evocado (250ms após o estímulo), e para o grupo PTZ-noES foi escolhido o maior disparo pre-ictal (100ms antes do pico máximo voltagem na janela e 150ms depois). A distribuição de frequência tanto do potencial evocado quanto dos disparos pre-ictais foram analisadas pelo método *wavelet* do programa MATLAB. Em seguida, a média dos valores absolutos das escalas de wavelet. referentes a cada banda de frequência, foi normalizada pela média dos valores encontrados no 1 segundo anterior aos picos máximos e potenciais evocados. Posteriormente, os valores normalizados para cada banda de frequência foram comparados entre os grupos PTZ-noES e PTZ+ES. As bandas de frequência foram separadas da seguinte forma:

- Gama: entre 100 a 30 Hz
- Beta: entre 30 a 12 Hz
- Alfa: entre 12 a 8 Hz
- Teta: entre 8 a 4 Hz

3.3 Materiais e métodos protocolos modulação de peso sináptico por pareamento de estimulação elétrica no ANT e crise epiléptica eletrográfica

3.3.1 Grupos experimentais da estimulação talâmica – protocolo 1

Foram utilizados 17 ratos wistar machos (300 – 320g) provenientes do CEBIO-ICB-UFMG *vivarium*. O protocolo foi realizado sob a licença nº 150/06 aprovada pelo comitê de ética e

experimentação animal (CETEA – UFMG). Os animais foram divididos em três grupos: PTZ-noES (infusão de pentilenetetrazol), ES-noPTZ (estimulação elétrica) e PTZ+ES (estimulação elétrica concomitante com infusão de PTZ).

3.3.2 Cirurgia estereotáxica – protocolo 1

O implante dos eletrodos no ANT dos animais para ES, bem como dos micro-parafusos no córtex parietal para aquisição do EEG seguiu o mesmo delineamento descrito na secção 3.2.2.

3.3.3 Infusão de pentilenotetrazol e estimulação elétrica cerebral profunda – protocolo 1

Tanto a infusão de PTZ quanto a estimulação elétrica no ANT foi realizada conforme descrito na secção 3.2.3.

3.3.4 Aquisição de sinal EEG, atividade epileptiformes – protocolo 1

O EEG dos animais deste protocolo foi adquirido seguindo a mesma metodologia descrita na secção 3.2.4.

3.3.5 Desenho experimental – protocolo 1

O protocolo experimental foi dividido em três períodos temporais sequenciais distintos, sendo que os dois primeiros estão presentes em todos os grupos e em todos os dias de experimentação: período basal (120s de registro sem estimulação elétrica ou infusão de PTZ), período estimulação elétrica (120s de estimulação elétrica, conforme tópico 3.2.3) e período experimental que é dependente do grupo a que pertence o animal (PTZ-noES: infusão de PTZ até o animal alcançar a crise mioclonica; ES-noPTZ: 600s de estimulação; PTZ+ES: infusão de PTZ até o animal alcançar a crise mioclônica concomitante com ES

desde o início da infusão, até o tempo de 120s após a crise convulsiva). A execução destes passos completa o dia zero. Os animais então retornam às suas caixas para um período de recuperação de 24h. Após esse período os animais são novamente submetidos aos períodos de registro basal e ES (dia 1), sendo novamente repetidos após de sete dias (dia 7).

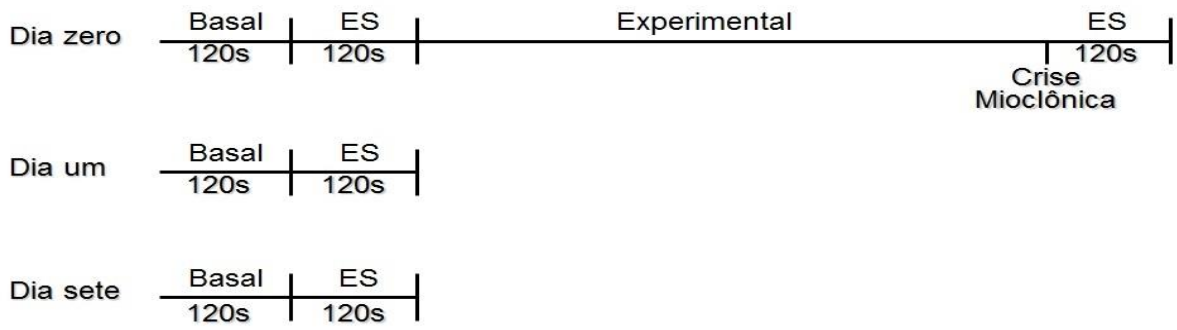

Figura 2: Esquemático do desenho experimental da sondagem de circuitos neurais por estimulação elétrica no ANT de ratos acordados pareado à crise epiléptica como forma de indução de alteração nos pesos sinápticos. No dia zero, os animais eram submetidos a três etapas sequenciais, sendo elas a basal (sem qualquer influencia de fármaco (PTZ) ou estimulação elétrica, período ES no qual todos os animais recebiam pulsos elétricos no ANT sem a influência do fármaco e período experimental que era dependente do grupo a que o animal pertencia (PTZ+ES, PTZ-noES, ES-noPTZ). Nos dias 1 e 7, os períodos basal e ES eram repetidos.

3.3.6 Análise da resposta à estimulação elétrica – protocolo 1

O instante no qual a ES era fornecida ao animal foi armazenado juntamente com o EEG e usado para separar o sinal do córtex parietal em janelas de 2 segundos (500ms depois da ES e 1500ms antes). A energia normalizada do sinal (250ms após a estimulação elétrica normalizada 250ms imediatamente anterior a mesma) foi calculada para os períodos basal e ES. A média da energia do período basal e ES dos dias 1 e 7 foram referenciadas pelas respectivas energias do dia zero e comparadas entre os grupos.

3.3.7 Grupos experimentais da estimulação talâmica – protocolo 2

Foram utilizados 6 ratos wistar machos (300 – 320g) provenientes do CEBIO-ICB-UFMG *vivarium* que compuseram o grupo PTZ+ES CRISE. O protocolo foi realizado sob a licença nº 150/06 aprovada pelo comitê de ética e experimentação animal (CETEA – UFMG).

3.3.8 Cirurgia estereotáxica – protocolo 2

O implante dos eletrodos no ANT dos animais para ES, bem como dos micro-parafusos no córtex parietal para aquisição do EEG seguiu o mesmo delineamento descrito na secção 3.2.2.

3.3.9 Infusão de pentilenotetrazol e estimulação elétrica cerebral profunda – protocolo 2

Tanto a infusão de PTZ quanto a estimulação elétrica no ANT foi realizada conforme descrito na secção 3.2.3.

3.3.10 Aquisição de sinal EEG, atividade epileptiformes – protocolo 2

O EEG dos animais deste protocolo foi adquirido seguindo a mesma metodologia descrita na secção 3.2.4.

3.3.11 Desenho experimental – protocolo 2

O protocolo experimental foi dividido em dois dias e cada dia continha três períodos temporais sequenciais distintos, sendo que os dois primeiros estão presentes em todos os todos os dias de aquisição: período basal (120s de registro sem estimulação elétrica ou infusão de PTZ), período estimulação elétrica (120s de estimulação elétrica, conforme tópico 3.2.3).

Dia zero: após os períodos basal e ES, PTZ era então infundido pela veia da cauda dos animais até que eles apresentassem crise mioclônicas. A estimulação elétrica neste dia era apresentada por 120s a começar após o animal ter apresentado o primeiro abalo mioclônico. Dia um: os mesmos animais foram novamente submetidos ao período basal, ES, e seguidos de infusão de PTZ concomitante com ES (agora desde o início da infusão de PTZ) até a crise mioclônica.

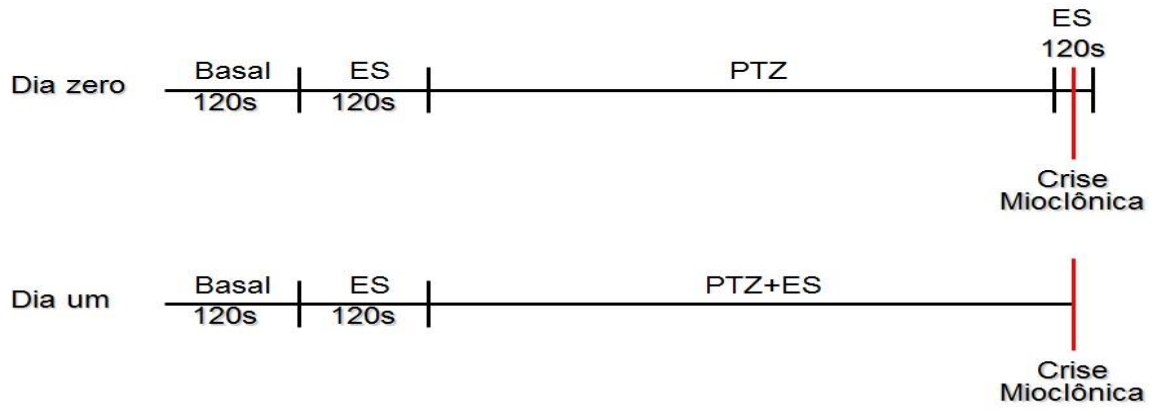

Figura 3: Esquemático do desenho experimental da sondagem de circuitos neurais por estimulação elétrica no ANT de ratos acordados pareado à somente crise epiléptica como forma de indução de alteração nos pesos sinápticos. No dia zero, os animais eram submetidos a três etapas sequenciais, sendo elas: a basal (sem qualquer influencia de fármaco (PTZ) ou estimulação elétrica; período ES no qual todos os animais recebiam pulsos elétricos no ANT sem a influência do fármaco, e indução de crise (PTZ) no qual os animais eram levados à crise epiléptica por infusão de PTZ. Quando os animais apresentavam o primeiro abalo mioclônico, eram então submetidos a 120s de ES. No dia 1, os períodos basal e ES eram repetidos, seguidos de um período no qual os animais recebiam infusão de PTZ concomitantemente com a ES até apresentar a crise epiléptica.

Foi então calculada a energia normalizada (energia 250ms após o estímulo, normalizada por 250ms antes do mesmo) do dia 1 para o grupo PTZ+ES CRISE nos dois minutos iniciais da infusão de PTZ concomitante a ES (0 a 120s) e nos dois minutos que antecedem

a crise epiléptica (-120 até Tzero). Posteriormente, a essa energia normalizada foi comparada com os grupos PTZ-noES e PTZ+ES do protocolo do ítem 3.2.2 (animais que não foram submetidos à crise epiléptica anteriormente, como forma de controle).

3.4 Materiais e métodos protocolo sondagem por estimulação cerebral no complexo amigdaloide em animal acordado

3.4.1 Grupos experimentais

Foram utilizados 20 ratos wistar machos (300 – 320g) provenientes do CEBIO-ICB-UFMG *vivarium*. Os protocolos foram realizados sob a licença nº 150/06 aprovada pelo comitê de ética e experimentação animal (CETEA – UFMG). Os animais foram divididos em três grupos: PTZ-noES (infusão de pentilenetetrazol), ES-noPTZ (estimulação elétrica) e PTZ+ES (estimulação elétrica concomitante com infusão de PTZ).

3.4.2 Cirurgia estereotáxica

Todos os animais foram anestesiados com Ketamina e Xilasina (proporção, 1 de ketamina para 0,7 de xilasina, sendo as concentrações da solução estoque de 10g/100ml e 2g/100ml respectivamente; 0.10 mL/100 g de peso animal i.p.) e posicionados no estereotáxico. Foram implantados eletrodos bipolares no complexo amigdaloide (AP: -2,8 referenciam no bregma, ML: -5,0, DV: -7,2) para a realização de estimulação elétrica e micro parafusos em ambos os córtex parietais para a aquisição do EEG. Os eletrodos, bem como os parafusos foram então soldados em um conector RJ11 (6 pinos) e fixado ao crânio com acrílico dental. Foi permitido um tempo de recuperação de 5 dias antes do experimento.

3.4.3 Infusão de pentilenotetrazol e estimulação elétrica cerebral profunda

Seguiu-se a mesma metodologia descrita na secção 3.2.3

3.4.4 Aquisição de sinal EEG

Seguiu-se a mesma metodologia descrita na secção 3.2.4.

3.4.5 Desenho experimental

O protocolo foi dividido em três períodos temporais sequencias distintos: período basal (120s de registro sem estimulação elétrica ou infusão de PTZ), período estimulação elétrica (120s de estimulação elétrica, conforme tópico 3.2.3) e período experimental que é dependente do grupo a que pertence o animal (PTZ-noES: infusão de PTZ até o animal alcançar a crise mioclonica; ES-noPTZ: 600s de estimulação; PTZ+ES: infusão de PTZ até o animal alcançar a crise mioclônica concomitante com ES desde o início da infusão, até o tempo de 120s após a crise convulsiva).

3.4.6 Atividade elétrica epileptiforme

Seguiu-se a mesma metodologia descrita na secção 3.2.6.

3.4.7 Análise da atividade pre-ictal (120 segundos anteriores à crise epiléptica)

Seguiu-se a mesma metodologia descrita na secção 3.2.7.

3.4.8 Resposta cortical perante estimulação elétrica profunda pré-crise epiléptica

Seguiu-se a mesma metodologia descrita na secção 3.2.8, com exceção do cálculo pós crise epiléptica.

3.4.9 Bandas de frequência que compõem o potencial evocado

Seguiu-se a mesma metodologia descrita na secção 3.2.9.

3.5 Materiais e métodos protocolos modulação de peso sináptico por pareamento de estimulação elétrica no complexo amigdaloide e crise epiléptica eletrográfica

3.5.1 Grupo experimental da estimulação amigdaloide

Foram utilizados 10 ratos wistar machos (300 – 320g) provenientes do CEBIO-ICB-UFMG *vivarium* que compuseram o grupo PTZ+ES CRISE. O protocolo foi realizado sob a licença nº 150/06 aprovada pelo comitê de ética e experimentação animal (CETEA – UFMG).

3.5.2 Cirurgia estereotáxica

Eletrodos bipolares foram cirurgicamente implantados no complexo amigdaloide dos animais seguindo a metodologia descrita na secção 3.4.2.

3.5.3 Infusão de pentilenotetrazol e estimulação elétrica cerebral profunda

A droga PTZ foi infundida pela veia da cauda dos animais seguindo mesma metodologia descrita na secção 3.2.3.

3.5.4 Aquisição de sinal EEG, atividade epileptiformes

O sinal de EEG do córtex parietal foi adquirido conforme a metodologia descrita na secção 3.2.4.

3.5.5 Desenho experimental

O protocolo experimental foi dividido em dois dias e cada dia continha três períodos temporais sequenciais distintos, sendo que os dois primeiros estão presentes em todos os todos os dias de aquisição: período basal (120s de registro sem estimulação elétrica ou infusão de PTZ), período estimulação elétrica (120s de estimulação elétrica, conforme tópico 3.2.3).

Dia zero: após os períodos basal e ES, PTZ era então infundido pela veia da cauda dos animais até que eles apresentassem crise mioclônicas. A estimulação elétrica neste dia era apresentada por 120s a começar após o animal ter apresentado o primeiro abalo mioclônico.

Dia um: os mesmos animais foram novamente submetidos ao período basal, ES, e seguidos de infusão de PTZ concomitante com ES (agora desde o início da infusão de PTZ) até a crise mioclônica.

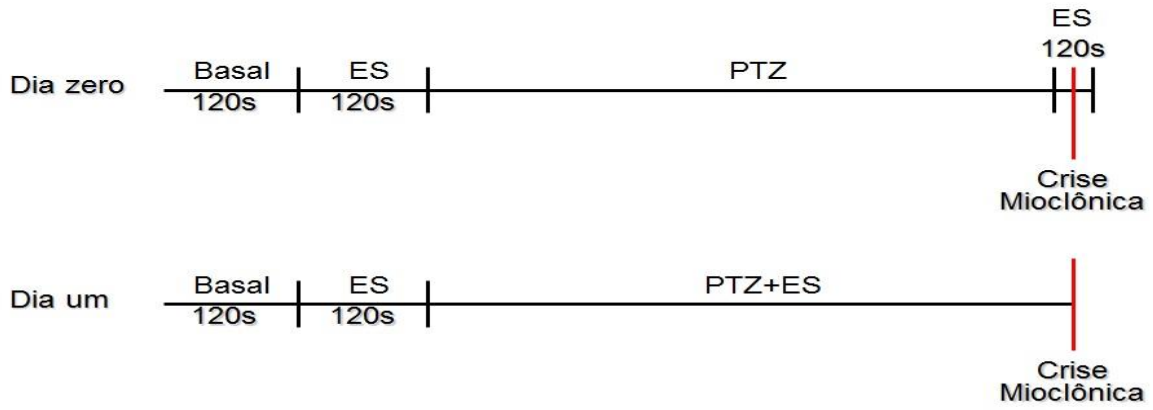

Figura 4: Esquemático do desenho experimental da sondagem de circuitos neurais por estimulação elétrica no AMG de ratos acordados pareado à somente crise epiléptica como forma de indução de alteração nos pesos sinápticos. No dia zero, os animais eram submetidos a três etapas sequenciais, sendo elas: a basal (sem qualquer influencia de fármaco (PTZ) ou estimulação elétrica; período ES no qual todos os animais recebiam pulsos elétricos no AMG sem a influência do fármaco, e indução de crise (PTZ) no qual os animais eram levados à crise epiléptica por infusão de PTZ. Quando os animais apresentavam o primeiro abalo mioclônico, eram então submetidos a 120s de ES. No dia 1, os períodos basal e ES eram repetidos, seguidos de um período no qual os animais recebiam infusão de PTZ concomitantemente com a ES até apresentar a crise epiléptica.

4.0 Resultados

4.1 Protocolo sondagem em animal anestesiado

A evolução representativa do EEG de um animal PTZ-noES para a crise convulsiva é mostrada na figura 1, assim como a transição do período pré-ictal para o ictal. A figura 5B e 5C representa o intervalo entre os disparos no período de 600 segundos antes da crise convulsiva. Pode-se notar uma prevalência em torno de 1-2 segundos o que indica que as oscilações de animais anestesiados por uretana e infusão gradativa de PTZ pela veia da cauda está entre 1 e 0.5Hz.

A estimulação elétrica em complexo amigdaloide não demonstrou padrão pró-convulsivo, pois não interferiu na latência para começo da crise eletrográfica, sua duração ou distribuição de frequência; não houve diferença estatística entre os grupos PTZ-noES e PTZ+ES, como mostrado na figura 6A, 6B e 6C (p=0.1548 teste T não-pareado, p=0.5887 Mann Whitney teste, p>0.05 2-way ANOVA Bonferroni post-hoc teste, respectivamente). No entanto, a estimulação elétrica foi capaz de alterar a atividade celular, evidenciada pela expressão de c-Fos (figura 7). O grupo PTZ+ES demonstrou um padrão de expressão de c-Fos diferente dos grupos PTZ-noES e ES-noPTZ, e significativamente para as regiões talâmicas, hipotalâmicas e do complexo amigdaloide (THAL p<0.001, AMY e Hth p<0.05, one way ANOVA Newman-Keuls post-hoc test). É importante ressaltar que nenhum dos animais do grupo c-Fos apresentou crise eletrográfica.

A estimulação elétrica não alterou a ocorrência de disparos pre-ictais (Figura 8A, comparação entre os grupos PTZ+ES e PTZ-noES - p>0.05 2-way ANOVA Bonferroni

post-hoc test) nem o total de energia do EEG (Figura 8B, comparação entre todos os grupos experimentais - $p>0.05$ 2-way ANOVA Bonferroni post-hoc test) ao longo da janela de 600s que precedem a crise eletrográfica. No entanto, a energia após o estímulo normalizada pelo basal (anterior ao estímulo) é significativamente superior no grupo PTZ+ES quando comparado aos outros grupos ($p<0.001$, 2-way ANOVA Bonferroni post-hoc test) 80 segundos antes do começo da crise eletrográfica conforme mostrado na figura 8C.

Além disso, a estimulação elétrica foi capaz de sincronizar os disparos máximos na sequencia de janelas de 2 segundos do grupo PTZ+ES comparado aos demais grupos cerca de 400s antes da crise eletrográfica. A figura 9 mostra cada grupo sendo representado por uma cor específica: ES-noPTZ preto; PTZ-noES vermelho e PTZ+ES azul. Na parte superior da figura são demonstrados traços típicos de EEG para cada grupo. É importante salientar que o grupo ES-noPTZ não evoluiu para crise eletrográfica, e, logo não apresentou disparos pre-ictais de grande amplitude. Abaixo dos traçados do EEG, são mostrados três distintos intervalos de 20 segundos (I0 -420s to -400s, I_1 -220s to -200s and I_2 -20s to T_{zero} segundos antes da crise convulsiva) que foram divididos em janelas de 2 segundos e posteriormente sobrepostos. Os histogramas mostram as diferenças entre os intervalos TMPs e sugerem que um oscilador externo (a estimulação elétrica) forçou a sincronização dos disparos máximos minutos antes do começo da crise para o grupo PTZ+ES. Como esperado, a distribuição no começo do EEG seguiu uma distribuição Gausiana (T_{zero}-600 até T_{zero}-400 segundos) para todos os grupos (Figure 9A - $p>0.05$, 2-way ANOVA Bonferroni post-hoc test). Porém, o grupo PTZ+ES demonstrou um aumento de ocorrências de valor zero entre os intervalos de pico máximos nos dois terços finais do registro (EEG de -400 até -200, $p<0.01$ e -200 até T_{zero}, $p<0.001$, 2-way ANOVA Bonferroni post-hoc teste),

enquanto os outros grupos permaneceram com distribuição normal. O valor zero reflete uma sincronia entre os disparos pre-ictais e o estímulo elétrico a 0.5Hz.

Três formas de ondas distintas de um animal representativo do grupo PTZ-noES (figura 10A) e do PTZ+ES (figura 6B) são mostradas na figura 10. O painel direito mostra a ocorrência das três formas de onda em janelas de tempo de 2 segudos (de 0,5 a 1,5 do sinal de *trigger*). Pode ser notado que as ondas ocorrem randomicamente no início do registro de EEG para ambos os animais representativos. Porém, as ondas do animal PTZ+ES gradualmente sincronizam com o ES antes da crise convulsiva, concomitante com o surgimento do potencial evocado, mostrado no painel à esquerda. As formas de onda do animal PTZ-noES se mantêm aleatoriamente distribuídas ao longo de todo o tempo do registro.

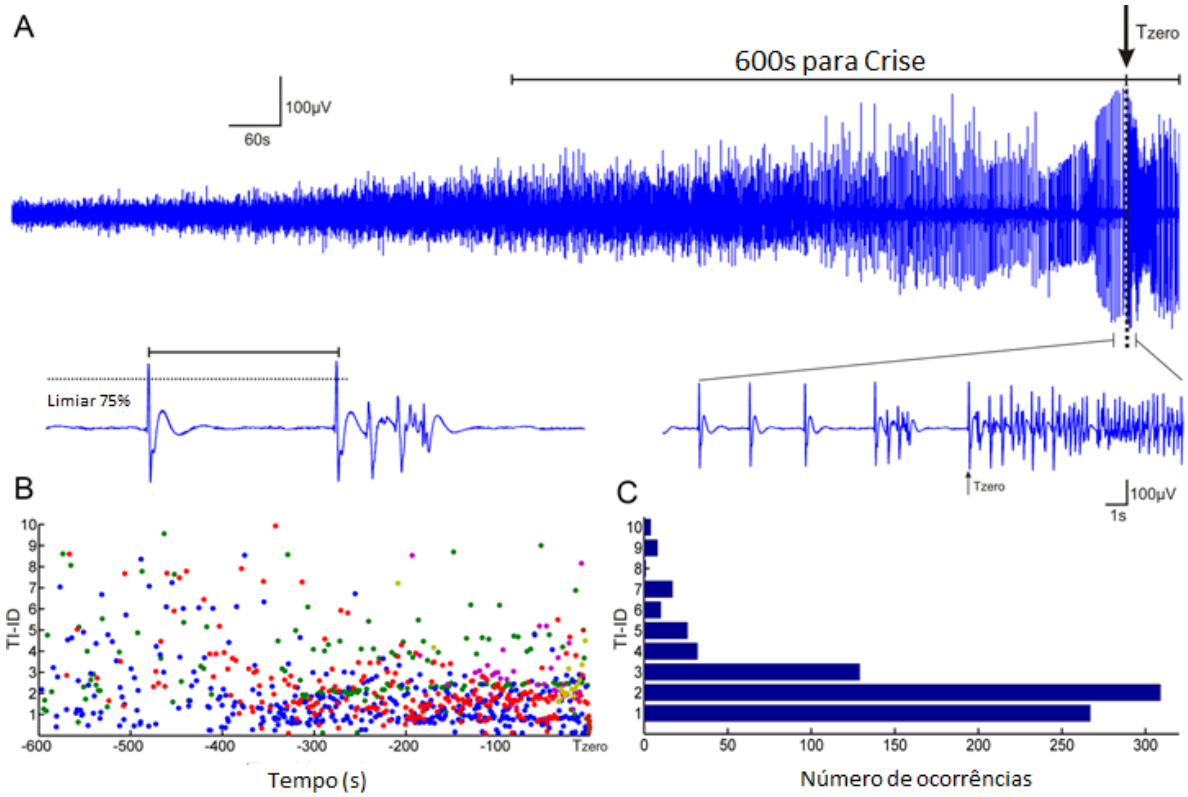

Figura 5 - Atividade pre-ictal do grupo PTZ-noES. A) Evolução de um EEG representativo do grupo PTZ-noES. B) Cada cor representa um animal e cada ponto representa uma ocorrência de disparo pré-ictal supra-limiar. C) Histograma de todos os intervalos das oscilações dos animais PTZ-noES

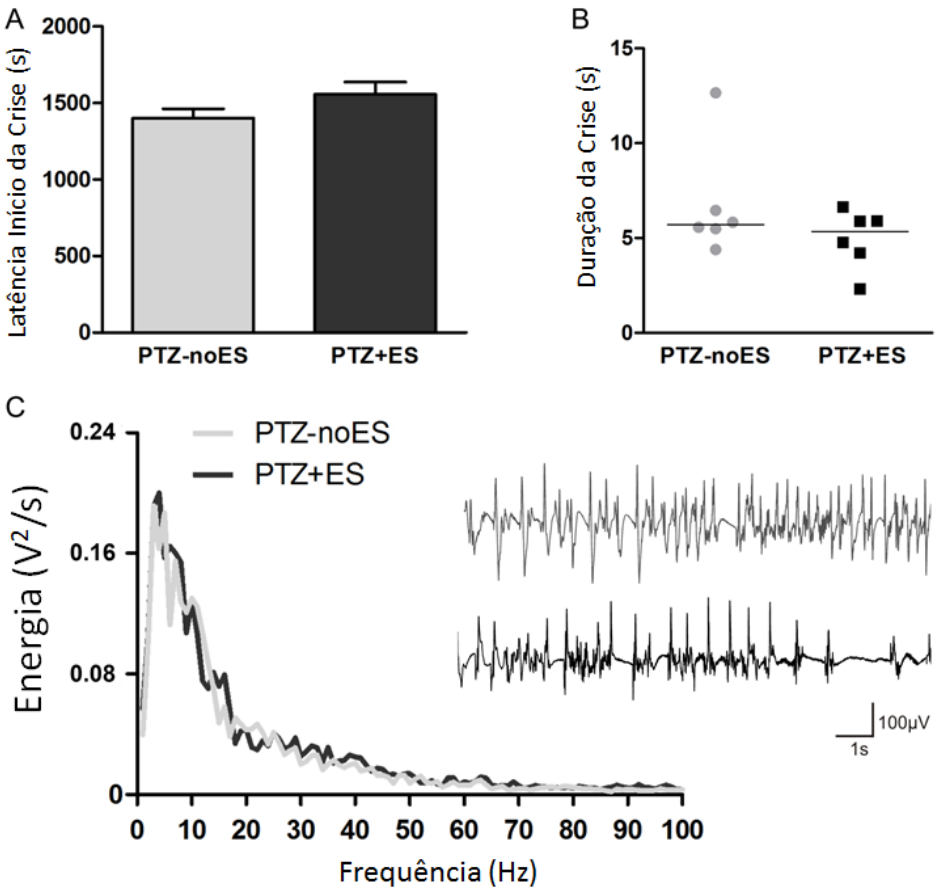

Figura 6 – Análise de parâmetros relacionados às crises epilépticas eletrográficas para o grupo PTZ+ES e PTZ-noES. A) Latência para início da crise eletrográfica (começo da infusão do PTZ até os primeiros disparos epileptiformes). B) Duração da atividade ictal. C) Distribuição em frequência dos disparos epileptiformes.

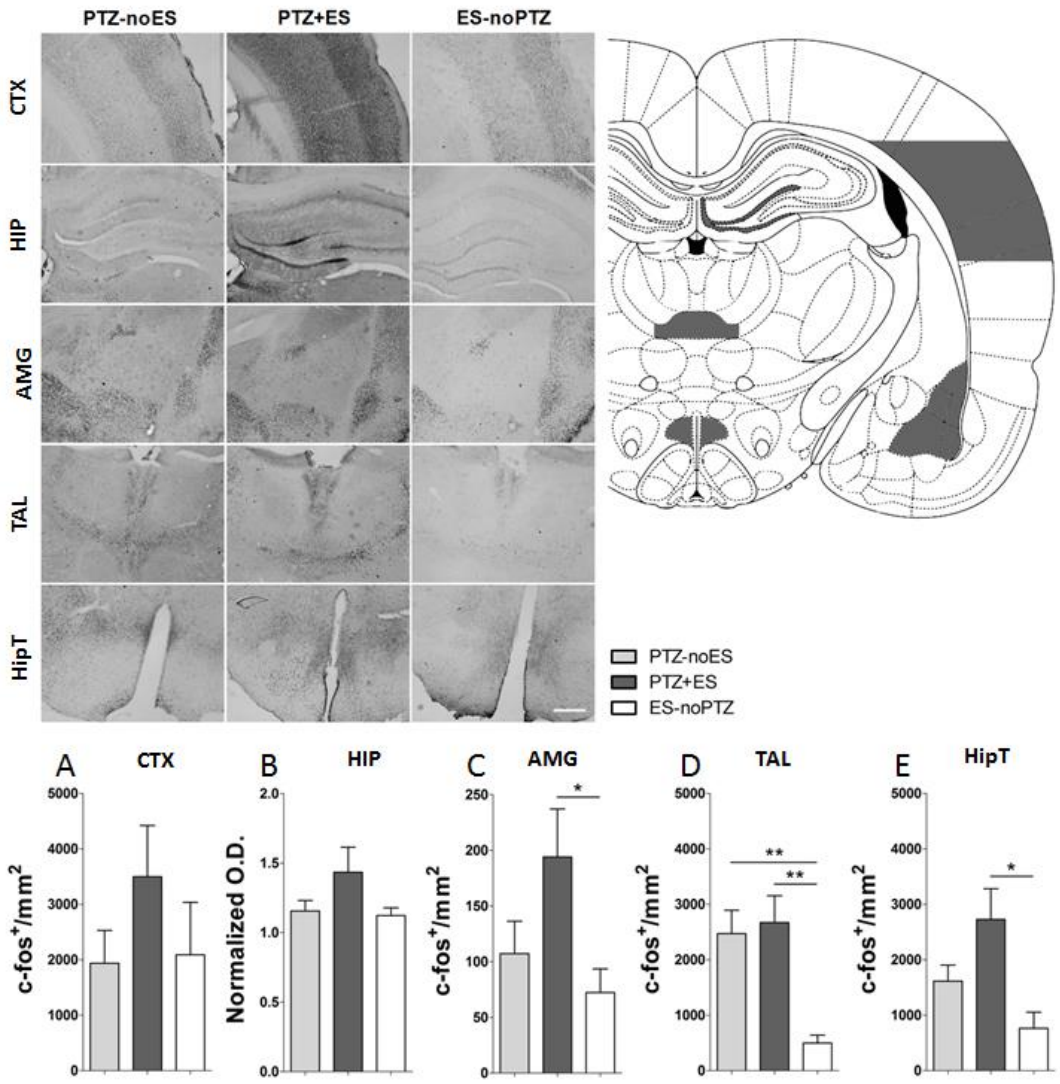

Figura 7 - Expressão de c-Fos em fatias de cérebro durante período pré-ictal. O painel superior demonstra imagens representativas das regiões de interesse analisadas: córtex (CTX), hipocampo (HIP), complexo amigdaloide esquerdo (AMG), tálamo (TAL) e hipotálamo (Hipt). As áreas destacadas no diagrama esquemático do atlas cerebral de rato indicam as áreas de interesse analisadas. Gráficos A, C, D, E demonstram número de células c-Fos positivas por unidade de área (mm2). Gráfico B, densitometria ótica normalizada. (*P<0.05; **P<0.01, média ± desvio padrão).

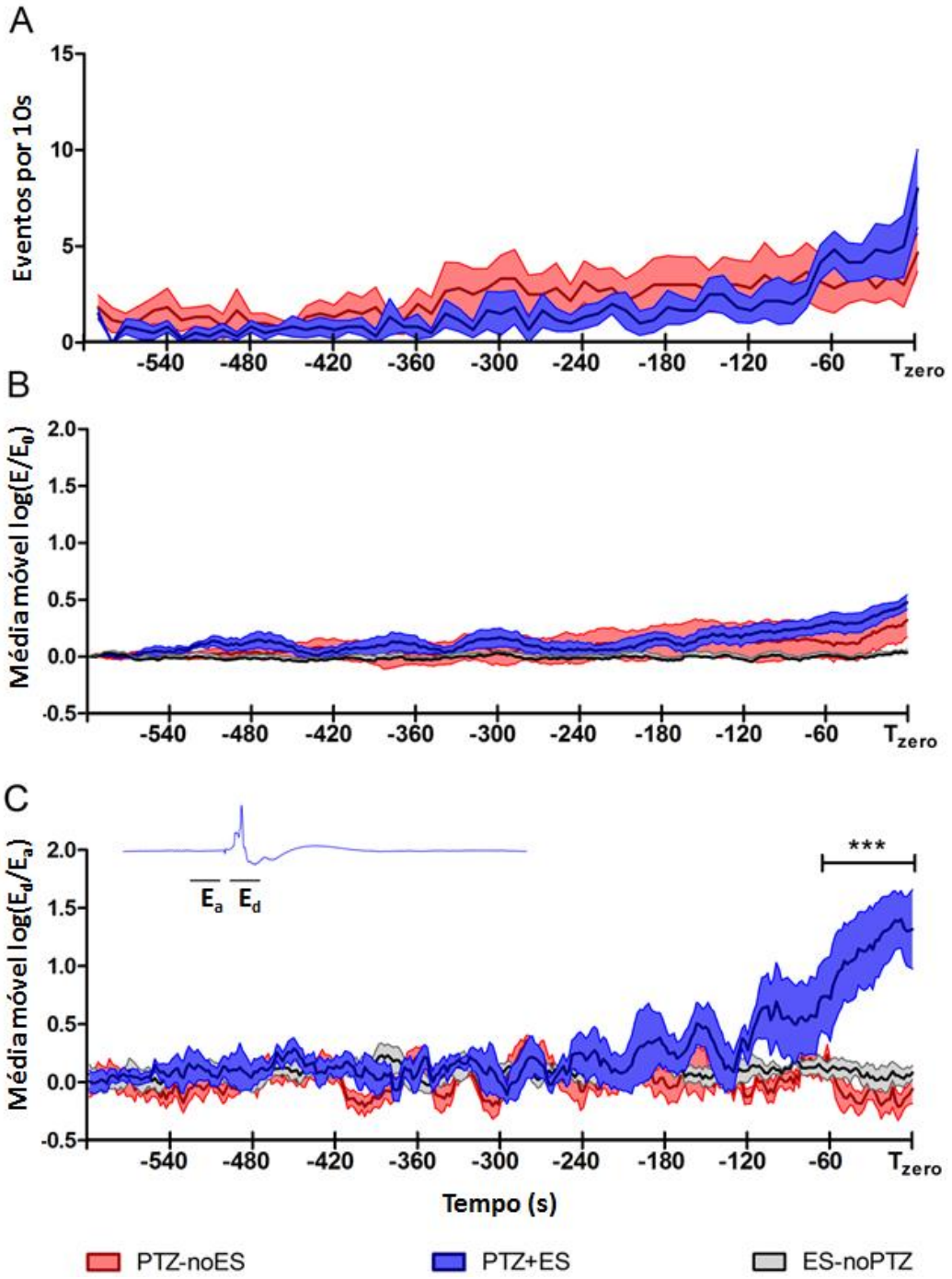

Figura 8 - Efeito da estimulação elétrica sobre os disparos pre-ictais ao longo de uma janela temporal de 600s antes da crise epiléptica eletrográfica. A) Os 600s foram divididos em 60 partes (10s cada) e o número total de disparos pre-ictais (acima de um limiar – ver metodologia) foi quantificado para cada parte de 10s. B) Média móvel (20s) da energia total normalizada (E/E_0) do EEG para cada 2s. C) Energia normalizada do EEG (Ed/Ea) para cada 2s usando a mesma média móvel que B (***P <0.001, média ± desvio padrão).

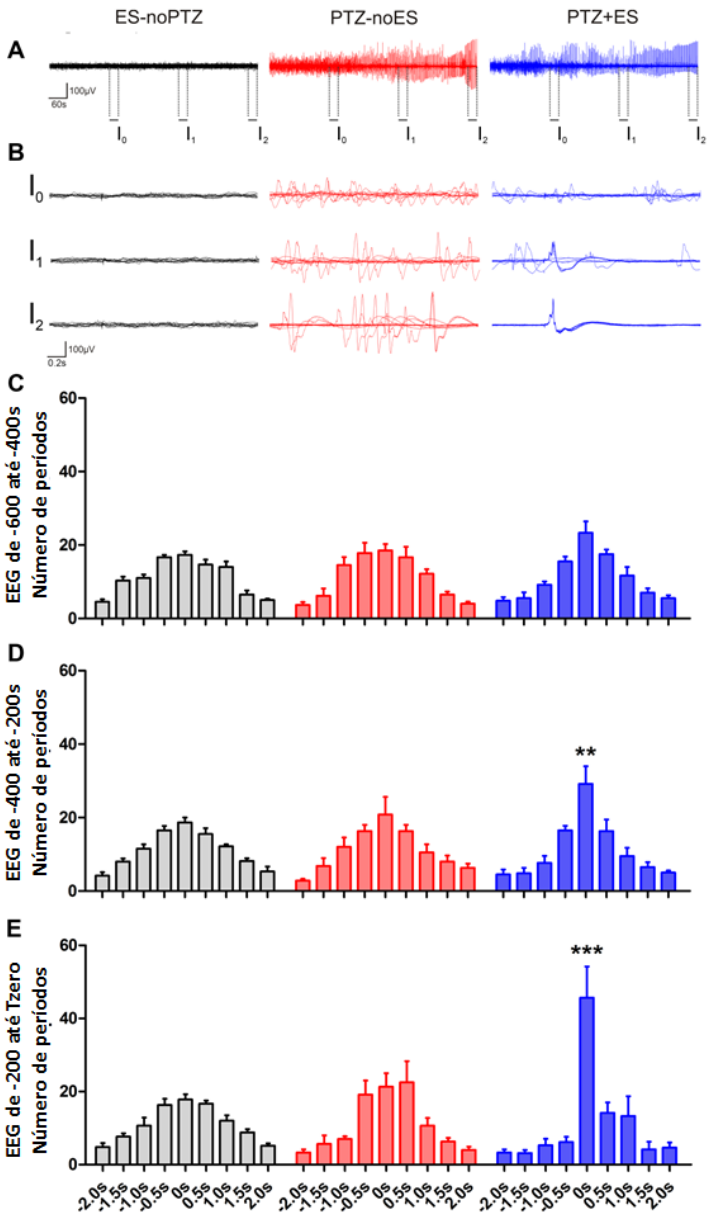

Figura 9 - Sincronia entre da atividade eletrográfica pre-ictal. Cada cor representa um grupo experimental, ES-noPTZ (preto), PTZ-noES (vermelho) and PTZ+ES (azul). A) Traçado de EEG representativo (600s pre-ictal) para cada grupo. Para cada animal, 3 intervalos foram selecionados: I0 (-420 até -400s), I1 (-220 até -200), I2 (-20 até Tzero). B) Os intervalos selecionados foram divididos em janelas de 2s (referenciados pelo ES – 0,5s antes do estímulo e 1,5s após) e sobrepostos. C, D, E) Os 600s de EEG que antecedem a crise epiléptica eletrográfica foi dividida em três partes. Cada terço foi subdividido em séries de 100 janelas de 2s. O pico máximo de voltagem para cada janela de 2s foi usado para produzir um marcador temporal (TMP). Os gráficos mostram os histogramas de -2s a +2s produzidos pela subtração dos TMP subsequentes pelos anteriores.

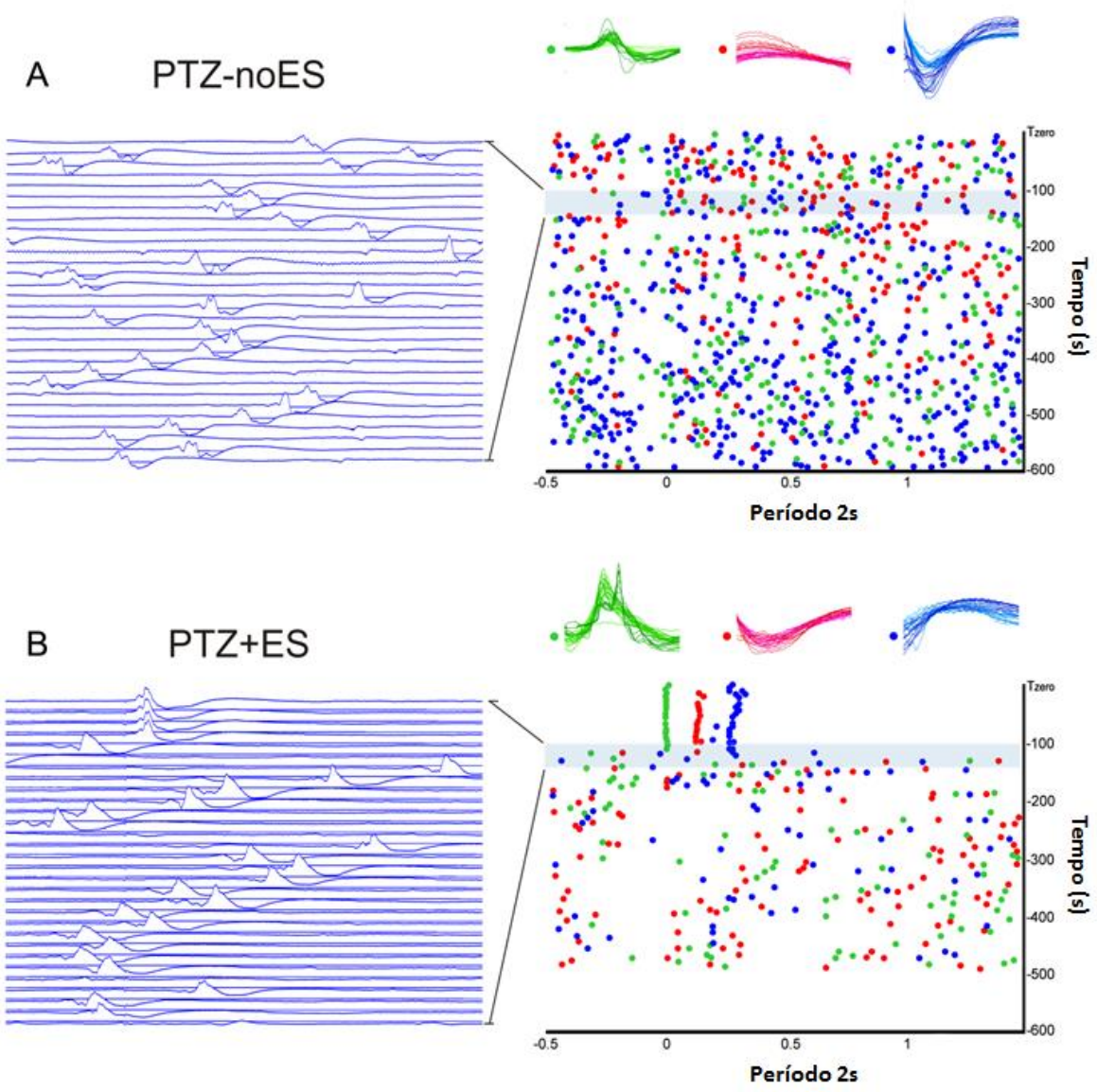

Figura 10 – Reconhecimento de padrões de onda e o tempo de ocorrência dos mesmos ao longo de uma janela de 600s de EEG que precedem a crise epiléptica eletrográfica. Três diferentes formas de onda foram arbitrariamente selecionadas para cada animal representativo do grupo PTZ-noES (A) e PTZ+ES (B). O painel esquerdo mostra a progressão do EEG (-160s até -100s) em sequenciais janelas de 2s (0,5 antes do estímulo e 1,5s após). Os pontos coloridos no painel à direita correspondem à ocorrência de determinado formato de onda (as cores de cada formato de onda são mostradas na parte superior da figura).

4.2 Protocolos sondagem em animal acordado perante estimulação talâmica

A estimulação elétrica profunda no ANT não alterou significativamente a latência para o início da crise nem a duração da mesma, mostrando assim que os pulsos elétricos não possuem características pró-convulsivas, quando aplicadas nesta estrutura (figura 11 - p=0,5 e p =0,7 respectivamente – Teste T não-pareado). Análises como energia (figura 12A gráfico p =0,9 teste T não pareado) e espectro de frequência (figura 12 C-D - inspeção visual) também não demonstraram diferença entre o grupos PTZ+ES e PTZ-noES. Porém, quando o sinal cortical é submetido a uma análise da energia normalizada (250ms após o estímulo normalizado por 250ms imediatamente anterior), que tem por finalidade ressaltar a influencia da ES nos circuitos neurais, percebe-se um aumento significativo para o grupo PTZ+ES doze segundos antes da crise epiléptica, quando comparada com os outros grupos (figura 13 - grupo PTZ+ES é significativamente diferente do grupo PTZ-noES e ES-noPTZ, p<0,05, 2-way ANOVA Bonferroni *post-hoc teste*). E a análise deste potencial evocado perante as diferentes bandas de frequência (figura 13 B-E) indica que a faixa beta (12 a 30Hz) contribuiu significativamente para o surgimento deste (PTZ+ES demonstrou maior energia na banda beta comparada com PTZ-noES e ES-noPTZ p <0.05, ONEWAY ANOVA, Newman-Keuls *post-hoc test*). Porém, quando se compara a distribuição de frequência do penúltimo potencial evocado do grupo PTZ+ES com o maior disparo pre-ictal (na janela de -4 a -2s antes da crise), não se nota diferença significativa em nenhuma banda de frequência (figura 14 - banda teta p =0,2; banda alfa p =0,3; banda beta p =0,5; banda gama p =0,5; teste T não pareado - figura 11).

A figura 15 mostra o cálculo da energia normalizada no grupo PTZ+ES após a crise eletrográfica (30s). É possível perceber que há um aumento significativo desta energia, comparado tanto com o mesmo grupo (PTZ+ES) 10s antes da crise quanto com o grupo PTZ-noES (figura 15 - p <0,05, ONEWAY ANOVA, Newman-Keuls post-hoc test) o que demonstra uma possível interferência da crise epiléptica na resposta cortical à estimulação talâmica. Essa afirmativa é também abordada na figura 16, onde a média da energia normalizada do dia 1, perante o estímulo, mostrou que, quando há a junção de estimulação elétrica e crise epiléptica, há um aumento significativo da resposta cortical perante a ES 24h após os disparos epileptiformes (figura 16 – período estimulação, grupo PTZ+ES difere significativamente dos grupos PTZ-noES e PTZ+ES p<0,05, ONEWAY ANOVA, Newman-Keuls post-hoc test). Interessante ressaltar que essa diferença desaparece quando o mesmo teste é realizado 7 dias após o pareamento entre a crise epiléptica e a ES. A comparação do período basal não revelou qualquer diferença estatística, demonstrando que a atividade intrínseca do sistema não foi alterada (figura 16 – período basal p>0,05, ONEWAY ANOVA, Newman-Keuls post-hoc test). Mesmo quando a estimulação elétrica é executada somente no período ictal (120s após o primeiro abalo muscular), é também capaz de aumentar a resposta cortical **pre-ictal** 24h após o pareamento (figura 17). Grupo PTZ+ES CRISE obteve aumento significativo da energia normalizada quando comparado com os grupos PTZ+ES e PTZ-noES, que não haviam tido qualquer crise epiléptica anteriormente (grupo PTZ+ES CRISE é significativamente diferente do grupo PTZ-noES 12s antes da crise, p<0,001, e do grupo PTZ+ES 2s antes da crise p <0,05; 2-way ANOVA Bonferroni *post-hoc teste)*. Porém, esse pareamento não foi capaz de aumentar o período de previsão (manteve-se em 12s quando se compara o grupo PTZ+ES CRISE e PTZ-noES). A

resposta cortical do grupo PTZ+ES CRISE teve o mesmo padrão de composição de frequencia do grupo PTZ+ES, sendo um aumento da energia normalizada (10s antes da crise) das bandas beta e gama, sendo essa última significativamente diferente dos outros grupos (figura 17 D-E; PTZ+ES CRISE demonstrou maior energia normalizada na banda gama comparada com PTZ+ES e PTZ-noES $p<0,001$, ONEWAY ANOVA, Newman-Keuls *post-hoc test*). Um fato interessante é que esse pareamento entre a ES e a crise não alterou os parâmetros de latência para o início e nem a duração da crise epiléptica no dia 1 em comparação com o dia zero (figura 18 A-B; latência para início da crise $p=0,7$ e duração da crise $p=0,8$; teste T pareado); e nem mesmo alterou significativamente a resposta cortical na ausência de PTZ (figura 19C; média da energia normalizada do período ES sobre período basal do dia 1 não difere do dia zero; $p=0,3$ teste T pareado). A única alteração considerável foi da energia total 10s antes da crise (de -10s até Tzero) do grupo PTZ+ES CRISE em comparação aos grupos PTZ+ES e PTZ-noES (figura 18; $p<0,01$, ONEWAY ANOVA, Newman-Keuls *post-hoc test*).

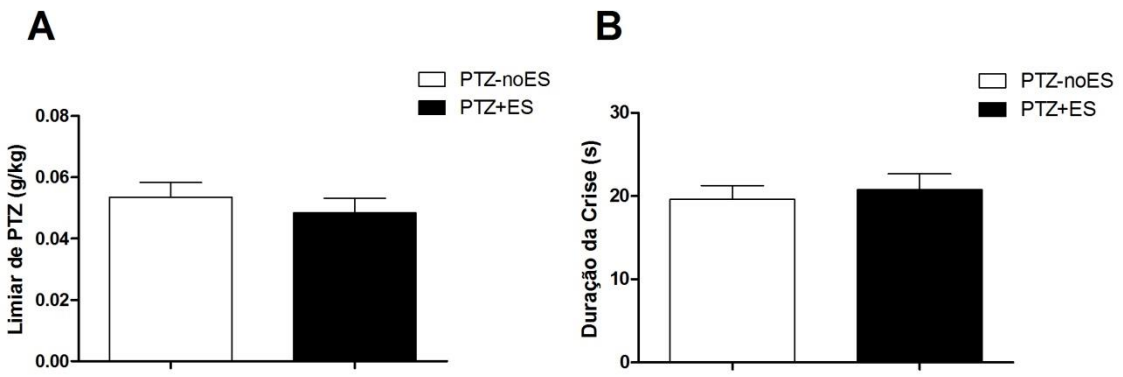

Figura 11 – Comparação de parâmetros da crise epiléptica eletrográfica dos grupos PTZ-noES e PTZ+ES. A) Limar de PTZ necessário para evocar crise epiléptica eletrográfica. B) Duração da atividade epileptiforme.

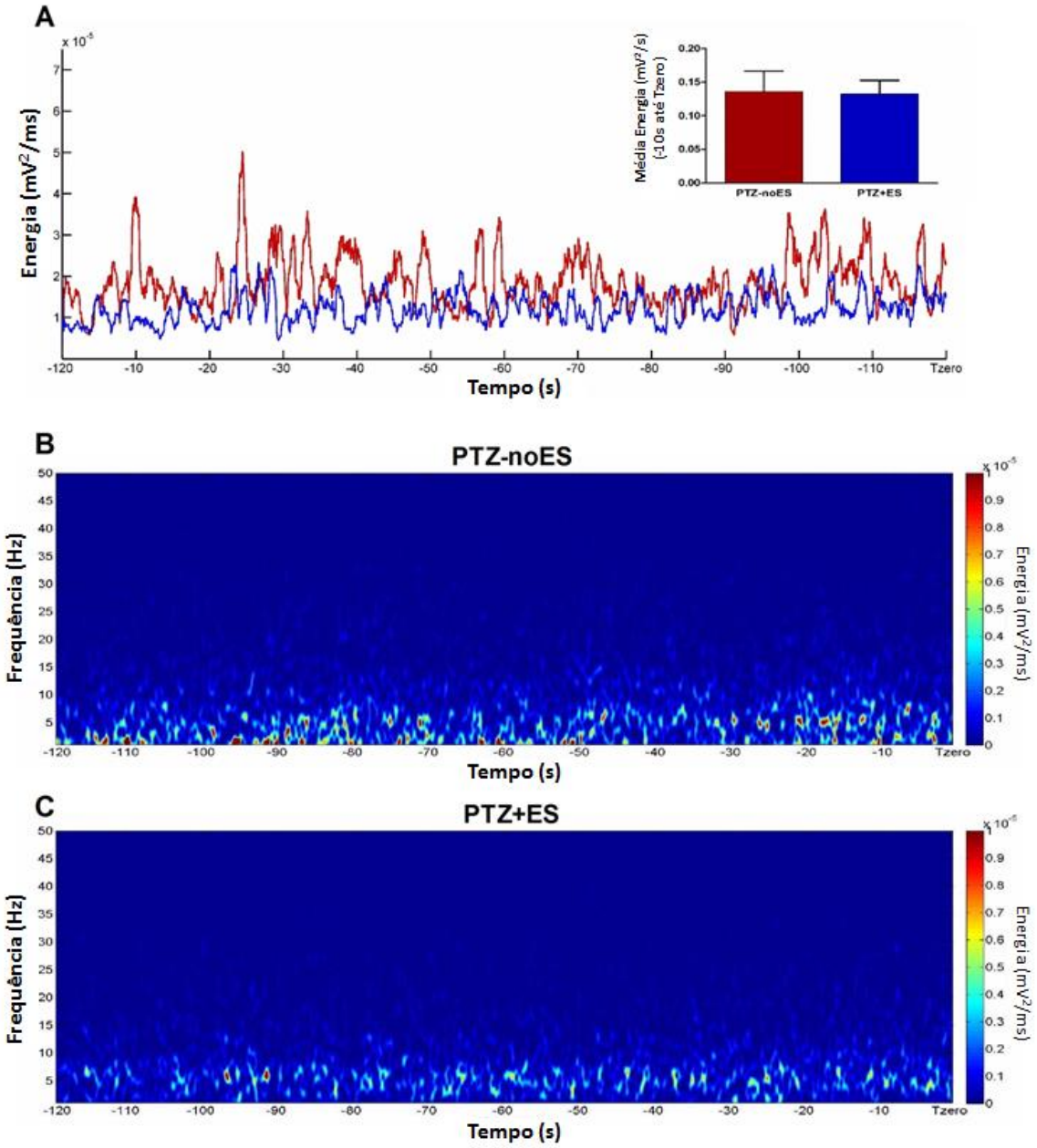

Figura 12 – Análise dos dois minutos de EEG que antecedem a crise epiléptica eletrográfica para os grupos PTZ+ES e PTZ-noES. A) Média da energia do EEG (V^2) para o grupo PTZ+ES (AZUL) e PTZ_noES (VERMELHO). Gráfico à direita mostra a média desta energia dos 10 segundos que antecedem a crise. Note que não há diferença significativa entre os grupos. B,C) Média da análise espectral dos 120 segundos anteriores à crise eletrográfica para os grupos PTZ-noES (A) PTZ+ES (B). Note a ausência de mudança expressiva no padrão de distribuição das frequências ao longo do tempo.

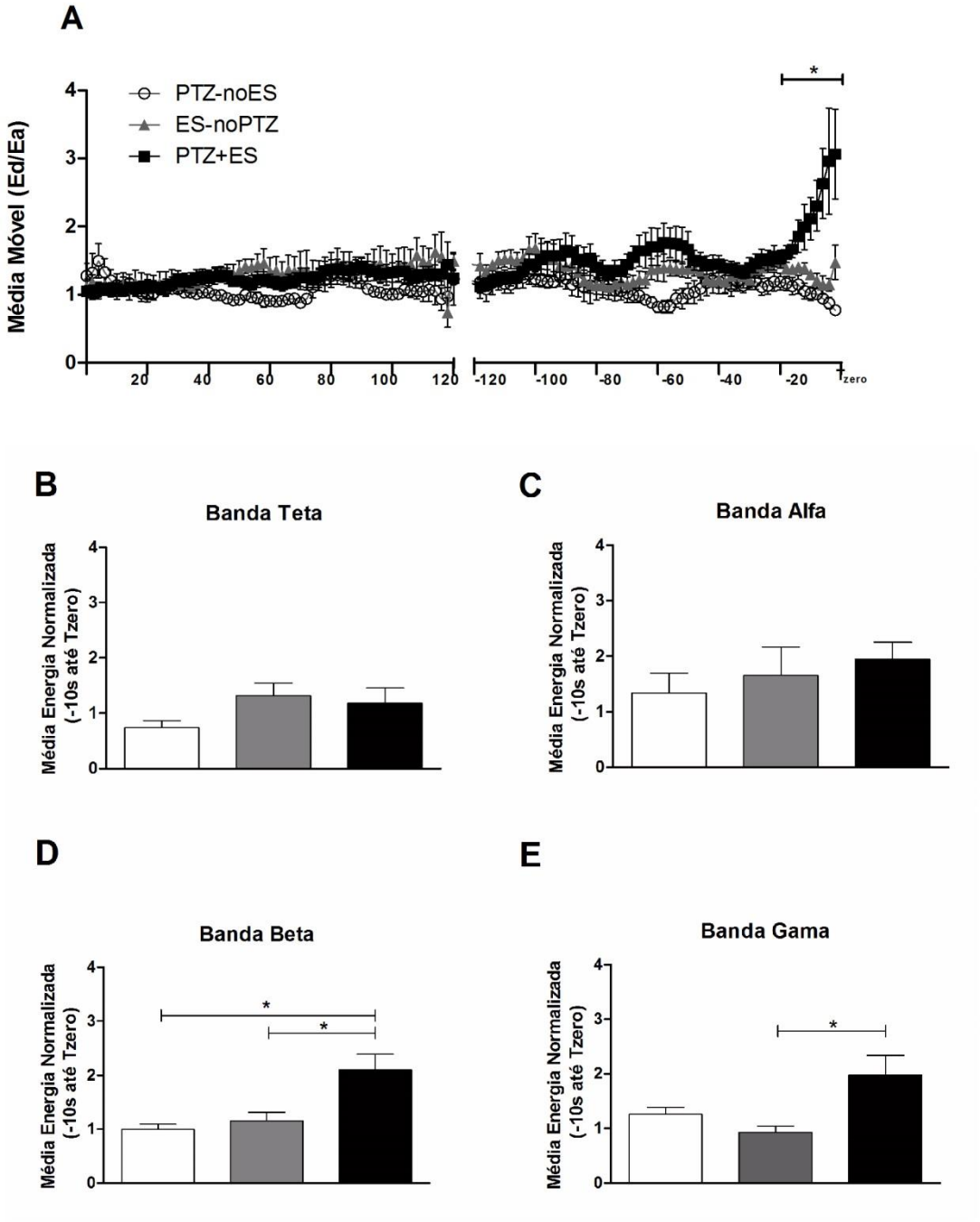

Figura 13 – Resposta cortical perante estimulação elétrica do ANT de baixíssima frequência. A) Média móvel da energia normalizada (E_d/E_a) nos períodos iniciais do EEG (de 0 a 120s) e nos dois minutos que antecedem a crise convulsiva (de -120 até Tzero). B,C,D,E) Média da energia normalizada dos últimos 10 segundos antes da crise convulsiva, de acordo com as bandas de frequência, teta, alpha, beta e gama (*P <0,05, média ± desvio padrão).

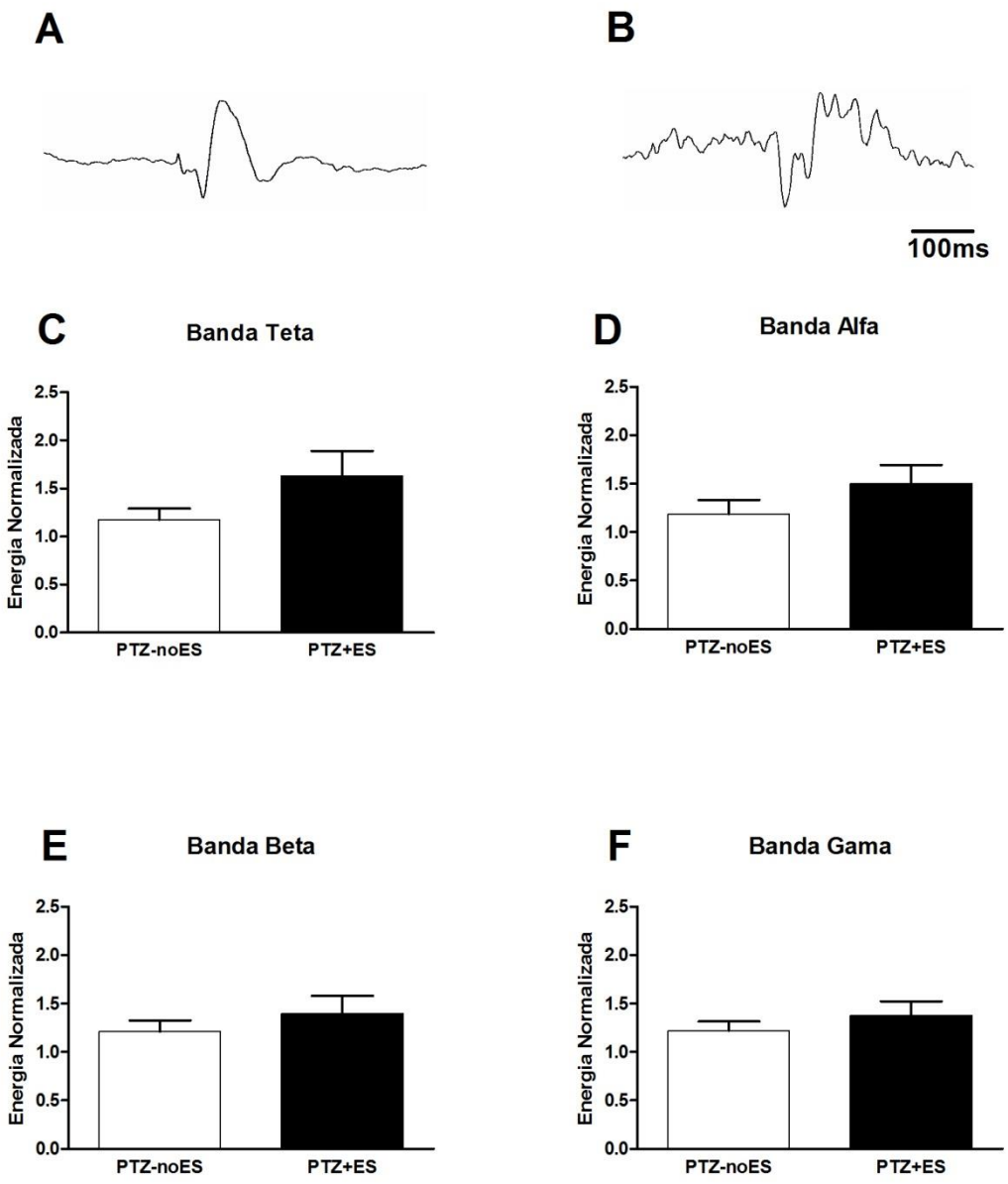

Figura 14 – Analise das bandas de frequência que compõem os potenciais evocados (grupo PTZ+ES) e os disparos pre-ictais (PTZ-noES) 4 segundos antes da crise. Os picos máximos do grupo PTZ-noES foram selecionados e uma janela de 250ms foi analisada por *wavelet*, assim como 250ms após o estímulo do grupo PTZ+ES e posteriormente normalizados por 1s anterior. A-B) figuras representativas de potencial evocado e disparo pre-ictal. C-F) comparação da média do valor absoluto das escalas do *wavelet* que representam as bandas de frequência.

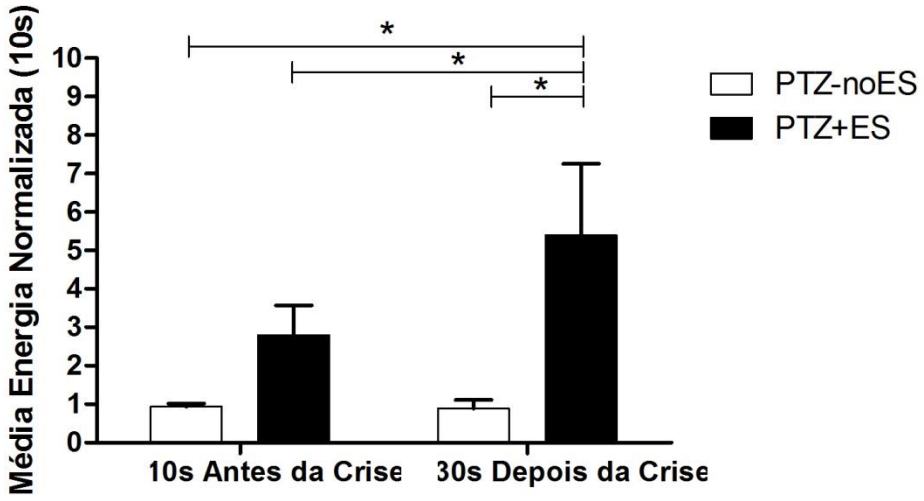

Figura 15 - Média da energia normalizada (Ed/Ea) 10 segundos antes da crise convulsiva (de -10s até Tzero) e 30 segundos depois da crise convulsiva (de 26s a 35s depois da crise epiléptica) para os grupos PTZ-noES e PTZ+ES (*P <0,05, média ± desvio padrão).

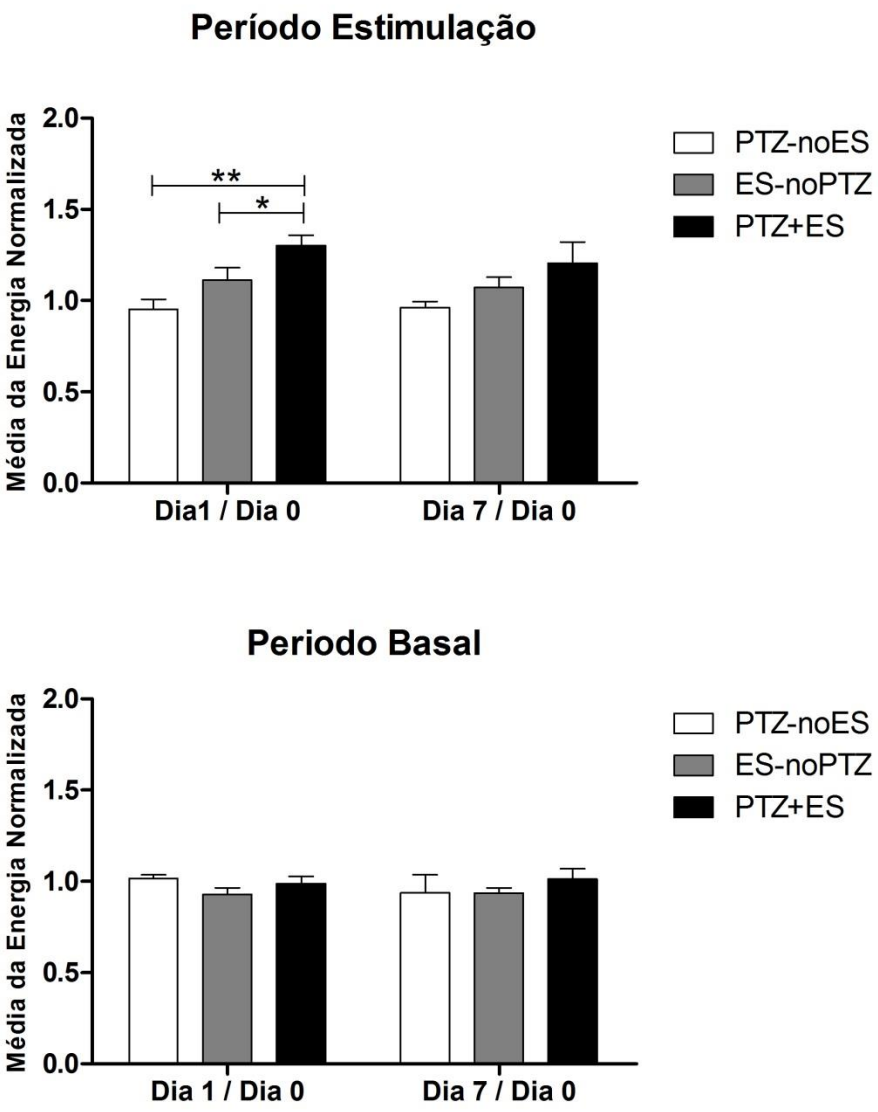

Figura 16 – Atividade cortical basal (sem qualquer intervenção farmacológica ou elétrica) e perante estimulação elétrica no ANT nos dias 1 e 7 após o dia zero experimental. Os gráficos mostram a média da energia normalizada (Ed/Ea) dos períodos estímulo (120s de estimulação elétrica – (figura A) e basal (120s – (figura B) em referência aos valores obtidos no dia zero (*P <0,05, média ± desvio padrão).

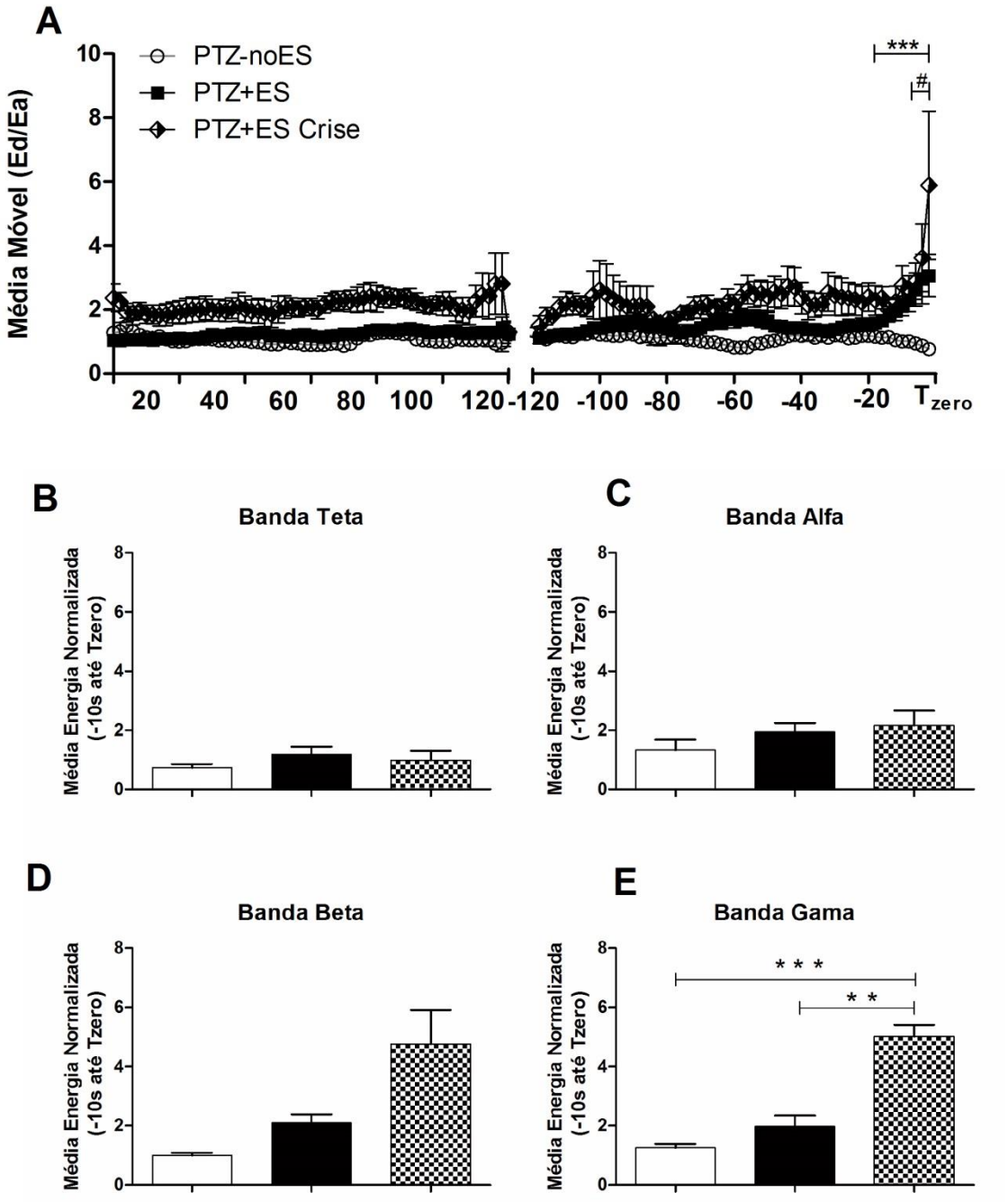

Figura 17 - Resposta cortical perante estimulação elétrica do ANT. A) Média móvel da energia normalizada (E_d/E_a) nos períodos iniciais do EEG (de 0 a 120s) e nos dois minutos que antecedem a crise convulsiva (de -120 até Tzero). Grupo "PTZ+ES crise" foi previamente estimulado (24h antes) por 120s durante a crise epiléptica B,C,D,E) Média da energia normalizada nos últimos 10 segundos antes da crise convulsiva de acordo com as bandas de frequência, teta, alpha, beta e gama (**P <0,01, ***P<0,001; média ± desvio padrão) .

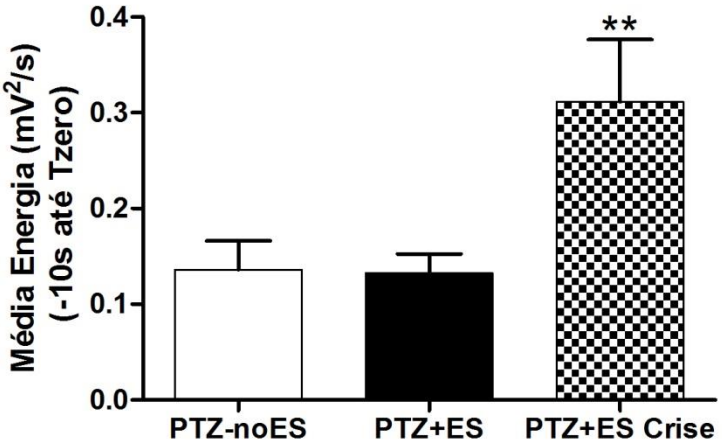

Figura 18 - Média da energia do EEG dos 10s anteriores à crise epiléptica eletrográfica (de -10s até Tzero; **P <0.01, média ± desvio padrão). Os grupos PTZ-noES e PTZ+ES (não foram submetidos a crise epiléptica anteriormente a essa avaliação) e o grupo PTZ+ES CRISE, a ES no ANT foi pareada à crise epiléptica 24h antes deste teste.

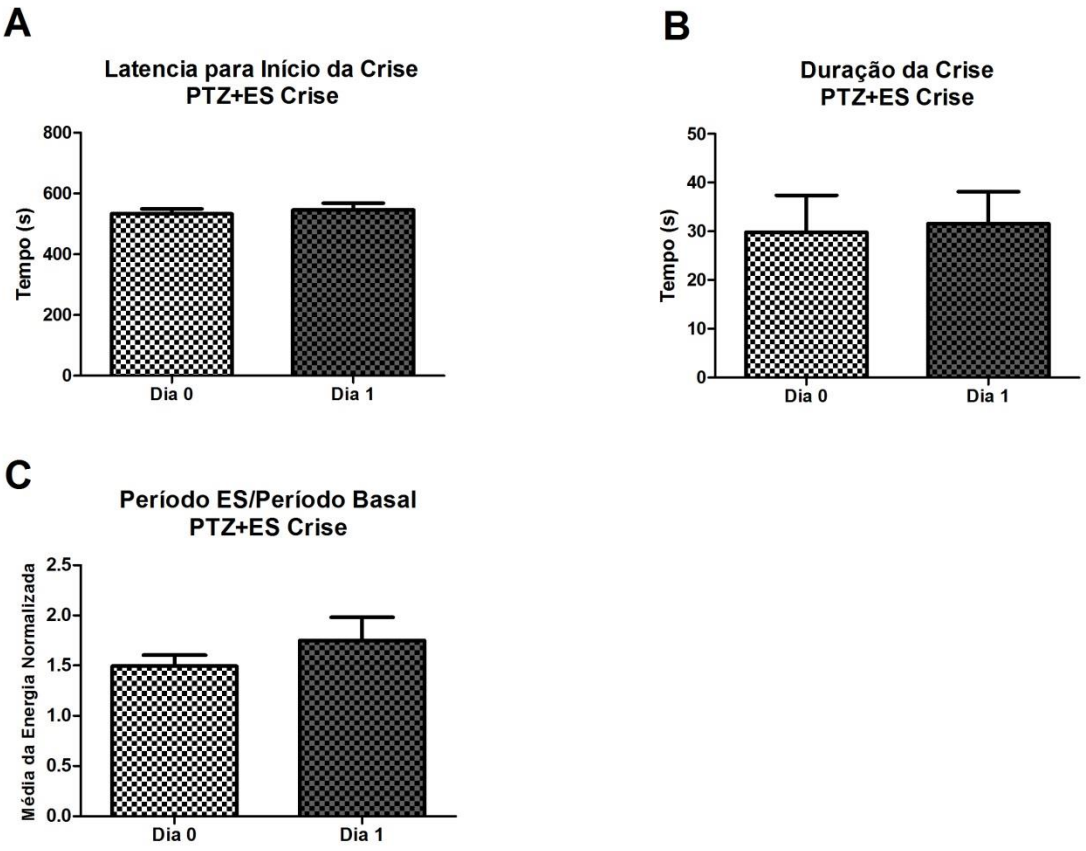

Figura 19 - Comparação de parâmetros da crise epiléptica eletrográfica referente ao grupo "PTZ+ES crise" nos dias zero e um. A) Latência em segundos para início da crise eletrográfica. B) Duração da atividade epileptiforme. C) Resposta do sistema neural perante a estimulação elétrica no núcleo do tálamo anterior. Gráfico mostra média da energia normalizada (Ed/Ea) do período estímulo (120s de estimulação elétrica) dividido pela média da energia normalizada (Ed/Ea) do período basal.

4.2 Protocolos sondagem em animal acordado perante estimulação no complexo amigdaloide

A estimulação elétrica no complexo amigdaloide não alterou significativamente a latência para o começo da crise, nem a duração das mesmas, indicando que o ES nesta estrutura não demonstra padrão pró-epiléptico (PTZ-noES comparado com PTZ+ES - figura 20 A-B; $p>0,05$ teste T student não pareado). A ES não demonstrou alterar também a energia do EEG do grupo PTZ+ES em comparação com o grupo PTZ-noES nos 120s anteriores aos disparos epileptiformes (figura 21 – gráfico $p=0,7$ teste T não pareado), mesmo que, por inspeção visual da análise espectral, pode-se notar um aumento da energia de frequências abaixo de 10Hz 10s antes da crise epiléptica no grupo PTZ+ES (figura 21 C). Porém, esse aumento do grupo PTZ+ES não se refletiu na análise da energia normalizada antes da crise, pois a ES no AMG não evocou qualquer alteração desta energia quando comparada com os grupos PTZ-noES e ES-noPTZ (figura 22A - $p>0,05$ 2-way ANOVA Bonferroni *post-hoc teste*), mesmo quando analisada pelas bandas de frequência (figura 22B-E $p>0,05$, ONEWAY ANOVA, Newman-Keuls *post-hoc test*).

No entanto, quando os animais que foram previamente estimulados (24h antes) durante a crise (grupo PTZ+ES CRISE) houve um aumento significativo na energia normalizada 12s antes da crise epiléptica (figura 23A - PTZ+ES CRISE comparado com PTZ+ES e PTZ-noES $p<0,001$ 2-way ANOVA Bonferroni *post-hoc teste*), sendo a banda beta (12-30Hz) prioritária na composição deste potencial evocado (figura 23B-E PTZ+ES CRISE significativamente maior que groupo PTZ-noES - $p<0,05$, ONEWAY ANOVA, Newman-Keuls *post-hoc test*). É importante ressaltar que esse pareamento prévio entre a estimulação

elétrica no AMG e a crise epiléptica não aumentou a energia do EEG antes da crise epiléptica quando comparado com os grupos PTZ+ES e PTZ-noES (grupo PTZ+ES CRISE não difere nos demais grupos quanto a energia no período -10s até Tzero - figura24 $p>0,05$, ONEWAY ANOVA, Newman-Keuls *post-hoc test*). Esse pareamento prévio entre ES e a crise também não demonstrou ser pró-convulsivo, pois não alterou padrões como latência para crise e duração da mesma, quando se compara o dia zero e o dia 1 do grupo PTZ+ES CRISE (figura 25 A-B - $p>0,05$ teste T student não pareado); e o aumento da resposta cortical perante a ES ocorreu somente em momentos prévios à crise, pois na ausência de PTZ a resposta cortical perante a ES (período ES normalizado pelo período basal) do dia 1 não difere do dia zero (figura 25C - $p>0,05$ teste T student não pareado).

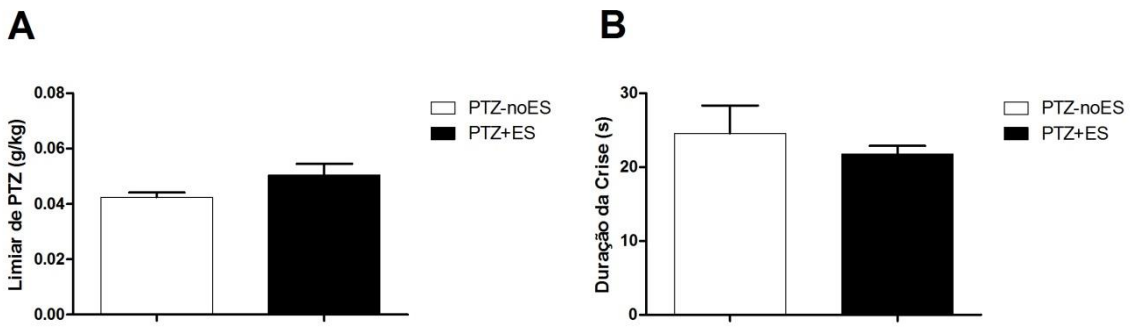

Figura 20 - Comparação de parâmetros da crise epiléptica eletrográfica dos grupos PTZ-noES e PTZ+ES. A) Limar de PTZ necessário para evocar crise epiléptica eletrográfica. B) Duração da atividade epileptiforme..

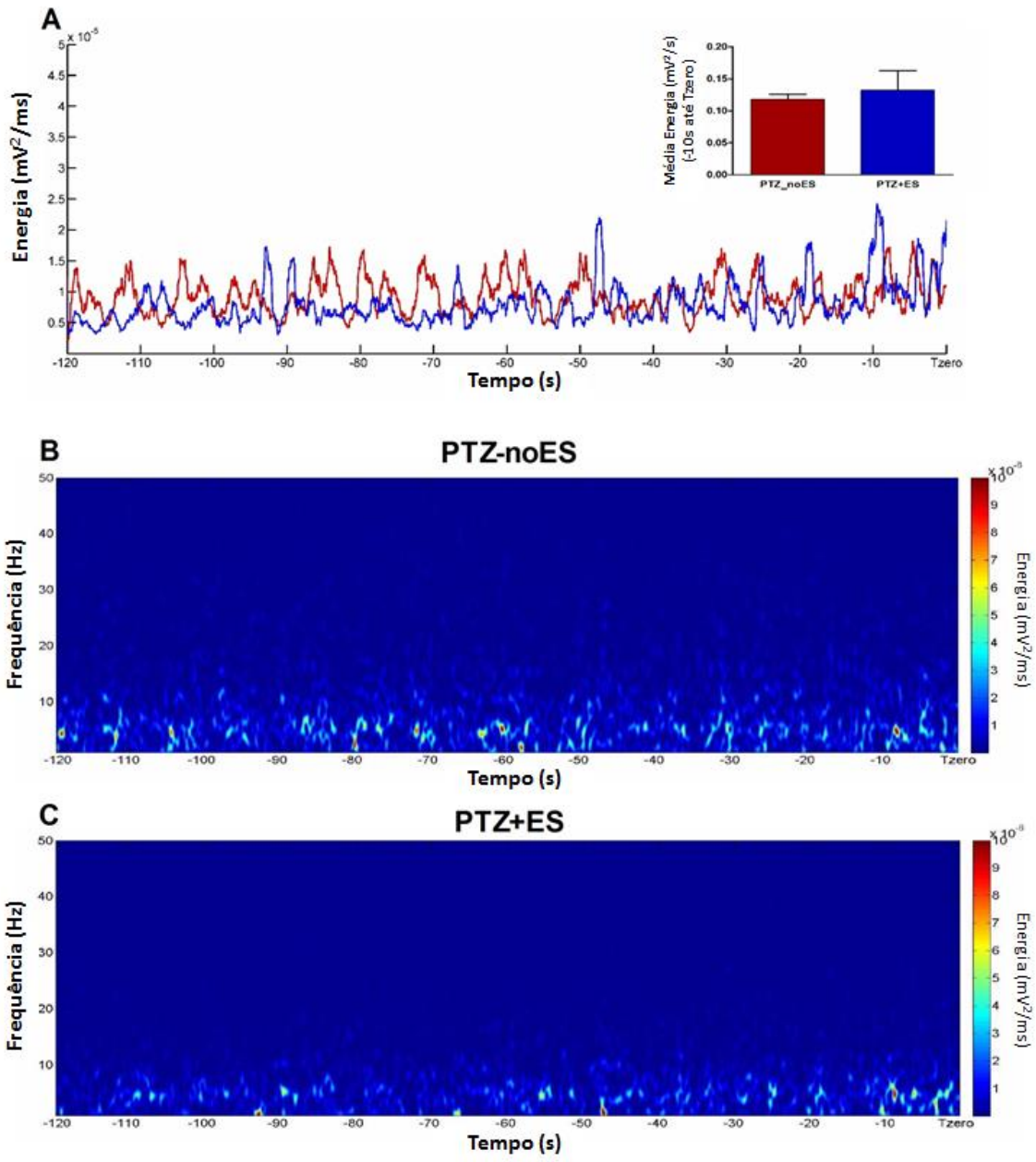

Figura 21 - Análise dos dois minutos de EEG que antecedem a crise epiléptica eletrográfica para os grupos PTZ+ES e PTZ-noES. A) Média da energia do EEG (V^2) para o grupo PTZ+ES (AZUL) e PTZ_noES (VERMELHO). Gráfico à direita mostra a média desta energia dos 10 segundos que antecedem a crise. Note que também não há diferença significativa entre os grupos. B,C) Média da análise espectral dos 120 segundos anteriores à crise eletrográfica para os grupos PTZ-noES (A) PTZ+ES (B). Note a ausência de mudança expressiva no padrão de distribuição das frequências ao longo do tempo

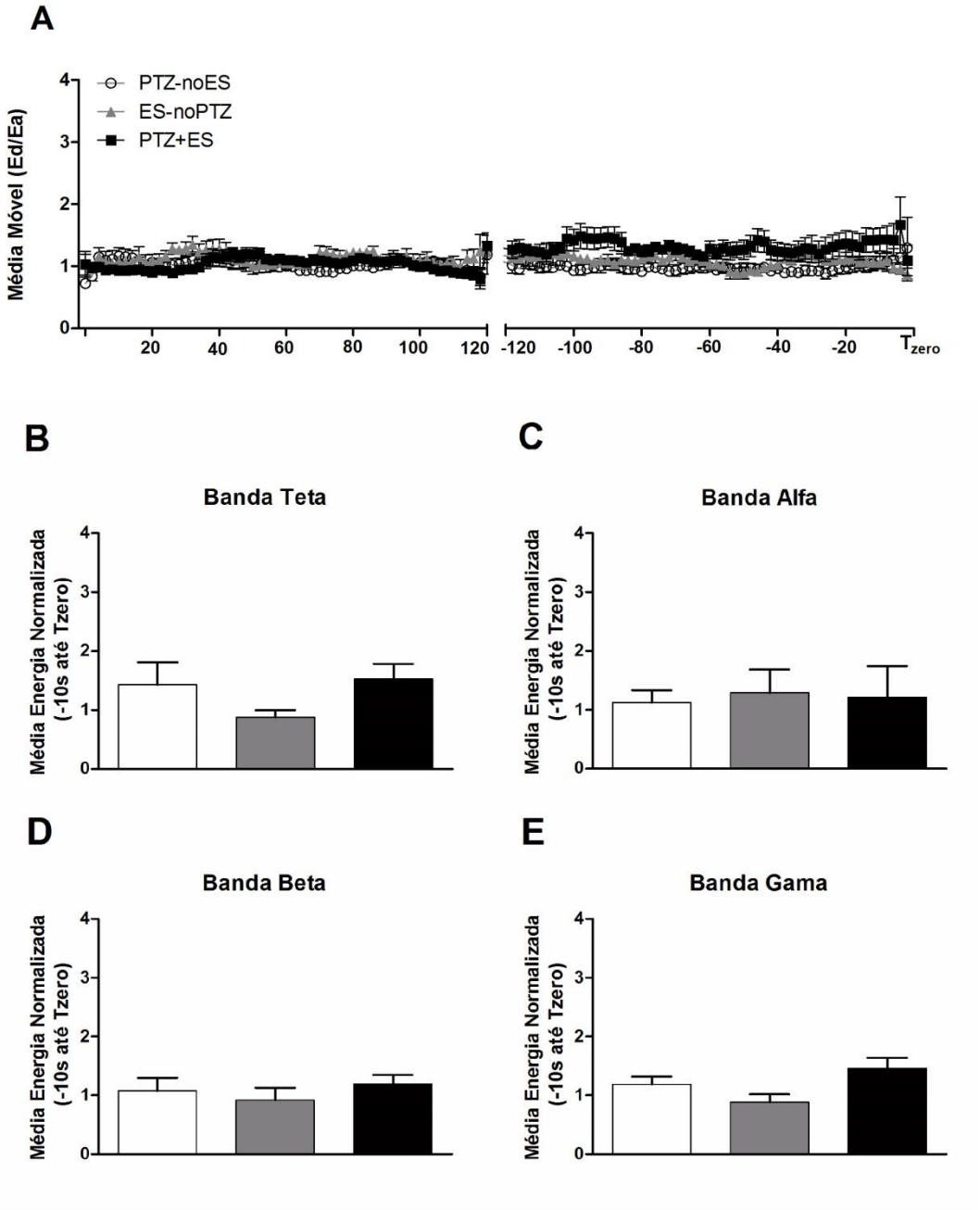

Figura 22 - Resposta cortical perante estimulação elétrica de baixíssima frequência na AMG. A) Média móvel da energia normalizada (E_d/E_a) nos períodos iniciais do EEG (de 0 a 120s) e nos dois minutos que antecedem a crise convulsiva (de -120 até Tzero). B,C,D,E) Média da energia normalizada dos últimos 10 segundos antes da crise convulsiva, de acordo com as bandas de frequência, teta, alpha, beta e gama.

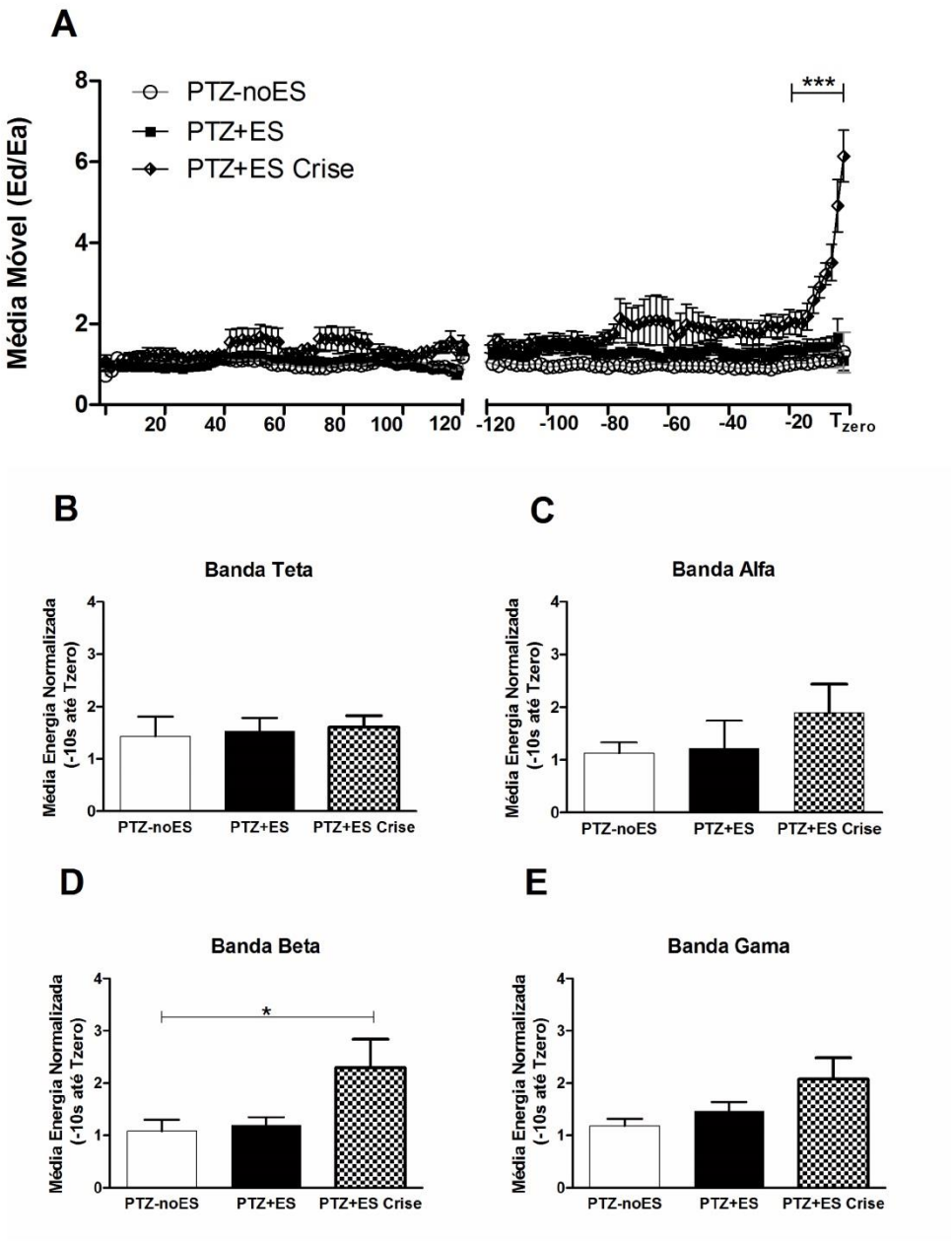

Figura 23 - Resposta cortical perante estimulação elétrica do AMG A) Média móvel da energia normalizada (Ed/Ea) nos períodos iniciais do EEG (de 0 a 120s) e nos dois minutos que antecedem a crise convulsiva (de -120 até Tzero). Grupo PTZ+ES CRISE foi previamente estimulado (24h antes) por 120s durante a crise epiléptica B,C,D,E) Média da energia normalizada nos últimos 10 segundos antes da crise convulsiva de acordo com as bandas de frequência, teta, alpha, beta e gama (*P <0,05, média ± desvio padrão).

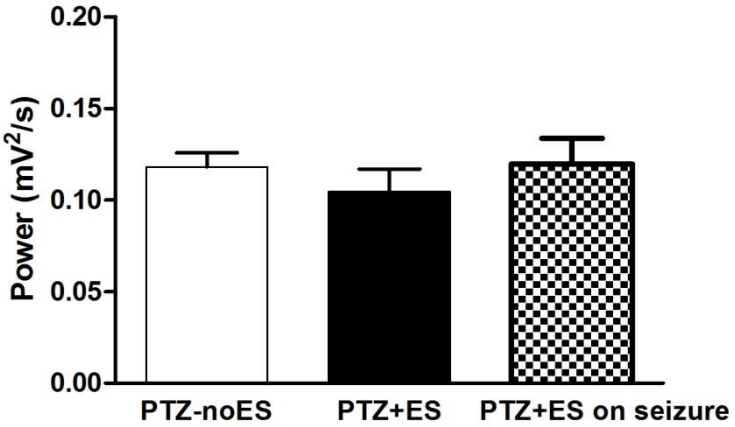

Figura 24 - Média da energia do EEG dos 10s anteriores à crise epiléptica eletrográfica para os grupos PTZ-noES e PTZ+ES (não foram submetidos a crise epiléptica anteriormente a essa avaliação) e grupo PTZ+Es CRISE, cuja ES no AMG foi pareada à crise epiléptica 24h antes deste teste.

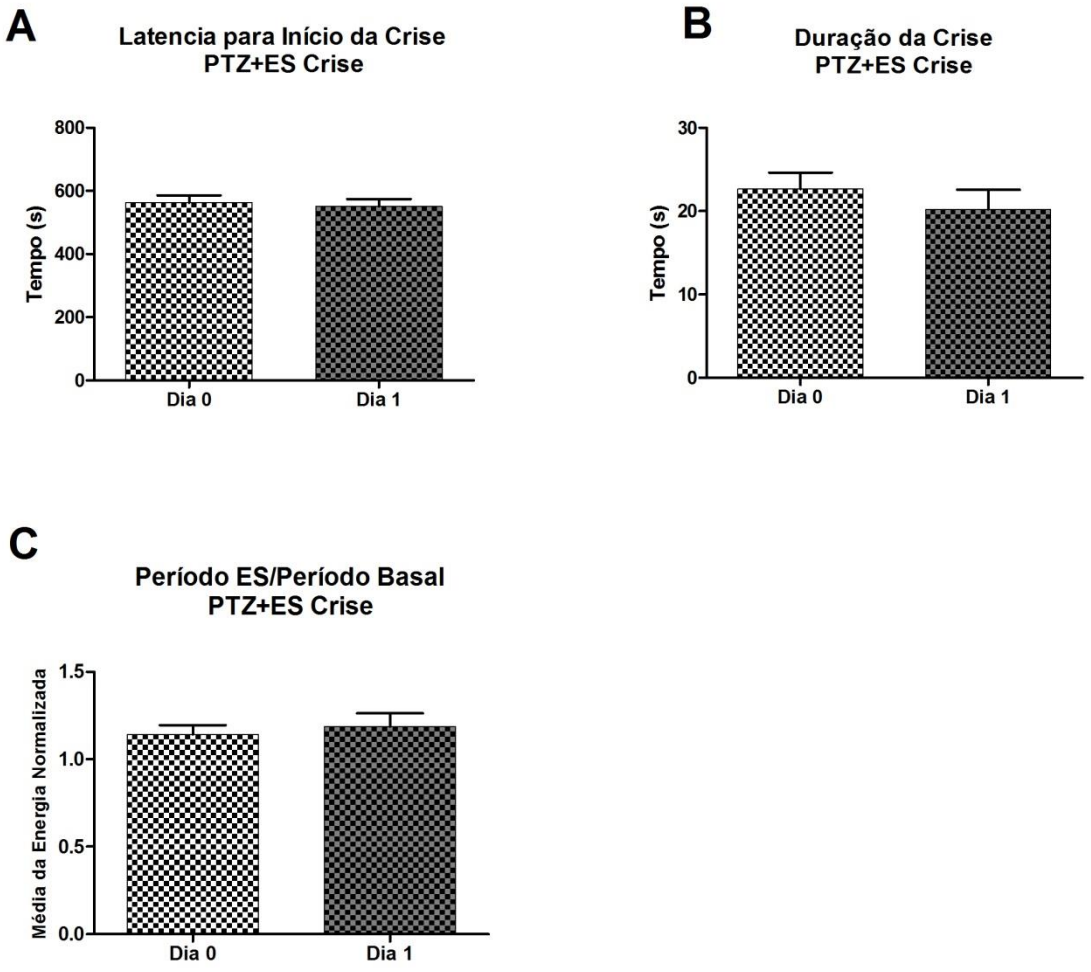

Figura 25 – Comparação de parâmetros da crise epiléptica eletrográfica referente ao grupo PTZ+ES CRISE nos dias zero e um. A) Latência em segundos para início da crise eletrográfica. B) Duração da atividade epileptiforme. C) Resposta do sistema neural perante a estimulação elétrica no núcleo do tálamo anterior. Gráfico mostra média da energia normalizada (Ed/Ea) do período estímulo (120s de estimulação elétrica) dividido pela média da energia normalizada (Ed/Ea) do período basal.

5.0 Discussão

5.1 Resposta cortical perante estimulação cerebral profunda

Em nosso estudo, a estimulação elétrica cerebral profunda agiu sobre o sistema neural como um oscilador externo que gradativamente modulou circuitos corticais ao ponto de evocar, momentos antes da crise epiléptica eletrográfica, potenciais de campo no EEG de ratos submetidos à infusão de PTZ pela veia da cauda. É importante ressaltar que, em todos os protocolos realizados, a estimulação elétrica não demonstrou caraterísticas pró-convulsivas, sem qualquer alteração significativa no valor da duração das crises eletrográficas ou latência para o início das mesmas, demonstrado na comparação entre os grupos PTZ+ES e PTZ-noES (figuras 6, 11, 20).

A sincronia neural desempenha papel fundamental no fluxo e processamento de informação ao longo dos substratos neurais (Singer, 1999). Certas desordens cerebrais estão associadas com uma sincronização neural anormal, entre elas a epilepsia (Uhlhaas e Singer, 2006); cujos disparos ictais têm sido tradicionalmente assumidos como sendo resultado de intensa e extensa sincronização neural que (Penfield, Jasper *et al.*, 1954) que, por vezes, rompe com o funcionamento fisiológico das redes neurais. Porém, ainda é alvo de debates se essa hipersincronia é resultado de um gradual aumento de sincronia neural entre substratos neurais distantes (Jiruska, De Curtis *et al.*, 2013), tanto que alguns estudos têm encontrado evidencias de diminuição de sincronia (Le Van Quyen, Martinerie *et al.*, 2001; Mormann, Kreuz *et al.*, 2003) momentos antes da crise epiléptica. Todavia, nossos resultados mostram que estruturas talâmicas (figuras 13,17,) e amigdalalares (figuras 8,9,23) (quando ativadas por estimulação elétrica) sincronizaram suas atividades neurais com regiões corticais

momentos antes da crise epiléptica induzida PTZ. A disparidade de resultados pode ter suas razões na diferença de metodologia aplicada. Enquanto os trabalhos que encontraram uma diminuição da sincronia utilizaram métodos passivos de análise do EEG, como correlação, coerência e sincronia em fase em diferentes áreas do cérebro; nosso trabalho se assenta na análise do eletrogencefalograma perante uma perturbação, ativamente realizada pela ES. Por nossa técnica, a sincronia foi mensurada minutos antes do começo da crise em animais anestesiados, (figura 8 e 9) e em animais acordados, 12 segundos antes da mesma. Outro dado que corrobora com a afirmação de sincronia entre áreas distantes antes da crise epiléptica é mostrado pela análise de c-Fos nos animais anestesiados (figura 7). Por este resultado, a ES, mesmo de tão baixa frequência, foi capaz de aumentar a expressão dessa proteína, quando aplicado concomitante com infusão de PTZ. Como o c-Fos é um marcador indireto de atividade neural (Dragunow e Faull, 1989), poderia-se supor que a causa de sua elevação no grupo PTZ+ES foi causado pelo aumento da atividade neuronal geral. Porém, o cálculo da energia do EEG não se alterou significativamente entre os grupos (figura 8). Logo, é pertinente pensar que a causa do aumento da expressão de c-Fos se deve mais sincronismo causado pela aplicação de um oscilador externo (ES), que por somação espacial, aumentou a eficiência sináptica e logo, a expressão de c-Fos do que pelo simples aumento da atividade basal.

Um fato interessante sobre resposta cortical evocada pela ES em animais acordados é o fato deste possuir componentes de alta frequência (banda beta 12-30Hz e gama 30-100Hz) que se destacam da atividade basal. Essas duas bandas de frequência são conhecidas por ser resultado de atividade sincrônica corticais de longa e curta distancia (beta e gama respectivamente) (Kopell, Ermentrout *et al.*, 2000), e podem estar exacerbadas em

momentos que antecedem a crise epiléptica (Grasse, Karunakaran *et al.*, 2013). Porém é uma tarefa árdua captar o aumento da energia destas bandas de frequência antes da ocorrência da crise eletrográfica somente pela análise espectral do EEG como mostram as figuras 12 e 21, onde, por inspeção visual, não se percebe alteração drástica nos sinais de EEG tanto do grupo PTZ+ES quanto do grupo PTZ-noES. Uma característica importante do potencial evocado (PE) por estimulação elétrica é a sua temporalidade, pois ele restringe a um período temporal muito estreito, a ocorrência das oscilações, majoritariamente composto pela banda beta e gama, o que aumenta a energia normalizada do sinal e torna possível a mensuração da densidade destas bandas de frequência e da energia como um todo. É muito importante salientar que essas altas frequências (banda beta e gama) estão também presentes no EEG pre-ictal de animais que não receberam a ES (grupo PTZ-noES), tanto que a figura 14 mostra que não há diferença significativa entre os potenciais evocados (grupo PTZ+ES) e os disparos pre-ictais (PTZ-noES) quanto à análise por bandas de frequência, incluindo beta e gama. Logo é razoável afirmar que a estimulação elétrica não foi o causador do surgimento de bandas de alta frequência, e sim apenas evocou, em um espaço temporal muito delimitado, um padrão de disparo que já era inerente ao estado do sistema neural, naquele determinado momento. O estudo em humanos realizado por Dinesh Nayak e col. (Nayak, Dinesh *et al.,* 2014) utilizando também estimulação elétrica cerebral profunda corrobora com essa afirmativa. Por este trabalho, os potenciais evocados por ES foram comparados com disparos inter-ictais pela sua morfologia, topografia e distribuição. O trabalho revelou que os potenciais evocados e os disparos inter-ictais são similares, o que sugere que a ES aciona o mesmos mecanismos responsáveis pela geração do ultimo. O diferencial do nosso trabalho é justamente a evocação destes disparos pre-

ictais num espaço temporal muito bem delimitado, possibilitando assim a mensuração dos mesmos frente à atividade intrínseca do sistema.

5.2 Crise epiléptica como fator de aumento de conexão entre áreas distantes.

Nosso trabalho revelou que apenas um episódio crise epiléptica aumentou a sincronia entre áreas distantes (aumento da resposta cortical perante ES), tanto agudo (30 segundos após a crise - figura 15) quanto cronicamente (24h após a crise – figuras 16,17,23).

Durante a crise epiléptica há elevação nos níveis de vários neurotransmissores, entre eles do glutamato, cuja ação é majoritariamente excitatória no sistema nervoso central (Meurs, Clinckers *et al.*, 2008). O tônus excitatório exacerbado aumenta a sincronia entre os neurônios (Kudela, Franaszczuk *et al.*, 2003) e, logo, entre áreas cerebrais, que pode levar a alterações nos pesos sinápticos. Em 1949, Donald Hebb postulou que a força da conexão entre dois neurônios é aumentada por longo período de tempo quando os disparos do neurônio pré-sináptico e do pós-sináptico estão correlacionados no tempo (Hebb, 1949) (essa afirmativa foi confirmada por experimentos subsequentes (Bliss e Collingridge, 1993)). Logo, a crise epiléptica pode ser um fator de aumento dos pesos sinápticos entre os neurônios que, naquele momento, estão disparando em sincronia (Scharfman, 2002), seja devido aos próprios disparos ictais, ou até mesmo por disparos evocados pela estimulação elétrica, como provam nossos resultados. Pode-se notar pela figura 16, que a resposta cortical, sem a influência de PTZ, aumenta significativamente perante estimulação no ANT 24h após uma seção de ± 500s de ES no qual uma crise está presente (essa diferença

significativa desaparece 7 dias após o pareamento) Mesmo quando esse pareamento entre a ES no ANT ocorre apenas durante a crise (grupo PTZ+ES CRISE – estimulação elétrica por 120s a partir do primeiro abalo muscular), há um aumento da resposta cortical (energia normalizada) antes da crise epiléptica quando comparada com animais que não obtiveram esse pareamento prévio (PTZ+ES e PTZ-noES). Porém, dois pontos devem ser ressaltados quando ao pareamento de ES no ANT e a crise: houve um aumento significativo da energia do EEG do grupo PTZ+ES CRISE em comparação aos demais (mesmo sem alteração de latência e duração da crise) o que indica um aumento exacerbado de excitabilidade; e, mais importante, não houve um aumento na janela de previsão, pois a diferença entre o grupo PTZ+ES CRISE e o grupo PTZ-noES ainda se manteve de 12s, igual ao grupo que não foi pareado, PTZ+ES. Esse cenário se altera a crise é pareada a ES no AMG. Vinte e quatro horas após o pareamento, a resposta cortical (energia normalizada) pre-ictal aumenta significativamente, perante ES no AMG, 12s antes da crise (figura 23), quando comparado com outros grupos não pareados (PTZ+ES e PTZ-noES). Detalhe importante é, sem esse pareamento (grupo PTZ+ES) a ES não foi capaz de aumentar a energia normalizada, em comparação com os grupos PTZ-noES e ES-noPTZ. Logo, o pareamento entre ES no AMG e a crise estaria programando o circuito neural, por modificar os pesos sinápticos, e podendo ser usado como marcador pre-ictal (*programing a seizure surrogate marker*). Vale ressaltar também, que o grupo PTZ+ES CRISE não apresentou qualquer alteração significativa na latência e duração das crises entre os dias zero e 1 do protocolo experimental (figura 25), e nem aumentou a energia do EEG, indicando assim uma manutenção da atividade basal. Esse resultado do pareamento da ES na AMG com a crise se mostra promissor, pois abre a possibilidade de, com apenas um eletrodo fixado na amigdala, seja possível a previsão e a supressão de crise epiléptica.

5.3 Previsão de crise epiléptica por estimulação cerebral profunda

Nosso estudo revelou ser possível uma janela de previsão de crise epiléptica de 12 segundos em animais acordados utilizando-se estimulação elétrica cerebral profunda em apenas um ponto de registro cortical. É possível que essa janela de previsão seja ampliada se forem utilizadas técnicas multivariadas de análise de EEG associadas à estimulação elétrica. Apesar de ser pertinente a afirmativa que existam diferentes mecanismos para a geração de crise epiléptica e logo exigindo diferentes abordagens para a previsão (Mormann, Andrzejak *et al.*, 2007), nossos resultados se mostram promissores, principalmente pela possibilidade de se utilizar somente um ponto de estimulação para a previsão e supressão de crise convulsiva. Tanto o núcleo anterior do tálamo (Medeiros, Cota *et al.*, 2012) quanto a amigdala (Cota, Medeiros Dde *et al.*, 2009), se mostraram excelentes alvos terapêuticos para supressão de crise epiléptica utilizando-se estimulação elétrica. Logo seria possível o desenvolvimento de um sistema fechado de previsão e supressão de crise convulsiva, utilizando-se para isso a estimulação elétrica cerebral profunda.

6.0 Referências Bibliográficas

Adelson, P. D., E. Nemoto, *et al.* Noninvasive continuous monitoring of cerebral oxygenation periictally using near-infrared spectroscopy: a preliminary report. Epilepsia, v.40, n.11, Nov, p.1484-9. 1999.

Adolphs, R. Neural systems for recognizing emotion. Curr Opin Neurobiol, v.12, n.2, Apr, p.169-77. 2002.

Aggleton, J. P. e M. Mishkin. The amygdala: Sensory gateway to the emotions. In: R. Plutchik e H. Kellerman (Ed.). Emotion: Theory, Research, and Experience. Orlando: FL, Academic, 1985. The amygdala: Sensory gateway to the emotions, p.281-299

Aggleton, J. P., S. M. O'mara, *et al.* Hippocampal-anterior thalamic pathways for memory: uncovering a network of direct and indirect actions. Eur J Neurosci, v.31, n.12, Jun, p.2292-307. 2010.

Alving, J. e S. Beniczky. Epileptic prodromes: are they nonconvulsive status epilepticus? Seizure, v.22, n.7, Sep, p.522-7. 2013.

Andrzejak, R. G., D. Chicharro, *et al.* Seizure prediction: any better than chance? Clin Neurophysiol, v.120, n.8, Aug, p.1465-78. 2009.

Avoli, M. e P. Gloor. Interaction of Cortex and Thalamus in Spike and Wave Discharges of Feline Generalized Penicillin Epilepsy. Experimental Neurology, v.76, n.1, p.196-217. 1982.

Baumgartner, C., W. Serles, *et al.* Preictal SPECT in temporal lobe epilepsy: regional cerebral blood flow is increased prior to electroencephalography-seizure onset. J Nucl Med, v.39, n.6, Jun, p.978-82. 1998.

Behbehani, M. M. Functional characteristics of the midbrain periaqueductal gray. Prog Neurobiol, v.46, n.6, Aug, p.575-605. 1995.

Bernard, C., A. Anderson, *et al.* Acquired dendritic channelopathy in temporal lobe epilepsy. Science, v.305, n.5683, Jul 23, p.532-5. 2004.

Bertram, E. H., D. Zhang, *et al.* Multiple roles of midline dorsal thalamic nuclei in induction and spread of limbic seizures. Epilepsia, v.49, n.2, Feb, p.256-68. 2008.

Bliss, T. V. e G. L. Collingridge. A synaptic model of memory: long-term potentiation in the hippocampus. Nature, v.361, n.6407, Jan 7, p.31-9. 1993.

Bonda, E., M. Petrides, *et al.* Specific involvement of human parietal systems and the amygdala in the perception of biological motion. J Neurosci, v.16, n.11, Jun 1, p.3737-44. 1996.

Canals, S., M. Beyerlein, *et al.* Electric stimulation fMRI of the perforant pathway to the rat hippocampus. Magnetic Resonance Imaging, v.26, n.7, Sep, p.978-986. 2008.

Carney, P. R., S. Myers, *et al.* Seizure prediction: methods. Epilepsy Behav, v.22 Suppl 1, Dec, p.S94-101. 2011.

Cassidy, R. M. e K. Gale. Mediodorsal thalamus plays a critical role in the development of limbic motor seizures. J Neurosci, v.18, n.21, Nov 1, p.9002-9. 1998.

Cobb, S. R., E. H. Buhl, *et al.* Synchronization of neuronal activity in hippocampus by individual GABAergic interneurons. Nature, v.378, n.6552, Nov 2, p.75-8. 1995.

Cota, V. R., C. Medeiros Dde, *et al.* Distinct patterns of electrical stimulation of the basolateral amygdala influence pentylenetetrazole seizure outcome. Epilepsy Behav, v.14 Suppl 1, Jan, p.26-31. 2009.

Dailey, J. W., M. E. Reith, *et al.* Carbamazepine increases extracellular serotonin concentration: lack of antagonism by tetrodotoxin or zero Ca2+. Eur J Pharmacol, v.328, n.2-3, Jun 11, p.153-62. 1997.

Davis, R., D. H. Peters, *et al.* Valproic acid. A reappraisal of its pharmacological properties and clinical efficacy in epilepsy. Drugs, v.47, n.2, Feb, p.332-72. 1994.

Delamont, R. S., P. O. Julu, *et al.* Changes in a measure of cardiac vagal activity before and after epileptic seizures. Epilepsy Res, v.35, n.2, Jun, p.87-94. 1999.

Dong, H. W., G. D. Petrovich, *et al.* Topography of projections from amygdala to bed nuclei of the stria terminalis. Brain Res Brain Res Rev, v.38, n.1-2, Dec, p.192-246. 2001.

Dragunow, M. e R. Faull. The use of c-fos as a metabolic marker in neuronal pathway tracing. J Neurosci Methods, v.29, n.3, Sep, p.261-5. 1989.

Eells, J. B., R. W. Clough, *et al.* Comparative fos immunoreactivity in the brain after forebrain, brainstem, or combined seizures induced by electroshock, pentylenetetrazol, focally induced and audiogenic seizures in rats. Neuroscience, v.123, n.1, p.279-92. 2004.

Engel, J., Jr. Introduction to temporal lobe epilepsy. Epilepsy Res, v.26, n.1, Dec, p.141-50. 1996.

Esteller, R., J. Echauz, *et al.* Continuous energy variation during the seizure cycle: towards an on-line accumulated energy. Clinical Neurophysiology, v.116, n.3, Mar, p.517-526. 2005.

Fisher, R., V. Salanova, *et al.* Electrical stimulation of the anterior nucleus of thalamus for treatment of refractory epilepsy. Epilepsia, Mar 17. 2010.

Fisher, R. S., W. Van Emde Boas, *et al.* Epileptic seizures and epilepsy: definitions proposed by the International League Against Epilepsy (ILAE) and the International Bureau for Epilepsy (IBE). Epilepsia, v.46, n.4, Apr, p.470-2. 2005.

Fonseca, C. S., I. D. Gusmao, *et al.* Object recognition memory and temporal lobe activation after delayed estrogen replacement therapy. Neurobiol Learn Mem, Jan 5. 2012.

Freestone, D. R., L. Kuhlmann, *et al.* Electrical probing of cortical excitability in patients with epilepsy. Epilepsy & Behavior, v.22, Dec, p.S110-S118. 2011.

Fridley, J., J. G. Thomas, *et al.* Brain stimulation for the treatment of epilepsy. Neurosurg Focus, v.32, n.3, Mar, p.E13. 2012.

Fritschy, J. M. Epilepsy, E/I Balance and GABA(A) Receptor Plasticity. Front Mol Neurosci, v.1, p.5. 2008.

Gallagher, M. e P. C. Holland. The amygdala complex: multiple roles in associative learning and attention. Proc Natl Acad Sci U S A, v.91, n.25, Dec 6, p.11771-6. 1994.

Gauriau, C. e J. F. Bernard. Pain pathways and parabrachial circuits in the rat. Exp Physiol, v.87, n.2, Mar, p.251-8. 2002.

Gotman, J. A few thoughts on "What is a seizure?" Epilepsy Behav, v.22 Suppl 1, Dec, p.S2-3. 2011.

Grasse, D. W., S. Karunakaran, *et al.* Neuronal synchrony and the transition to spontaneous seizures. Exp Neurol, v.248, Oct, p.72-84. 2013.

Gwinn, R. P. e D. D. Spencer. Fighting fire with fire: brain stimulation for the treatment of epilepsy. Clinical Neuroscience Research, v.4, n.1-2, p.95-105. 2004.

Halpern, C. H., U. Samadani, *et al.* Deep brain stimulation for epilepsy. Neurotherapeutics, v.5, n.1, Jan, p.59-67. 2008.

Hamann, S. Cognitive and neural mechanisms of emotional memory. Trends Cogn Sci, v.5, n.9, Sep 1, p.394-400. 2001.

Harrison, M. A., M. G. Frei, *et al.* Accumulated energy revisited. Clin Neurophysiol, v.116, n.3, Mar, p.527-31. 2005.

Hebb, D. O. The organization of behaviour : a neuropsychological theory. [S.l.]: Chapman and Hall. 1949

Jankowski, M. M., K. C. Ronnqvist, *et al.* The anterior thalamus provides a subcortical circuit supporting memory and spatial navigation. Front Syst Neurosci, v.7, p.45. 2013.

Jiruska, P., M. De Curtis, *et al.* Synchronization and desynchronization in epilepsy: controversies and hypotheses. Journal of Physiology-London, v.591, n.4, Feb, p.787-797. 2013.

Johnston, D. e T. H. Brown. The synaptic nature of the paroxysmal depolarizing shift in hippocampal neurons. Ann Neurol, v.16 Suppl, p.S65-71. 1984.

Kalitzin, S. N., D. N. Velis, *et al.* Stimulation-based anticipation and control of state transitions in the epileptic brain. Epilepsy & Behavior, v.17, n.3, Mar, p.310-323. 2010.

Kaneko, S., M. Okada, *et al.* Carbamazepine and zonisamide increase extracellular dopamine and serotonin levels in vivo, and carbamazepine does not antagonize adenosine effect in vitro: mechanisms of blockade of seizure spread. Jpn J Psychiatry Neurol, v.47, n.2, Jun, p.371-3. 1993.

Kerem, D. H. e A. B. Geva. Forecasting epilepsy from the heart rate signal. Med Biol Eng Comput, v.43, n.2, Mar, p.230-9. 2005.

Kopell, N., G. B. Ermentrout, *et al.* Gamma rhythms and beta rhythms have different synchronization properties. Proc Natl Acad Sci U S A, v.97, n.4, Feb 15, p.1867-72. 2000.

Kudela, P., P. J. Franaszczuk, *et al.* Changing excitation and inhibition in simulated neural networks: effects on induced bursting behavior. Biol Cybern, v.88, n.4, Apr, p.276-85. 2003.

Kuga, N., T. Sasaki, *et al.* Large-Scale Calcium Waves Traveling through Astrocytic Networks In Vivo. Journal of Neuroscience, v.31, n.7, Feb 16, p.2607-2614. 2011.

Le Van Quyen, M., J. Martinerie, *et al.* Characterizing neurodynamic changes before seizures. J Clin Neurophysiol, v.18, n.3, May, p.191-208. 2001.

Ledoux, J. The emotional brain, fear, and the amygdala. Cell Mol Neurobiol, v.23, n.4-5, Oct, p.727-38. 2003.

Ledoux, J. E. Emotion circuits in the brain. Annu Rev Neurosci, v.23, p.155-84. 2000.

Litt, B. e J. Echauz. Prediction of epileptic seizures. Lancet Neurol, v.1, n.1, May, p.22-30. 2002.

Litt, B., R. Esteller, *et al.* Epileptic seizures may begin hours in advance of clinical onset: a report of five patients. Neuron, v.30, n.1, Apr, p.51-64. 2001.

Lopes Da Silva, F., W. Blanes, *et al.* Epilepsies as dynamical diseases of brain systems: basic models of the transition between normal and epileptic activity. Epilepsia, v.44 Suppl 12, p.72-83. 2003.

Lopes Da Silva, F. H. e G. F. Harding. Transition to seizure in photosensitive epilepsy. Epilepsy Res, v.97, n.3, Dec, p.278-82. 2011.

Loscher, W. Critical review of current animal models of seizures and epilepsy used in the discovery and development of new antiepileptic drugs. Seizure, v.20, n.5, Jun, p.359-68. 2011.

Loscher, W., C. P. Fassbender, *et al.* The role of technical, biological and pharmacological factors in the laboratory evaluation of anticonvulsant drugs. II. Maximal electroshock seizure models. Epilepsy Res, v.8, n.2, Mar, p.79-94. 1991.

Lothman, E. W., D. A. Rempe, *et al.* Changes in excitatory neurotransmission in the CA1 region and dentate gyrus in a chronic model of temporal lobe epilepsy. J Neurophysiol, v.74, n.2, Aug, p.841-8. 1995.

Mangan, P. S., D. A. Rempe, *et al.* Changes in inhibitory neurotransmission in the CA1 region and dentate gyrus in a chronic model of temporal lobe epilepsy. J Neurophysiol, v.74, n.2, Aug, p.829-40. 1995.

Mcdonald, A. J. Topographical organization of amygdaloid projections to the caudatoputamen, nucleus accumbens, and related striatal-like areas of the rat brain. Neuroscience, v.44, n.1, p.15-33. 1991.

Mcdonald, A. J. Cortical pathways to the mammalian amygdala. Prog Neurobiol, v.55, n.3, Jun, p.257-332. 1998.

Mcgaugh, J. L. Memory consolidation and the amygdala: a systems perspective. Trends Neurosci, v.25, n.9, Sep, p.456. 2002.

Mcnamara, J. O. Cellular and molecular basis of epilepsy. J Neurosci, v.14, n.6, Jun, p.3413-25. 1994.

Medeiros, D. D., V. R. Cota, *et al.* Anatomically dependent anticonvulsant properties of temporally-coded electrical stimulation. Epilepsy & Behavior, v.23, n.3, Mar, p.294-297. 2012.

Mesquita, M. B. S., D. D. Medeiros, *et al.* Distinct temporal patterns of electrical stimulation influence neural recruitment during PTZ infusion: An fMRI study. Progress in Biophysics & Molecular Biology, v.105, n.1-2, Mar, p.109-118. 2011.

Meurs, A., R. Clinckers, *et al.* Seizure activity and changes in hippocampal extracellular glutamate, GABA, dopamine and serotonin. Epilepsy Res, v.78, n.1, Jan, p.50-9. 2008.

Moga, M. M., H. Herbert, *et al.* Organization of cortical, basal forebrain, and hypothalamic afferents to the parabrachial nucleus in the rat. J Comp Neurol, v.295, n.4, May 22, p.624-61. 1990.

Morel, A., M. Magnin, *et al.* Multiarchitectonic and stereotactic atlas of the human thalamus. J Comp Neurol, v.387, n.4, Nov 3, p.588-630. 1997.

Mormann, F., R. G. Andrzejak, *et al.* Seizure prediction: the long and winding road. Brain, v.130, n.Pt 2, Feb, p.314-33. 2007.

Mormann, F., T. Kreuz, *et al.* Epileptic seizures are preceded by a decrease in synchronization. Epilepsy Res, v.53, n.3, Mar, p.173-85. 2003.

Morrell, M. J. Responsive cortical stimulation for the treatment of medically intractable partial epilepsy. Neurology, v.77, n.13, Sep 27, p.1295-304. 2011.

Nayak, D. *et al*. Can single pulse electrical stimulation provoke responses similar to spontaneous interictal epileptiform discharges? Clinical Neurophysiology, 2014

Pare, D., D. R. Collins, *et al.* Amygdala oscillations and the consolidation of emotional memories. Trends Cogn Sci, v.6, n.7, Jul 1, p.306-314. 2002.

Penfield, W., H. H. Jasper, *et al.* Epilepsy and the Functional Anatomy of the Human Brain. By W. Penfield ... and Herbert Jasper ... Chapter XIV by Francis McNaughton, etc. [With plates and a bibliography.]. London; printed in U.S.A.: J. & A. Churchill. 1954

Petrovich, G. D., N. S. Canteras, *et al.* Combinatorial amygdalar inputs to hippocampal domains and hypothalamic behavior systems. Brain Res Brain Res Rev, v.38, n.1-2, Dec, p.247-89. 2001.

Pitkanen, A., V. Savander, *et al.* Organization of intra-amygdaloid circuitries in the rat: an emerging framework for understanding functions of the amygdala. Trends Neurosci, v.20, n.11, Nov, p.517-23. 1997.

Rho, J. M. e R. Sankar. The pharmacologic basis of antiepileptic drug action. Epilepsia, v.40, n.11, Nov, p.1471-1483. 1999.

Rizvi, T. A., M. Ennis, *et al.* Connections between the central nucleus of the amygdala and the midbrain periaqueductal gray: Topography and reciprocity. The Journal of Comparative Neurology, v.303, n.1, p.121-131. 1991.

Rogan, M. T. e J. E. Ledoux. Emotion: systems, cells, synaptic plasticity. Cell, v.85, n.4, May 17, p.469-75. 1996.

Sah, P., E. S. Faber, *et al.* The amygdaloid complex: anatomy and physiology. Physiol Rev, v.83, n.3, Jul, p.803-34. 2003.

Scharfman, H. E. Epilepsy as an example of neural plasticity. Neuroscientist, v.8, n.2, Apr, p.154-173. 2002.

Scharfman, H. E. The neurobiology of epilepsy. Curr Neurol Neurosci Rep, v.7, n.4, Jul, p.348-54. 2007.

Schulze-Bonhage, A., F. Sales, *et al.* Views of patients with epilepsy on seizure prediction devices. Epilepsy Behav, v.18, n.4, Aug, p.388-96. 2010.

Silva Brum, L. F. e E. Elisabetsky. Antiepileptogenic properties of phenobarbital: behavior and neurochemical analysis. Pharmacol Biochem Behav, v.67, n.3, Nov, p.411-6. 2000.

Singer, W. Neuronal synchrony: a versatile code for the definition of relations? Neuron, v.24, n.1, Sep, p.49-65, 111-25. 1999.

Steriade, M. Sleep, epilepsy and thalamic reticular inhibitory neurons. Trends in Neurosciences, v.28, n.6, Jun, p.317-324. 2005.

Takebayashi, S., K. Hashizume, *et al.* Anti-convulsant effect of electrical stimulation and lesioning of the anterior thalamic nucleus on kainic acid-induced focal limbic seizure in rats. Epilepsy Res, v.74, n.2-3, May, p.163-70. 2007.

Tehovnik, E. J., A. S. Tolias, *et al.* Direct and indirect activation of cortical neurons by electrical microstimulation. Journal of Neurophysiology, v.96, n.2, Aug, p.512-521. 2006.

Traub, R. D., H. Michelson-Law, *et al.* Gap junctions, fast oscillations and the initiation of seizures. Adv Exp Med Biol, v.548, p.110-22. 2004.

Tunnicliff, G. Basis of the antiseizure action of phenytoin. Gen Pharmacol, v.27, n.7, Oct, p.1091-7. 1996.

Uhlhaas, P. J. e W. Singer. Neural synchrony in brain disorders: relevance for cognitive dysfunctions and pathophysiology. Neuron, v.52, n.1, Oct 5, p.155-68. 2006.

Valentin, A., G. Alarcon, *et al.* Single-pulse electrical stimulation identifies epileptogenic frontal cortex in the human brain. Neurology, v.65, n.3, Aug 9, p.426-35. 2005.

Valentin, A., G. Alarcon, *et al._*. Single pulse electrical stimulation for identification of structural abnormalities and prediction of seizure outcome after epilepsy surgery: a prospective study. Lancet Neurol, v.4, n.11, Nov, p.718-26. 2005.

Van Der Kooy, D., L. Y. Koda, *et al.* The organization of projections from the cortex, amygdala, and hypothalamus to the nucleus of the solitary tract in rat. J Comp Neurol, v.224, n.1, Mar 20, p.1-24. 1984.

Van Groen, T., I. Kadish, *et al.* Efferent connections of the anteromedial nucleus of the thalamus of the rat. Brain Res Brain Res Rev, v.30, n.1, Jul, p.1-26. 1999.

Veening, J. G., L. W. Swanson, *et al.* The organization of projections from the central nucleus of the amygdala to brainstem sites involved in central autonomic regulation: a

combined retrograde transport-immunohistochemical study. Brain Res, v.303, n.2, Jun 15, p.337-57. 1984.

Viglione, S. S. e G. O. Walsh. Proceedings: Epileptic seizure prediction. Electroencephalogr Clin Neurophysiol, v.39, n.4, Oct, p.435-6. 1975.

Weinand, M. E., L. P. Carter, *et al.* Cerebral blood flow and temporal lobe epileptogenicity. J Neurosurg, v.86, n.2, Feb, p.226-32. 1997.

Wichmann, T. e M. R. Delong. Deep brain stimulation for neurologic and neuropsychiatric disorders. Neuron, v.52, n.1, Oct 5, p.197-204. 2006.

Wiegell, M. R., D. S. Tuch, *et al.* Automatic segmentation of thalamic nuclei from diffusion tensor magnetic resonance imaging. Neuroimage, v.19, n.2 Pt 1, Jun, p.391-401. 2003.

Yan, Q. S., P. K. Mishra, *et al.* Evidence that carbamazepine and antiepilepsirine may produce a component of their anticonvulsant effects by activating serotonergic neurons in genetically epilepsy-prone rats. J Pharmacol Exp Ther, v.261, n.2, May, p.652-9. 1992.

7.0 Anexos

UNIVERSIDADE FEDERAL DE MINAS GERAIS
COMITÊ DE ÉTICA EM EXPERIMENTAÇÃO ANIMAL
- C E T E A -

CERTIFICADO

Certificamos que o **Protocolo nº 150/2006,** relativo ao projeto intitulado "***Redes neurais hiperexcitáveis e hipersincrônicas em modelos animais de epilepsia: aspectos da dinâmica temporal de recrutamento neural na epileptogênese***", que tem como responsável **Márcio Flávio Dutra Moraes** , está de acordo com os Princípios Éticos da Experimentação Animal, adotados pelo ***Comitê de Ética em Experimentação Animal*** **(CETEA/UFMG),** tendo sido aprovado na reunião de **28/ 02/2007.**

Este certificado expira-se em **28/ 02 / 2012.**

CERTIFICATE

We hereby certify that the **Protocol nº 150/2006,** related to the project entitled "***Hyperexcitable and hypersynchronic neural networks in animal models of epilepsy: temporal dynamics aspects of neuronal recruitment in epileptogenesys***", under the supervision of **Márcio Flávio Dutra Moraes,** is in agreement with the Ethical Principles in Animal Experimentation, adopted by the ***Ethics Committee in Animal Experimentation*** **(CETEA/UFMG),** and was approved in **February 28, 2007.**

This certificate expires in **February 28, 2012.**

Belo Horizonte, 28 de Fevereiro de 2007.

Prof. Humberto Pereira Oliveira
Presidente do CETEA/UFMG

Universidade Federal de Minas Gerais
Avenida Antônio Carlos, 6627 – Campus Pampulha
Unidade Administrativa II – 2º Andar, Sala 2005
31270-901 - Belo Horizonte, MG - Brasil
Telefone: (31) 3499-4516 – Fax: (31) 3499-4516
www.ufmg.br/bioetica/cetea - cetea@prpq.ufmg.br

(Mod.Cert. v1.0)

Artigo Resultante desta tese

ARTICLE IN PRESS

Brain Stimulation xxx (2013) 1–9

Contents lists available at ScienceDirect

Brain Stimulation

journal homepage: www.brainstimjrnl.com

Original Research

Temporal Rearrangement of Pre-ictal PTZ Induced Spike Discharges by Low Frequency Electrical Stimulation to the Amygdaloid Complex

Daniel Castro Medeiros [a,b], Luciano Borges Oliveira [c], Flávio Afonso Gonçalves Mourão [a], Cristiane Perácio Bastos [a], Norberto Garcia Cairasco [d], Grace Schenatto Pereira [a], Eduardo Mazoni Andrade Marçal Mendes [b,c], Márcio Flávio Dutra Moraes [a,b,*]

[a] Núcleo de Neurociências (NNC), Departamento de Fisiologia e Biofísica, Instituto de Ciências Biológicas – Universidade Federal de Minas Gerais, Belo Horizonte, Minas Gerais CEP 31270-901, Brasil
[b] Centro de Tecnologia e Pesquisa em Magneto-Ressonância, Escola de Engenharia, Universidade Federal de Minas Gerais, Belo Horizonte, Minas Gerais CEP 31270-901, Brasil
[c] Departamento de Engenharia Eletrônica – Escola de Engenharia – Universidade Federal de Minas Gerais, Belo Horizonte, Minas Gerais CEP 31270-901, Brasil
[d] Departamento de Fisiologia, Faculdade de Medicina de Ribeirão Preto, Universidade de São Paulo, Ribeirao Preto, São Paulo CEP 14049-900, Brasil

ARTICLE INFO

Article history:
Received 12 July 2013
Received in revised form 7 November 2013
Accepted 17 November 2013
Available online xxx

Keywords:
Epilepsy
Pentylenetetrazole
Low frequency electric stimulation
Phase-locking
Seizure prediction

ABSTRACT

Background: Epilepsy is a common neurological disease affecting over 40 million people worldwide. The foremost important challenge of epileptologists has been to control and predict the recurrent and spontaneous seizures of epileptic patients. The application of low frequency electrical stimulation (LFS) in deep brain structures has shown promising results in seizure control. However, the use of LFS as a probing strategy for seizure prediction, thus contributing to a closed loop solution, is still poorly explored.
Objective: To improve seizure prediction by producing gradually increasing phase-locked pre-ictal electrographical responses, due to the short-term plastic changes in epileptogenic neural networks, thus behaving as a "programmed" surrogate marker.
Methods: Urethane anesthetized rats were divided into 3 groups: the PTZ-noES group was injected with pentylenetetrazole (PTZ 4 mg/ml/min flow rate) i.v. without electrical stimulation (ES); the ES-noPTZ group received ES (0.5 Hz, 0.1 ms pulse width and 0.6 mA) to the amygdaloid complex and the PTZ + ES group received simultaneously i.v. PTZ infusion and ES. After each condition, electrographical parameters and c-Fos expression of regions of interest were evaluated.
Results: Although the PTZ + ES group had no evident change in the sustained electrographic seizure onset, duration and/or frequency spectrum; c-Fos labeling showed a different expression pattern when compared to the PTZ-noES and ES-noPTZ. Also, PTZ + ES formed a gradually increasing evoked potential; confirming the strong coupling of reverberant neural networks induced by ES – phase locked to stimuli.
Conclusion: ES induces a detectable temporal rearrangement of pre-ictal activity, which has suggestive applicability to seizure prediction.

Introduction

Epilepsy is one of the most common neurological diseases worldwide [1]. Although most epileptic conditions are satisfactorily controlled by medication, about 30% of the patients are resistant to pharmacological treatment [2]. The deep-brain-electrical stimulation (DBS) is an emerging therapeutic alternative to an otherwise untreatable medical scenario. It has been hypothesized that DBS seizure control is achieved by inactivating ictogenic networks, using high-frequency stimulation, or by activating inhibitory networks, through low-frequency stimulation (LFS) [3]. If periodic LFS is applied to ictogenic areas, it may facilitate seizure occurrence [4].

Previous research has shown that 4 Hz periodic pulses applied to the amygdaloid complex (AMY) of pentylenetetrazole (PTZ) treated animals increases the susceptibility to seizure [4] and enhances neural activity in limbic system structures [5]. Adding to the complexity of the phenomena, the fixed time interval between

Conflict of interest: The authors declare no competing financial interests.

* Corresponding author. Núcleo de Neurociências, Departamento de Fisiologia e Biofísica Instituto de Ciências Biológicas, Universidade Federal de Minas Gerais. Av. Antônio Carlos, 6627, CEP 31270-901, Campus Pampulha, Belo Horizonte, MG, Brazil. Tel.: +55 31 3409 2930; fax: +55 31 3409 2924.
E-mail addresses: mfdm@icb.ufmg.br, marcionnc@me.com (M.F.D. Moraes).

1935-861X/$ – see front matter © 2013 Elsevier Inc. All rights reserved.
http://dx.doi.org/10.1016/j.brs.2013.11.005

electrical stimulation (ES) pulses is determinant to produce the pro-convulsive effect. Conversely, a non-periodic ES applied to the AMY, with the same 4 pulses-per-second paradigm, induces an anti-convulsant effect [4,5]. One possible explanation is that non-periodic ES delays seizure outcome by interfering with the excessive coupling between oscillators. In contrast, periodic ES promotes the coupling of endogenous neural oscillators, leading to abnormal neural synchronization and seizure. This hypothesis is quite consonant with the concept of several microseizure neural circuits being abnormally connected to form a full-scale epileptic event [6]. The present work explores the abnormal coupling (i.e. hypersynchronicity) within a different perspective: seizure prediction.

It is our understanding that if ES is to be applied to seizure prediction at least a couple of guidelines must be convened: 1) The ES may not promote or induce seizures in non-epileptogenic and/or epileptogenic neural networks and 2) The probing of epileptogenic circuits must improve the detection of abnormal coupling when compared to ES-free seizure progression.

Although the use of the PTZ model is not ideal for studying seizure prediction, its choice is quite adequate for evaluating gradual changes previous to the sustained epileptiform onset; therefore, much better suited for testing our hypothesis. Also, urethane anesthetized rats were used in order to lower overall brain excitability and the frequency of endogenous pre-ictal isolated discharges. The occurrence of pre-ictal discharges in the PTZ-noES group was quantified in terms of its mean overall frequency to determine an adequate ES periodic stimulation. In sequence, ES-noPTZ, PTZ-noES and PTZ + ES groups were evaluated by means of electrographical parameters and c-Fos expression. The results show that ES induces a phase-locked coupling of reverberant neural networks during the pre-ictal period, without evident change to epileptiform activity onset (sustained spike discharges), duration of burst activity and frequency spectrum during the electrographic seizure. In summary, ES promotes a detectable temporal rearrangement of pre-ictal activity, which has suggestive applicability to seizure prediction.

Material and methods

Animals

Male Wistar rats ($n = 32$, weighing 300–320 g), supplied by the CEBIO-ICB-UFMG vivarium, were housed under controlled environmental conditions (22 ± 1 °C), with a 12:12-h light–dark cycle and free access to food and water. All experiments were executed under the Protocol License n° 150/06 approved by the University's Ethical Committee for Animal Experimentation (CETEA – UFMG). The CETEA directives are in compliance to NIH guidelines for the care and use of animals in research.

Experimental procedure

Experimental groups

Rats were divided into 2 main groups: EEG ($n = 18$) and c-Fos ($n = 18$) groups. Both were further divided into 3 sub-groups: PTZ infusion (PTZ with no ES, $n = 6$ – PTZ-noES), electrically stimulated (ES with noPTZ, $n = 6$ – ES-noPTZ) and PTZ infusion associated with electric stimulation (PTZ + ES, $n = 6$). The EEG recording, the i.v. PTZ infusion and the ES started simultaneously for all animals.

Surgical procedures

All rats were anesthetized (urethane 140 mg/ml; 10 ml/kg, i.p.) and positioned in a stereotaxic frame (Stoelting Co., Wood Dale, IL, USA). Bipolar electrodes (2 mm separation dipole), made of a twisted pair of stainless-steel teflon-coated wires (Model 791400, A-M Systems Inc., Carlsborg, WA, USA), were surgically implanted in the right amygdala (AMY - AP: −2.8 referenced from the bregma, ML: −5.0, DV: −7.2) [7]. In addition, surface electrode micro-screws were positioned over both parietal cortices (AP: +1.0 referenced from the lambda, ML: ±2.0) for EEG recordings. The electrodes were then soldered to a phone connector (RJ 11–6 pins), which in turn was fixed to the rat's skull with dental acrylic cement.

PTZ infusion and ES

Immediately after surgery, the medial tail vein was cannulated (BD Angiocath Catheter I.V. – $24_{GA} \times 0.75_{IN} - 0.7 \times 19$ mm) for infusion of PTZ (40 mg/ml – Sigma–Aldrich, diluted in saline 0.9%) or saline (ES-noPTZ group). The infusion pump (KDS100 – KD Scientific®) was set at 4 mg/ml/min flow rate. The PTZ infusion was interrupted at the beginning of the electroencephalographic seizure for EEG groups and at half necessary PTZ dose to evoke seizure for the c-Fos group (150 g/kg or 790 ± 30 s). For the ES-noPTZ and PTZ + ES groups, electrical stimuli consisted of monophasic square pulse (0.1 ms pulse width and 0.6 mA intensity) delivered at 0.5 Hz by an isolated constant current stimulator (Digitimer® DS3 Constant Current Stimulator) to the AMY bipolar electrodes. The use of monophasic instead of biphasic ES pulses in this work was not a relevant issue for the experimental design. One possible consideration would be that monophasic pulses might induce greater tissue damage by electrolysis. However, not only the pulse duration used was very short (100 μs) but also the repetition rate was extremely low (0.5 Hz). In fact, according to Merrill et al. [8] our K factor ($2 \log Q - \log A$) would be 0.77 ($K < 2$ @50 Hz is considered safe practice; $Q = 0.06$ μC/phase and $A = 0.000613$ cm^2), posing no harm to surrounding tissue due to ES. In addition, the total duration of ES was also short (approximately 25 min), when compared to other reported studies [9]. The widespread efferent connections from AMY to sensory cortex [10], hippocampus [11], hypothalamus [12] and thalamus [13] were the main reason for choosing this area as the ES target.

Electrophysiology

The EEG signal from both parietal cortices were amplified (5000 × gain) and filtered (1 Hz High pass, 500 Hz Low pass) by a signal conditioner (Aisha4 – Kananda® Ltd). Data were sampled at 1 kHz and recorded in a computer hard disk for offline analyses. The EEG group was recorded for over 1 min after PTZ infusion was interrupted; while the c-Fos group was monitored for another 90 min to guarantee no electrographic seizure occurred. Immediately after EEG recording was halted, anesthetized animals were injected with a urethane overdose (1.4 mg/kg) and immediately underwent transcardial perfusion with 0.01 M phosphate buffer saline (PBS), followed by 4% paraformaldehyde (PFA) in PBS. The brains were removed and embedded in the perfusion solution. At this point, the brains for the EEG and c-Fos group diverged in the way they were processed.

Brain tissue preparation

The brains from EEG group rats were removed, sliced (Cryostat 300 – ANCAP® Ltd), and stained with neutral red (2%) for histological identification of electrode position. For c-Fos immunohistochemistry, brains were transfer to a solution of 30% sucrose in PBS and maintained at 4 °C for three days. Brains were frozen in 99% isopentane, at − 45 °C and cryo-sectioned (rostro-caudal extent – Cryostat 300 – ANCAP® Ltd) at 40 μm thickness. Slices were stored at −20 °C in PBSAF [PBS, 20% sucrose, 15% ethylene glycol, 0.05% NaN_3]. The sections were washed three times for 6 min (3 × 6 min) in 0.01 M Trizma base saline buffer (TBS) before being placed in hydrogen peroxide (3% H_2O_2/TBS) for 10 min. Next, the sections were washed 3 × 6 min in TBS followed by 2 h of incubation in a

blocking solution [3% normal goat serum (NGS) in TBS/0.3% Triton X-100]. The primary antibody against c-Fos (Santa Cruz, sc-52), diluted 1:5000, was added and incubated overnight at room temperature. Next day, the sections were washed 3 × 6 min in TBS with 0.3% Triton X-100 and incubated with the secondary antibody (1:1000, biotinylated anti-IgG antibody goat antirabbit; Vector Laboratories) for 2 h at room temperature. After, the sections were washed 3 × 6 min in TBS with 0.3% Triton X-100 and incubated with avidin–biotin horseradish peroxidase complex (1:500 in TBS with 0.3% Triton X-100; Vector Laboratories) during 1 h at room temperature. Subsequently, the sections were washed 3 × 6 min in TBS and 3 × 6 min in 174 mM acetate buffer. The sections were developed with a solution containing 0.2 mg/ml diaminobenzidine (DAB), 25 mg/ml nickel sulfate and 0.0025% H_2O_2 in acetate buffer for 15 min. Finally, the sections were washed 3 × 6 min in 174 mM acetate buffer and mounted on gelatin-coated slides, air-dried, dehydrated in xylene, and embedded in Entellan® [14].

Data analysis

c-Fos expression

Immunostaining images of coronal slices (from Bregma −2.5 to −3.3) were obtained using an AxioImager M2 (Zeiss) microscope, Plan-Apochromat ×5 objective. Photomicrographs of stained brain sections were taken with a digital camera (AxioCam MRm, Zeiss) through the software Carl Zeiss Axiovision 4.8 (1388 × 1420 pixels image; 1.02 μm × 1.02 μm pixel size). The TIFF-format micrographs were analyzed using ImageJ software (http://rsbweb.nih.gov/ij/). The ImageJ threshold tool was used to construct a mask separating stained cells from the background (same pixel threshold level was held for all images analyzed). An identified object was only counted as a cell if the overall diameter was within 5–100 μm. Total counts were made within Regions of Interest (ROIs), depicted in the schematic diagram of the rat brain atlas shown in Fig. 3 – right inset, as follows (contralateral to ES electrode placement): cortex, amygdaloid complex, thalamus and hipotalamus. The mechanical lesions of areas ipsi-lateral to the ES electrode placement (i.e. cortex and amygdaloid complex) rendered the analysis inconclusive and therefore were removed from the results (data not shown). In order to provide proper inter-ROI comparison; the total number of cell counts was normalized by the area of each ROI in mm^2 (Fig. 3 – bottom bar graphs). Due to the high density of cells within the hippocampus ROI (see Fig. 3 brain atlas diagram inset), with continuous overlapping of cell bodies, the analysis of this region was conducted by optical-densitometry (OD). The hippocampus ROI-OD gray scale average was normalized against background (i.e. corpus callosum OD), see Fig. 3.

Epileptiform EEG activity (onset, duration and spectral analysis)

The latency from the beginning of the PTZ infusion and the emerging of typical polyspike epileptiform discharge on the EEG recording was used as the seizure onset value. The duration of polyspike epileptiform discharge activity was also determined (seizure duration) in order to quantify seizure severity. The frequency spectrum of the ictal EEG activity of the PTZ-noES and PTZ + ES groups were calculated using a MATLAB® routine (fast Fourier transform – FFT) within the first 2 s after seizure onset.

Pre-ictal EEG analyses

Time zero (T_{zero}) was set at the beginning of the typical polyspike epileptiform discharge pattern characteristic of PTZ induced seizures (seizure onset – Fig. 1A). The subsequent analyses were conducted within the 600 s time window before EEG seizure onset (T_{zero}-600 s–T_{zero}), using MATLAB® routines (The MathWorks) and functions. For both groups injected with PTZ, a threshold voltage for pre-ictal discharge detection was set to be at 75% of the maximum amplitude of the last discharge immediately before seizure onset (inset of the Fig. 1B). An algorithm was design to detect every electrographical event that surpassed threshold and returned the time-stamp of all events detected. In order to determine the average pre-ictal discharge time interval of repetition in the PTZ-noES group, the time of occurrence of the (N + 1)th event was subtracted from the previous Nth event (time interval between pre-ictal discharges – TI-ID). This data was used to produce a histogram

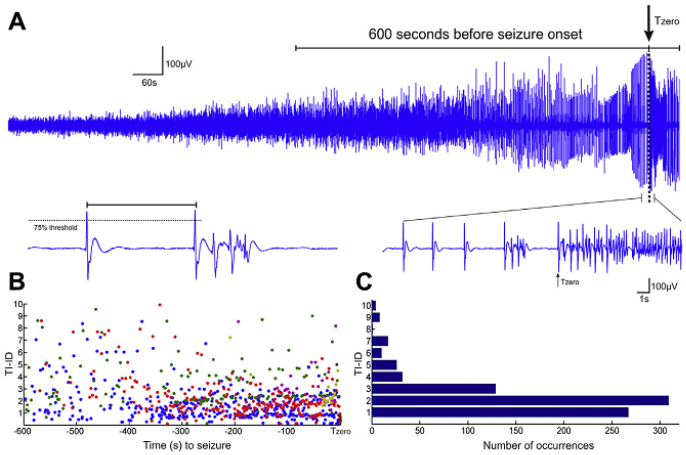

Figure 1. PTZ-noES pre-ictal electrographic activity. (A) Time segment of a typical electrographic recording from the PTZ-noES group. Only the 600 s time window preceding electrographic ictal activity onset (T_{zero} – black arrow) was used for analysis. Inset is a zoomed view depicting the transition between pre-ictal and epileptiform EEG. (B) Time-stamp of TI-ID (time interval between pre-ictal discharges). Each color represents one animal from the PTZ-noES group, with every dot representing the occurrence of a pre-ictal event. The pre-ictal event is defined as the spike activity exceeding 75% of the last pre-ictal discharge before seizure onset (inset of panel B). (C) TI-ID histogram from all animals of the PTZ-noES group (1 s bin interval). (For interpretation of the references to color in this figure legend, the reader is referred to the web version of this article.)

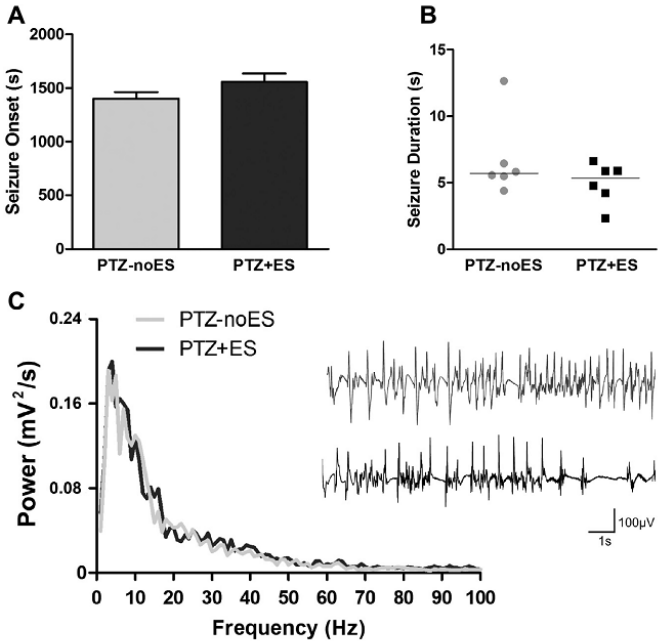

Figure 2. Electrographic seizure onset, duration and frequency spectrum of the PTZ-noES and PTZ + ES groups. (A) Latency (in seconds) from the beginning of the PTZ infusion to the onset of electrographic epileptiform discharges ($P = 0.1548$, mean ± SEM). (B) Duration of the polyspike epileptiform discharge activity ($P = 0.5887$, median ± (5/25) – (75/95) quartiles). (C) Frequency spectrum of the ictal discharge pattern for both groups ($P > 0.05$). The inset depicts a typical polyspike epileptiform discharge for an animal from each group (PTZ-noES and PTZ + ES).

of 1 s-bins (Fig. 1C). The ES frequency chosen for subsequent experiments was established at constant inter-stimuli intervals of 2 s (i.e. 0.5 Hz).

It is paramount to evaluate if the low frequency ES, in PTZ injected animals, did not significantly change the frequency of occurrence of pre-ictal discharge events. Thus, the 600 s analysis window was divided into 60 epochs (10 s window width) and the total number of pre-ictal discharge events quantified for each epoch (Fig. 4A).

For the purpose of evaluating phase synchronization to ES, the trigger signal from the ES was also recorded in a different channel of the A/D converter. Therefore, it was possible to trigger the electrographic response with the ES presentation, depicting EEG activity before (500 ms) and after (1500 ms) stimuli were applied (Fig. 6, left panel). Consequently, a sequence of 300 consecutives 2 s windows epochs (600 s EEG analyses) was used to evaluate the temporal rearrangement of the pre-ictal discharges. Nevertheless, the EEG energy (V^2) of each 2 s epochs was calculated and normalized by basal energy (E_0: EEG from the first 2 s epoch, −600 to −598 s), in order to show that ES did not significantly change the total energy of the signal – depicted in Fig. 4B. Evidence of temporal synchronization to stimuli is clear from the emergence of an evoked potential recorded from cortical leads (Fig. 4C). The normalized energy ratio (E_a/E_b: $E_b = -250$ to 0 ms and $E_a = 10–260$ ms) was quantified for every 2-s epoch for all three groups.

An algorithm was designed for quantifying to what degree the ES was driving pre-ictal spike activity. The EEG was separated into a series of 2 s window segments and the time, within each 2 s segment, at which the maximum peak (TMP – time maximum peak) occurred was used to produce a time-stamp of event occurrences. By subtracting the instant of occurrence of the $(N + 1)$th from the previous Nth event, an histogram varying from −2 s to +2 s (9 bins) was produced (Fig. 5C, D, E). It is important to highlight that a completely stochastic process would generate a Gaussian distribution, since every 2 s interval would have a random positioned correspondent maximum value (Fig. 5B). Furthermore, in order to observe the gradual "phase-locking" effect driven by ES, the EEG analysis interval was subdivided into 3 portions of 100 epochs each: −600 s to −400 s, −400 s to −200 s and −200 s to T_{zero}.

In order to further address the temporal synchronization of different pre-ictal discharge components with an external trigger (i.e. the ES), a semi-automatic pattern recognition algorithm was designed to track specific waveforms throughout the EEG recording. The algorithm recognizes similar waveforms, from a given template, and adjusts the template pattern through time, as the neural network evolves to seizure. The initial waveform templates were arbitrarily chosen from a portion of the EEG recording in which they were clearly identifiable. The algorithm consisted of dividing the EEG signal into 20 s time windows until the seizure onset. In each window, the complement of Pearson's correlation coefficient (1-corr) was computed between the wave pattern and all the waveforms of the following window as a measure of distance. The minimum was located and the waveforms below a certain threshold were chosen as similar. The average of the three more similar waves was then stored and used as the pattern for the next time window, then resulting in a progressive waveform to the seizure onset. For each animal (Fig. 6), the algorithm was applied in

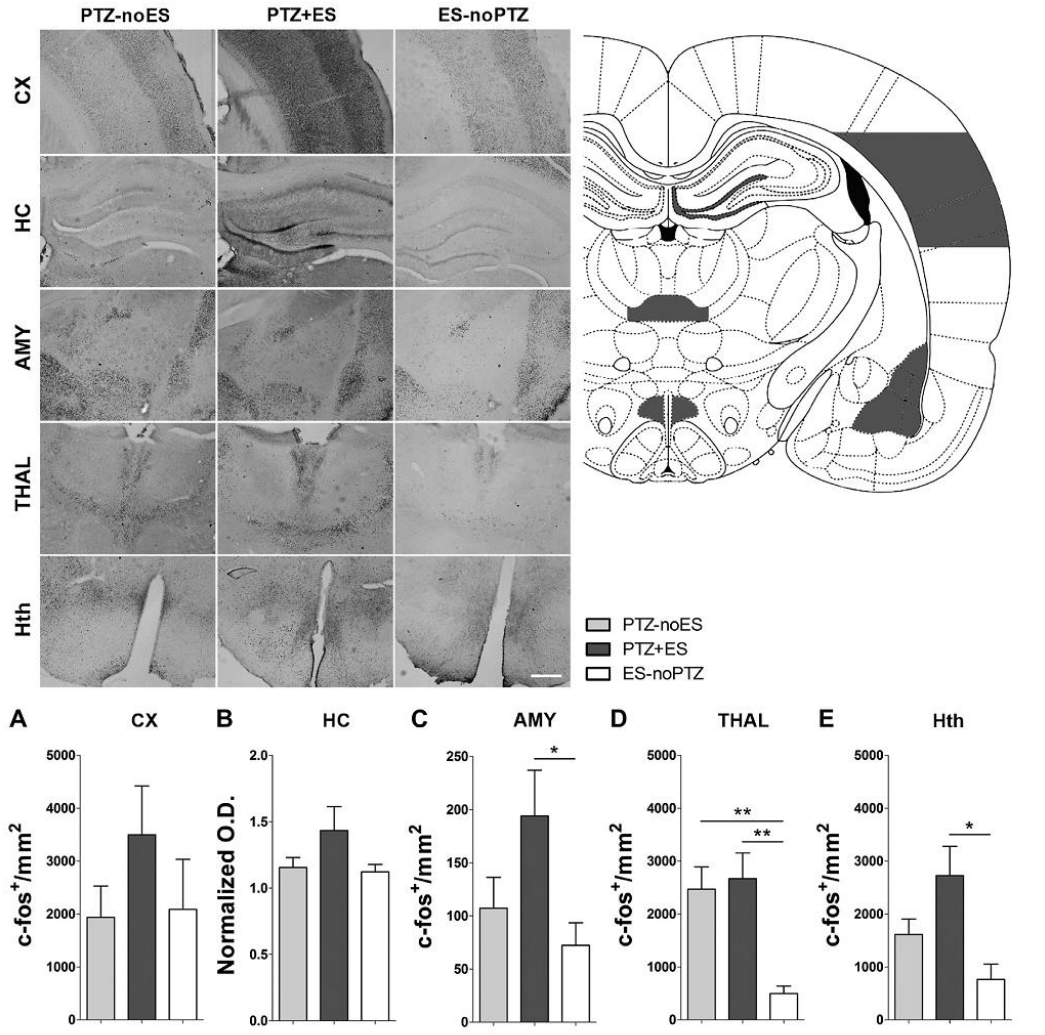

Figure 3. The c-Fos expression in brain slices. Panel to the left depicts typical c-Fos expression images for all regions of interest (ROIs) analyzed. ROIs: CX-cortex, HC-hippocampus, AMY-amygdala complex, THAL – thalamus, HTh – hypothalamus. Dark area images in a rat brain atlas schematic diagram demonstrate the ROIs analyzed. (A, C, D, E) Number of c-Fos labeled cells per unit of area (mm^2). (B) Normalized optical-densitometry. Scale bar 1 mm (*$P < 0.05$; **$P < 0.01$, mean ± SEM).

3 different waveforms (arbitrarily chosen as mentioned above) and the time of occurrence of each waveform was plot in a 2 s epochs window (synchronized with stimulus at 0 s) along the EEG analysis time frame (T_{zero}-600 s–T_{zero}).

Results

A typical EEG time series from a PTZ-noES group rat (600 s before seizure and 60 s after ictal activity onset) is shown in Fig. 1A; the inset depicts the transition between pre-ictal to ictal period. It should be noted that, despite of the anesthesia, the PTZ was able to lead the brain structures to a clear, easily recognizable, electrographic seizure. Fig. 1B presents the time interval between pre-ictal discharges (TI-ID time interval of interictal discharges) for the PTZ-noES group (each animal is represented by a specific color). A gradual organization of the TI-ID around 1–2 s can be observed. In order to determine the ES optimal presentation frequency, a histogram of all the TI-ID was made showing the 2-s time interval bin as highest incidence of occurrence (Fig. 1C).

The ES did not interfere on the latency for the seizure onset, on its duration or spectral energy distribution; no statistical difference was found between PTZ-noES and PTZ + ES groups as shown in Fig. 2A, B and C ($P = 0.1548$ unpaired t-student test, $P = 0.5887$ Mann Whitney test, $P > 0.05$ 2-way ANOVA Bonferroni post-hoc

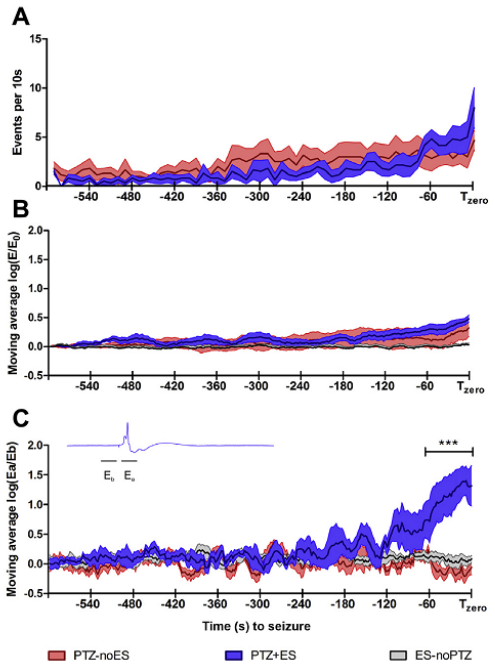

Figure 4. ES effect on the pre-ictal discharge events throughout the 600 s analysis window. (A) The 600 s was divided into 60 epochs (10 s each) and the total number of pre-ictal discharge events quantified for each epoch. (B) EEG normalized energy (E/E_0) from a 20 s moving average calculated for every 2 s. (C) EEG power ratio of intervals E_a/E_b (as shown in the inset) using the same moving average as B. (***$P < 0.001$, mean ± SEM).

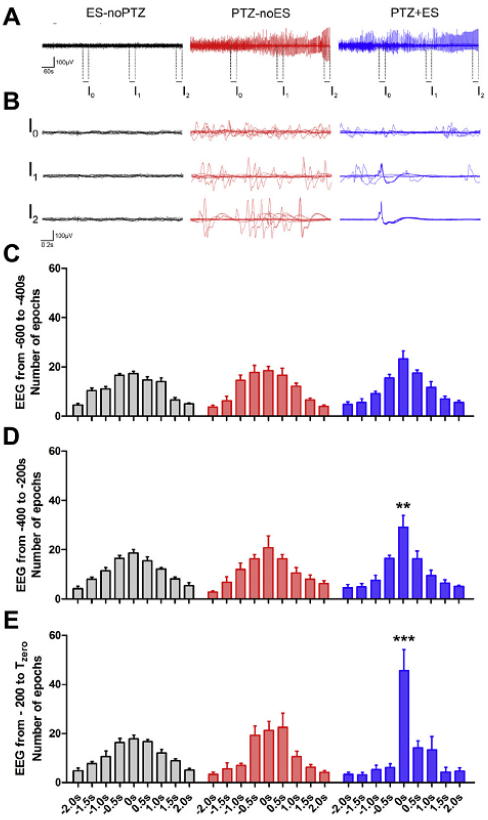

Figure 5. Phase-locking of pre-ictal electrographic activity. The colors represent the ES-noPTZ (black), PTZ-noES (red) and PTZ + ES (blue) groups. (A) EEG recordings (T_{zero}-600 s–T_{zero}) from a typical animal of each group. For each animal 3 intervals were selected I_0 (−420 to −400 s), I_1 (−220 to −200), I_2 (−20 to T_{zero}). (B) The selected intervals are shown as ten overlapped 2-s epochs triggered by ES (time window from −0.5 s to 1.5 s with reference to ES). (C, D, E) The 600-s time window preceding seizure onset (T_{zero}) was divided into 3 parts. Each third was subdivided into a series of 100 2-s-time windows. The maximum peak voltage of every 2-s epoch (TMP) was used to produce a time-stamp of occurrences. The graphics shows histograms varying from −2 s to +2 s (9 bins) produced by subtracting the TMP of the ($N + 1$)th from the previous Nth epoch (**$P < 0.01$; ***$P < 0.001$, mean ± SEM). (For interpretation of the references to color in this figure legend, the reader is referred to the web version of this article.)

test, respectively). Nevertheless, the ES was able to modify neural activity as shown by the c-Fos expression analyses. The PTZ + ES group demonstrated a different c-Fos expression pattern when compared to the PTZ-noES and ES-noPTZ (Fig. 3), statistically different from the latter for thalamus, amygdaloid complex, and hipotalamus (THAL $P < 0.001$, AMY and Hth $P < 0.05$, one way ANOVA Newman–Keuls multiple comparison post-hoc test). It is important to highlight that none of the animals from de c-Fos group had an identifiable electrographic seizure prior to brain tissue processing.

Pre-ictal discharge events throughout 600 s time window quantitative analyses are shown in Fig. 4. The low-frequency ES did not significant change the frequency of occurrence of pre-ictal discharge events (Fig. 4A – $P > 0.05$ 2-way ANOVA Bonferroni post-hoc test) or total energy of the signal (Fig. 4B – logarithm of normalized EEG – $P > 0.05$ 2-way ANOVA Bonferroni post-hoc test). Nevertheless, the logarithm of the ratio between EEG power after stimuli normalized by baseline energy for the PTZ + ES group is statistically higher compared with PTZ-noES ($P < 0.001$, 2-way ANOVA Bonferroni post-hoc test) and ES-noPTZ ($P < 0.001$, 2-way ANOVA Bonferroni post-hoc test) groups 80 s before seizure onset (Fig. 4C).

The Fig. 5 shows the three experimental groups represented by specific colors: ES-noPTZ (black), PTZ-noES (red) and PTZ + ES (blue). The upper traces depict typical EEG recordings from each group. It should be note the lack of large oscillations in representative EEG from the ES-noPTZ group, which obviously had no pre-ictal activity (Fig. 5A). Beneath the complete EEG time series recording, three distinct time intervals of 20 s, withdraw from EEG recording (I_0 −420 s to −400 s, I_1 −220 s to −200 s and I_2 −20 s to T_{zero} seconds before seizure onset) is shown. These intervals were further separated in 2-s epochs and overlapped in order to highlight the evoked potential for the PTZ + ES group only prior the seizure; Fig. 5B. The histograms show the difference between TMPs intervals; suggesting that the external ES oscillator forces neural synchronization several seconds before seizure onset for the PTZ + ES group. As expected, the distribution at the beginning of the EEG record (T_{zero}-600–T_{zero}-400 s) follows a Gaussian probability for all groups (Fig. 5A – $P > 0.05$, 2-way ANOVA Bonferroni

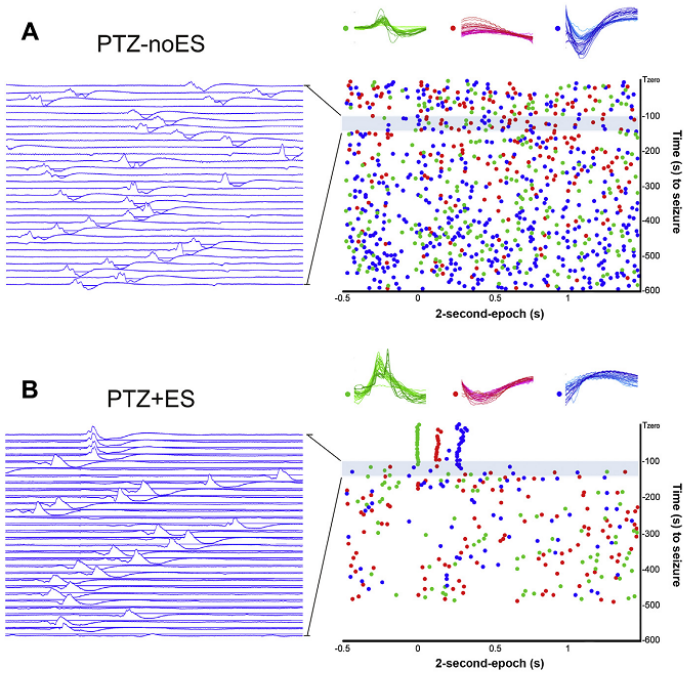

Figure 6. Semi-automatic pattern recognition. The algorithm tracked the relative time occurrence of specific waveforms during the EEG analysis time window (−600 s to T_{zero}). Three different waveforms were arbitrarily chosen for each recording of a representative animal of the (A) PTZ-noES and (B) PTZ + ES groups. The left panel shows the raw EEG time-series progression of the sequential 2-s-epochs (−0.5 to 1.5 s of the ES trigger) within the period depicted on the shadowed portion on the right (from T_{zero}-160 s—T_{zero}-100 s; thus, the evolution of 30 sequential 2-s-epochs). Each colored dot in the right panel corresponds to the occurrence of a particular waveform template (color code shown in the upper portion of the figure). (For interpretation of the references to color in this figure legend, the reader is referred to the web version of this article.)

post-hoc test). However, the PTZ + ES group demonstrated a significant increase of the zero value bin, of TMPs intervals difference, on the last two thirds of the recording (Fig. 5B and C) preceding seizure onset, compared with PTZ-noES and ES-noPTZ (EEG from −400 to −200, $P < 0.01$ and −200 to T_{zero}, $P < 0.001$, 2-way ANOVA Bonferroni post-hoc test). The value zero reflects the phase lock of pre-ictal discharges with the 0.5 Hz external ES drive.

In order to test if the evoked potential for the PTZ + ES group results from the merging of individual neural circuits, which become synchronized with the external oscillator, the pre-ictal pattern identification algorithm was used. Thus, considering that different neural circuits may be represented by different waveforms on the EEG, semi-automatic pattern recognition can track the relative time occurrence (phase locked to ES) of specific circuits gradually shifting before seizure onset. A representative animal from PTZ-noES (Fig. 6A) and PTZ + ES (Fig. 6B) group was chosen depicting three different waveforms for each animal. The right panel shows the occurrence of the 3 waveforms templates in 2 s-epochs (from −0.5—1.5 s of the ES trigger) along EEG recording time to seizure. The left panel shows the EEG progression of sequential 2 s epochs varying from T_{zero}-160 s—T_{zero}-100 s. It can be noted that the waveforms occur randomly at the beginning of the EEG recording for both representative rats. However, the waveforms from the animal PTZ + ES group gradually synchronize with the stimuli prior seizure onset as the evoked potential emerges. The waveforms from the PTZ-noES animal remain randomly distributed.

Discussion

In our study, the low frequency ES (0.5 Hz) applied to the AMY (i.e. PTZ + ES group) did not show pro-convulsive properties: not altering seizure onset, duration of electrographic ictal activity or epileptiform discharge spectral distribution. However, low frequency stimulation has been shown to delay the evolution of seizure phenotype on the electrical kindling of the amygdala [15]. Controversially, 8 Hz stimulation of the anterior thalamic nuclear complex has a pro-convulsive effect generating electrographic seizures and behavioral manifestations even without the PTZ injection [16]. The classical view is that low-frequency ES would produce a stimulation-induced modulation of areas that could, in turn, either inhibit or induce seizures depending on the target area chosen for electrode placement [3]. Nevertheless, the very low frequency ES (0.5 Hz) was able to increase c-Fos expression only when applied during the ictogenic process induced by PTZ (PTZ + ES compared with ES-noPTZ group) which suggests that ES promotes abnormal neural network activation [17,18] by a potentiated modulation of amigdalofugal pathways. The PTZ-noES groups showed a significantly higher c-Fos count in the thalamus, as well as the PTZ-ES group, when compared to the ES group. It is expected, due to its diffuse and massive cortical afferent and efferent projections, that thalamic structures would be significantly activated during the PTZ infusion [19]. Altogether, these results are suggestive of a potentiating effect ES might exert on the abnormal

PTZ induced coupling between diffuse microseizure circuits [20]. The ES may have worked as an exogenous pacemaker circuit driving PTZ triggered internal oscillators (pre-ictal EEG activity) to enhance coupling to a point as to promote visible evoked electrographical responses at the cortical leads (Figs. 4C, 5 and 6). It is important to highlight that neither the number of occurrences of pre-ictal events (Fig. 4A) nor the total energy of the electroencephalogram (Fig. 4B) showed significant changes between PTZ groups with or without ES.

The hypothesis that ictal neural circuitry may result from abnormal coupling between separate independent oscillatory substrates has been suggested by other studies using a myriad of different approaches. The GEPRs, a genetically strain of epilepsy prone rats, have a characteristic electrographic epileptiform signature that most likely results from the electric field propagation (within the conducting volume) generated by different, phase locked, neural substrates [21]. In the before mentioned work, after surgically disconnecting the brainstem-forebrain circuitry, although seizure could still be induced by sound stimuli, the ictal electrographic epileptiform signature was significantly altered. The same concept has also been addressed in hippocampal slice studies [22] where a sequential disruption of the 3-synaptic circuitry had a significant effect on the coupling of independent hippocampal epileptiform activity and overall ictal waveform discharge pattern. Our data also support the view that independent pre-ictal neural generators, gradually coupling with each other, come to form an apparent single coupled epileptogenic oscillator (Figs. 4C, 5 and 6).

Our results do not preclude the fact that neural circuits, otherwise silent during the pre-ictal period, may be recruited during seizure activity; though Fig. 5D does not show an increase on EEG energy after the evoked potential response emerges. In addition, the coupling of existing pre-ictal generators and the recruitment of new epileptogenic circuits may be interdependent factors for seizure onset. As an example, it has been shown that brain regions responsible for inter-ictal electrographic activity are not necessarily part of ictogenic foci [23]; although inter-ictal activity and localization is relevant for diagnostic purposes. Thus, it is not the authors' intention to defend, with current results, that exclusively the neural substrates generating pre-ictal activity are synchronizing to produce an epileptic circuit; rather, our data suggest that the mechanisms that underlie the excessive coupling between these pre-ictal generators might correlate to the same mechanisms of the ictogenesis process.

Although the chemical model used in this work (i.e. PTZ infusion seizures) is quite adequate to study the synchronization of pre-ictal activity; to assume that interictal patterns from patients having spontaneous seizures would behave in the same way would be an improper generalization of this principle. However, even under the paradigm of an ictogenesis chemical model, our results show that an external oscillator gradually drives/synchronizes the activity of endogenous ictogenic networks that can be measured before the onset of sustained epileptiform discharge, thus, potentially serving as a seizure predicting strategy. More so, if seen as a surrogate marker [24] for epileptic electrographic activity, the synchronization induced by ES was programmed by temporally pairing it to ictal activity, very much like it is done in an associative learning paradigm. It is important to highlight that the ES-noPTZ group did not give rise to any detectable evoked potential response at cortical EEG recordings. Nevertheless, although the present work lays ground for the concept of a programmed surrogate marker; further investigation is needed in order to test if the abnormal connectivity endures until the next epileptic event and if such plastic changes not change ES into a pro-convulsive stimuli.

In summary, our results show that very low frequency ES (0.5 Hz) may be used to probe neurogenic circuits without necessarily facilitating or promoting seizure activity (Fig. 2). Furthermore, the LFS promoted an abnormal coupling between endogenous neural circuits, as evidenced by c-Fos and electrographic data (Figs. 3–6), which gradually changed before seizure onset. The current results endorse the proposition that probing epileptogenic neural circuits with ES may provide a temporal time frame for seizure prediction that allows feedback devices, such as using anti-epileptogenic ES [4,5], to create a novel treatment for patients with refractory epilepsy.

Acknowledgments

FAPEMIG, CNPq, INCT-INCeMaq and CAPES.

References

[1] Engel J. Epilepsy: global issues for the practicing neurologist. New York, NY: Demos Medical Pub; 2005.
[2] French JA. Refractory epilepsy: clinical overview. Epilepsia 2007;48(Suppl. 1):3–7. PubMed PMID: 17316406. English.
[3] Gwinn RP, Spencer DD. Fighting fire with fire: brain stimulation for the treatment of epilepsy. Clin Neurosci Res 2004;4(1–2):95–105.
[4] Cota VR, Medeiros Dde C, Vilela MR, Doretto MC, Moraes MF. Distinct patterns of electrical stimulation of the basolateral amygdala influence pentylenetetrazole seizure outcome. Epilepsy Behav 2009 Jan;14(Suppl. 1):26–31. PubMed PMID: 18824246. English.
[5] Mesquita MBS, Medeiros DD, Cota VR, Richardson MP, Williams S, Moraes MFD. Distinct temporal patterns of electrical stimulation influence neural recruitment during PTZ infusion: an fMRI study. Prog Biophys Mol Biol 2011 Mar;105(1–2):109–18. PubMed PMID: ISI:000288635300011. English.
[6] Jiruska P, de Curtis M, Jefferys JGR, Schevon CA, Schiff SJ, Schindler K. Synchronization and desynchronization in epilepsy: controversies and hypotheses. J Physiol Lond 2013 Feb;591(4):787–97. PubMed PMID: ISI:000315150000007. English.
[7] Paxinos G, Watson C. The rat brain in stereotaxic coordinates. 4th ed. San Diego; London: Academic; 1998. xxvi, 236 pp.
[8] Merrill DR, Bikson M, Jefferys JG. Electrical stimulation of excitable tissue: design of efficacious and safe protocols. J Neurosci Methods 2005 Feb 15;141(2):171–98. PubMed PMID: 15661300. English.
[9] McCreery DB, Agnew WF, Yuen TG, Bullara L. Charge density and charge per phase as cofactors in neural injury induced by electrical stimulation. IEEE Trans Biomed Eng 1990 Oct;37(10):996–1001. PubMed PMID: 2249872. English.
[10] Aggleton JP. The amygdala: a functional analysis. 2nd ed. Oxford: Oxford University Press; 2000. xiv, 690 pp.
[11] Petrovich GD, Canteras NS, Swanson LW. Combinatorial amygdalar inputs to hippocampal domains and hypothalamic behavior systems. Brain Res 2001 Dec;38(1–2):247–89. PubMed PMID: 11750934. English.
[12] Kapp BS, Gallagher M, Underwood MD, McNall CL, Whitehorn D. Cardiovascular responses elicited by electrical stimulation of the amygdala central nucleus in the rabbit. Brain Res 1982 Feb 25;234(2):251–62. PubMed PMID: 7059829. English.
[13] Sah P, Faber ES, Lopez De Armentia M, Power J. The amygdaloid complex: anatomy and physiology. Physiol Rev 2003 Jul;83(3):803–34. PubMed PMID: 12843409. English.
[14] Fonseca CS, Gusmao ID, Raslan AC, Monteiro BM, Massensini AR, Moraes MF, et al. Object recognition memory and temporal lobe activation after delayed estrogen replacement therapy. Neurobiol Learn Mem 2013 Mar;101:19–25. PubMed PMID: ISI:000317088700003. English.
[15] Yang LX, Jin CL, Zhu-Ge ZB, Wang S, Wei EQ, Bruce IC, et al. Unilateral low-frequency stimulation of central piriform cortex delays seizure development induced by amygdaloid kindling in rats. Neuroscience 2006;138(4):1089–96. PubMed PMID: 16427743. English.
[16] Mirski MA, Rossell LA, Terry JB, Fisher RS. Anticonvulsant effect of anterior thalamic high frequency electrical stimulation in the rat. Epilepsy Res 1997 Sep;28(2):89–100. PubMed PMID: 9267773. English.
[17] Kalitzin SN, Velis DN, da Silva FHL. Stimulation-based anticipation and control of state transitions in the epileptic brain. Epilepsy Behav 2010 Mar;17(3):310–23. PubMed PMID: ISI:000276029900003. English.
[18] Valentin A, Alarcon G, Honavar M, Garcia Seoane JJ, Selway RP, Polkey CE, et al. Single pulse electrical stimulation for identification of structural abnormalities and prediction of seizure outcome after epilepsy surgery: a prospective study. Lancet Neurol 2005 Nov;4(11):718–26. PubMed PMID: 16239178. English.
[19] Jones EG, Azmitia EC, Javier DEG, Jones PRCE. Chapter 27 thalamic organization and function after Cajal. Progress in brain research, vol. 136. Elsevier; 2002. pp. 333–57.
[20] Stead M, Bower M, Brinkmann BH, Lee K, Marsh WR, Meyer FB, et al. Microseizures and the spatiotemporal scales of human partial epilepsy. Brain 2010 Sep;133:2789–97. PubMed PMID: ISI:000281529000028. English.

[21] Moraes MF, Mishra PK, Jobe PC, Garcia-Cairasco N. An electrographic analysis of the synchronous discharge patterns of GEPR-9s generalized seizures. Brain Res 2005 Jun 7;1046(1–2):1–9. PubMed PMID: 15885667. English.
[22] Imamura S, Tanaka S, Akaike K, Tojo H, Takigawa M, Kuratsu J. Hippocampal transection attenuates kainic acid-induced amygdalar seizures in rats. Brain Res 2001 Apr 6;897(1–2):93–103. PubMed PMID: 11282362. English.
[23] Keller CJ, Truccolo W, Gale JT, Eskandar E, Thesen T, Carlson C, et al. Heterogeneous neuronal firing patterns during interictal epileptiform discharges in the human cortex. Brain 2010 Jun;133:1668–81. PubMed PMID: ISI:000278226700010. English.
[24] Sunderam S, Gluckman B, Reato D, Bikson M. Toward rational design of electrical stimulation strategies for epilepsy control. Epilepsy Behav 2010 Jan;17(1):6–22. PubMed PMID: ISI:000273837700002. English.

ARTICLE IN PRESS

YEBEH-03720; No. of pages: 5; 4C:

Epilepsy & Behavior xxx (2013) xxx–xxx

Contents lists available at ScienceDirect

Epilepsy & Behavior

journal homepage: www.elsevier.com/locate/yebeh

Review

Focus on desynchronization rather than excitability: A new strategy for intraencephalic electrical stimulation

Daniel de Castro Medeiros [a], Márcio Flávio Dutra Moraes [a,b,*]

[a] Núcleo de Neurociências (NNC), Departamento de Fisiologia e Biofísica, Instituto de Ciências Biológicas, Universidade Federal de Minas Gerais, Belo Horizonte, Minas Gerais CEP 31270-901, Brazil
[b] Centro de Tecnologia e Pesquisa em Magneto-Ressonância, Escola de Engenharia, Universidade Federal de Minas Gerais, Belo Horizonte, Minas Gerais CEP 31270-901, Brazil

ARTICLE INFO

Article history:
Revised 27 December 2013
Accepted 28 December 2013
Available online xxxx

Keywords:
Epilepsy
Excitability
Synchronization
DBS
Temporally coded

ABSTRACT

Epilepsy is a severely debilitating brain disease, often associated with premature death, which has an urgent need for alternative methods of treatment. In fact, roughly 25% of patients with epilepsy do not have seizures satisfactorily controlled by pharmacological treatment, and 30% of these patients with treatment-refractory seizures are not even eligible for ablative surgery. Epilepsy is most readily identifiable by its seizures and/or paroxysmal events, mostly viewed as spontaneously recurrent and unpredictable, which are caused by stereotyped changes in neurological function associated with hyperexcitability and hypersynchronicity of the underlying neural networks. Treatment has strongly been based on the fixed goal of depressing neuronal activity, working under the veiled assumption that hyperexcitability would lead to synchronous neuronal activity and, therefore, to seizure. Over the last 20–30 years, the emergence of electrical (ES) of deep brain structures, a practicable option for treating patients with otherwise untreatable seizures, has broadened our understanding of anticonvulsant mechanisms that conceptually differ from those of pharmacological treatment. Conversely, the research on ES therapy applied to epilepsy is contributing significantly to untwine the phenomena of excitation from that of synchronization as potential target mechanisms for abolishing seizures and predicting paroxysmal events. This paper is, thus, an addendum to other reviews on the subject of ES therapy in epilepsy which focuses on the desynchronization effect ES has on epileptogenic neural networks rather than its effect on overall brain excitability.

This article is part of a Special Issue entitled "NEWroscience 2013".

1. Introduction

Epilepsy is a brain disease that afflicts approximately 1% of the world population [1], with an alarming one-fourth of these patients not having seizures satisfactorily controlled by pharmacological treatment [2]. Quite plainly, such a frustrating scenario is a direct result of the overwhelming number of possible pathophysiological causes that encompass various brain disorders under a single name: epilepsy. Thus, epilepsy is not in itself a single disease but rather a myriad of signs and symptoms caused by critical brain dysfunction nor is it a single diagnostic entity, as it may be considered a comorbidity or even a symptom for a large number of other diseases [3]. Nevertheless, even with such a complex synopsis, from the very beginning, an effort has been made to propose a comprehensive theory for the basic mechanisms that would embrace all epilepsies [4]. Before the exponential advances in neuroscience that took place in the late twentieth century, William Gordon Lennox, an American neurologist who pioneered the use of electroencephalography (EEG) as a clinical investigative tool in the diagnosis of epilepsy, summarized the disease using a pictorial model [5]. The model, most likely drawn from his experience as a medical practitioner, was depicted as a reservoir in which water represented the contributing and fundamental causes for epileptic seizures. Thus, water would fill the reservoir with contributing factors until an excitability threshold is reached, the dam breaches, and seizure befalls. Accordingly, the fundamental factors would work as predisposing agents for the epileptic condition, partially filling the reservoir to begin with. Drug therapy, dietary control, oxygenation, and other inhibitory physiological feedback mechanisms would be represented as controlled "spillways" diverging any excess amount of water. Hence the long-standing concept envisioned epilepsy is a constant struggle between inhibitory and excitatory factors regulating neuronal activity and that seizure is the inevitable result that comes from the incapacity of neural networks to enforce feedback mechanisms designed to contain abnormal excitation [6].

It is still a matter under debate if the disruption of such finely tuned excitation–inhibition balance, which swiftly shifts normal brain activity into the ictal state, is a widespread phenomenon or restricted to a

* Corresponding author at: Núcleo de Neurociências, Departamento de Fisiologia e Biofísica, Instituto de Ciências Biológicas, Universidade Federal de Minas Gerais, Av. Antônio Carlos, 6627, CEP 31270-901, Campus Pampulha, Belo Horizonte, Minas Gerais, Brazil. Fax: +55 31 3409 2924.
E-mail address: mfdm@ufmg.br (M.F.D. Moraes).

1525-5050/$ – see front matter © 2013 Published by Elsevier Inc.
http://dx.doi.org/10.1016/j.yebeh.2013.12.034

Please cite this article as: Medeiros DC, Moraes MFD, Focus on desynchronization rather than excitability: A new strategy for intraencephalic electrical stimulation, Epilepsy Behav (2013), http://dx.doi.org/10.1016/j.yebeh.2013.12.034

confined brain area. Accordingly, the categorization of focal and generalized epilepsies is challenged by findings that show that many focal types of epilepsy have widespread bilateral abnormalities [7] and that, supposedly, generalized seizures might have an initial focal cortical onset that secondarily spreads throughout adjacent areas [8]. Although such definitions are quite relevant for the field of epileptology, for the purpose of this paper, as a common ground between both hypotheses, ictogenesis is defined as a dynamic process that would gradually shift from a physiological controlled excitation–inhibition balance (normal brain function) towards an unbalanced state that could, in turn, recruit larger neuronal populations, thus spreading the seizure even further [9]. It is important to clarify terminology in order to restrict the scope of this review. The term ictogenesis is used instead of epileptogenesis because the latter refers to the plastic changes that contribute to the fundamental factors that predispose brain tissue to seize, not addressed in this text [10]. Accordingly, this paper will focus on the transition between normal brain activity and seizure manifestation, the spreading cascades that recruit neurons into an epileptogenic network and, finally, the use of temporally coded electrical stimulation (ES) to disrupt such abnormal connectivity. The "spreading" of the seizure activity may refer both to synaptic network connectivity and to nonsynaptic extracellular factors [11] that recruit neurons not primarily presenting abnormal activity. Thus, the article explores the hypothesis that temporally coded ES may interfere with the abnormal connectivity between neuronal microcircuits that would be necessary to induce a seizure.

2. Excitability and synchronism

The abnormal synchronous bursting of large neuronal populations [12] is as much a marker of seizure manifestation as is the excitability–inhibition unbalance. Many scholars defend that, in the epileptic condition, synchronization is a direct consequence of excitation–inhibition unbalance towards excitability [13]. Using simulated neural networks, Kudela et al. [14] showed that when changing the excitatory input strength, without proper inhibitory compensation, the end result is an increase in overall network synchronization. Under this framework, the concept of excitability and synchronization is entwined to an extent as to perceive them as two different manifestations of the same phenomena.

In practical terms, the boundary between the two distinct concepts of excitability and synchronism is blurred even further by the recording and analysis methods used to access neuronal activity. As an example, the reliability of local field potentials (LFPs) or EEG to reflect changes in neuronal excitation depends on the degree of synchronization of the underlying neural networks; otherwise, the uncoordinated activity of each individual cell would tend to cancel each other out and mask the activation of large neuronal populations [15]. In brief, the electrophysiological methodologies described above are ideal for detecting both excited and synchronous neuronal assemblies. In addition, since the transmembrane resting potential of neurons lay closer to the Nernst equilibrium of chloride and potassium, activated inhibitory synapses tend to exert a mild extracellular electrical field distribution, while depolarizing excitatory currents generate much more significant extracellular dipoles. In fact, if the extracellular field distribution caused by neuronal excitation was to be represented by an equivalent dipole, a synapse would have a comparatively bigger dipole moment (measure of the separation between positive and negative charges) than that of axonal propagation. Altogether, this sums up to understanding EEG/LFP recordings as, above all, the result of excitatory postsynaptic activation [16]. These are general guidelines – rules of thumb – to be considered with extreme caution, which have been shown to have several exceptions observed throughout literature. Just to illustrate, hippocampal/parahippocampal LFP recordings often show brief bursts of high-frequency oscillations (HFOs) that are most likely produced by synchronized inhibitory postsynaptic potentials [17,18], along with other important causal factors. However, even if grossly associated with inhibitory activity, some epileptic foci also present the HFO phenomena and have been suggested as surrogate markers of seizure-onset zones [19–21].

Digressing from the focus on excitability, the temporal relations between the activities of single neurons or even the phase coherence between LFP recordings of larger neuronal networks have, over the last two decades, interested many of the world's leading neuroscientists. Context-dependent phase synchronization between the oscillatory activities of different brain areas has been proposed as a key mechanism by which prior knowledge may facilitate/modulate a specific sensory signal input to dynamically activate a motor response for appropriate and flexible sensory–motor coordination [22]. This functional coupling among distributed neural populations, i.e., functional connectivity, has been observed in earlier measurements of covariance between the amplitude of oscillations for specific frequencies (or frequency bands) from electrodes positioned at different sites [23], named magnitude squared coherence between two signals. The interpretation is that if the amplitude of one specific oscillatory behavior localized at area **A** is varying together with another at area **B**, then **A** and **B** are probably functionally connected [24]. However, as mentioned in the above statements, researchers have devised mathematical tools to assess synchronicity (i.e., phase synchronization) independent of the amplitude of oscillations [25,26]. This was an important step in determining the degree of synchronicity without having to infer conclusions from amplitude measurements. Thus, in terms of normal physiological behavior, the phase synchronization of different neural circuits, even when not yet reflecting amplitude coherence, would dynamically facilitate the flow of signal processing throughout a specific pathway within the CNS, consequently resulting in proper function. This new vision of the mechanisms underlying cognitive processes is somehow evolving in parallel to our ability to separate the concepts of inhibition–excitation from those of synchronization. However, the epileptic condition would, in turn, corroborate correlated activation patterns of spatially distributed neural networks that should be otherwise decorrelated. In fact, the abnormal coupling would also disrupt the finely tuned balance of oscillatory circuitry correlation/decorrelation to the point of compromising the normal physiological brain function.

3. From microseizure circuits to full-scale seizures

Some highly localized EEG events have been shown to exist in interictal recordings from patients with epilepsy [27,28]. These distributed microseizure domains, predominant in seizure-onset zones, present an initially desynchronized activity that, as a seizure progresses, increasingly forces adjacent clusters to synchronize [29,30]. It has also been shown that subsequent seizure episodes, much like what has been termed the kindling phenomenon, strengthen and expand synchronization between clusters separated by even greater distances. The spreading of epileptiform activity through the synchronization of microseizure circuits suggests an important role of abnormal connectivity in the ictogenesis process. The traditional approach towards treatment would dictate that these microseizure domains should be surgically resected, thus removing the onset zone (i.e., foci) of seizure initiation. However, a few researchers have postulated that full-scale seizures are the consequence of merging several and distributed microseizure circuits rather than a localized "dominant" circuit spreading from a single onset region [28–30]. If correct, a new therapeutic strategy would be more effective if focusing on disrupting the oscillatory circuitry correlation using carefully devised and temporally precise interference to decorrelate activity between microseizure domains.

The spectral analysis of the electrographical activity of such microseizure domains falls usually within very high frequencies of oscillation [31]. Accordingly, the HFO phenomena have been suggested to play a key role in a number of physiological processes (see the last paragraph of the previous section). It is important to highlight that there is much controversy regarding the equivalence of physiological oscillations that partially overlap frequency bandwidth with known HFO

Please cite this article as: Medeiros DC, Moraes MFD, Focus on desynchronization rather than excitability: A new strategy for intraencephalic electrical stimulation, Epilepsy Behav (2013), http://dx.doi.org/10.1016/j.yebeh.2013.12.034

circuits. As an example, gamma oscillations (slow = 30–50 Hz, mid = 50–90 Hz, and high = >90 Hz) have been suggested to play an important role merging several microdomains into forming a visual percept — "the binding hypothesis" [32]; nevertheless, although quite similar, these mechanisms do not necessarily coincide with those proposed previously for microseizure circuitry hyperconnectivity and seizure spreading. A very elegant review on similarities and differences between physiological and epileptic HFOs may be found in Jefferys et al. [33]. Even under such considerations, although the intrinsic oscillatory mechanisms may differ, two different networks may increase their phase coherence by similar synchronization mechanisms that couple the oscillators. Thus, rather than enforcing poorly localized inhibitory mechanisms to the oscillators, a therapeutic approach that had a very fast effect on the underlying neural network (within the order of milliseconds) could disrupt abnormal synchronization, thus avoiding abnormal coupling and consequently inhibiting the spreading of activity to a full-scale seizure.

4. ES therapy for epilepsy control

In very plain terms, the ES of neural tissue consists of positioning a working electrode (WE) close to targeted receptors, nerves, and/or deep brain nuclei – a counter electrode (CE) to close the circuit – and then forcing a current through them by applying a controlled voltage. The distance between the WE and CE electrodes, amid a number of other parameters (e.g., electrode material, ES polarity, waveform, amplitude, and frequency), is quite relevant in predicting the electrical current distribution that will affect the underlying neural networks. However, a certain degree of "unpredictability" in calculating ES current distribution would rise from parenchymal nonlinearities (e.g., interaction of neurons, glia, and endothelium) that are unknown at the time that electrode implantation take place. In addition, ES current distribution could elicit very different outcomes in the underlying neural network depending on the particularities of the cells recruited. It is well known that ES current provokes nonspecific activation of excitatory/inhibitory neurons [34], indirectly modulates the astrocyte network [35], and may also affect vascular dynamics [35–37]. Nevertheless, despite the factors raised above, the ES essentially causes a disturbance on the neural network that may influence its permanence at any specific intrinsic state [38,39]. In fact, it has been shown that ES may even drive the activity of preictal oscillatory neural networks. Medeiros et al. have recently demonstrated that cortical preictal discharges, elicited by the pentylenetetrazole seizure model in rats, gradually synchronize with ES (applied to the amygdaloid complex) minutes before seizure onset [40].

Nevertheless, ES has been used in research and for clinical diagnostic purposes (e.g. sensory, nerve, and muscle stimulation) long before its suggested applications for seizure control. As an example, intraoperatory functional stimulation of brain areas, during resective surgery in patients with epilepsy, was of investigatory nature only, thus not designed for treatment (for review, see [41]). Other neurological diseases, most notably associated with movement disorders and pain, preceded epilepsy in using ES as a viable alternative treatment. It was not until the 80s that vagus nerve stimulation (VNS) treatment was proposed as an effective method for treating patients with refractory epilepsy, found unfit for resective surgery (for review, see [42]). Also, during the same period, cortical stimulation and deep brain stimulation (DBS) were evaluated as a reasonable therapeutic approach for some extreme cases (i.e., patients with spasticity, severe psychiatric disorders, etc.) but without the clear intent of developing and exploring ES as a new alternative treatment for epilepsy. Nowadays, there is a renewed interest from both basic science epileptologists and clinicians in understanding and improving the use of ES for the treatment of refractory epilepsy. Recently, data from large, randomized controlled trials have shown that ES applied to the anterior nucleus of thalamus (SANTE — Stimulation of the Anterior Nucleus of Thalamus for Epilepsy) [43] or ES applied to cortical structures [44] significantly reduces the frequency of occurrence of seizures [45]. In fact, the latter (NeuroPace®) has newly received United States Food and Drug Administration approval for the treatment of refractory epilepsy, increasing the therapeutic alternatives for this debilitating brain disease.

At a glance, it seems quite paradoxical that ES would aid already hyperexcitable circuits, such as those found in patients with epilepsy, to produce the proper inhibitory compensation for seizure control. In fact, transauricular electroshock in rats has been used for a very long time as an adequate animal model for preclinical trials of new anticonvulsant drugs [46]. However, the empirical tuning of ES parameters and the use of various stimulation protocols have been proven to be quite effective in controlling seizures. The ES therapy in epilepsy, when compared with pharmacotherapy or resective surgery, shows some advantages: better anatomically restricted target of action, faster effect on underlying circuits, greater flexibility on customizing treatment parameters, and apparently less invasive than resective surgery.

Although electronic/mathematical models of the electrochemical interface make it possible to devise safer, efficient, and efficacious strategies for ES, it is still a puzzling matter as to how exactly ES modulates overall neuronal activity in dysfunctional neuronal networks, in spite of a number of theories and very comprehensive reviews. The classical view is that high-frequency ES (HF-ES) – intermittent or continuous application – would functionally inhibit the targeted area, thus mimicking the effects of ablative surgery "resecting" the dysfunctional brain area [47]. Data from electrophysiological recordings, fMRI, microdialysis, and neural modeling suggest that HF-ES might cause a depolarization blockade, synaptic inhibition, or synaptic depression, which would render the pathologic network ineffective and consequently incapable of compromising proper brain function. Conversely, low-frequency ES (LF-ES) would produce a stimulation-induced modulation of areas that would contribute to restoring proper network functionality [47]. Although very elegant and scientifically sound, these hypotheses are more closely bound to principles of functional anatomy and pharmacology compared with those of neurodynamics. To explore the effect that ES could have on neuronal synchronization and microseizure circuit coupling falls outside the classical view of accepted anticonvulsant therapeutic approach strategies: excitability is the primary concern to be addressed. Accordingly, although commercially ES devices allow tampering with several ES parameters, the temporal disposition of pulses, although programmable, is invariably constant. That is, in terms of time distribution of stimuli, ES can be programmed in intermittent or continuous pulses of different frequencies — but always with fixed interpulse intervals (IPIs). Other parameters, such as pulse duration (measured in milliseconds), waveform type (e.g., monophasic or biphasic), intensity (electrical current), dipole moment (distance between the two poles), anatomical target of ES electrode placement, and type of electrode (e.g., material and contact area) are less related to the temporal dynamics of seizure propagation and more closely associated with excitation and inhibition of specific anatomical structures. However, even using fixed IPI stimulation, some very creative ES protocols have been proposed as means to disrupt synchronicity, even at the cost of increasing excitability, just by reorganizing spatial and temporal bursts of intermittent ES. The mathematical model proposed by Tass et al. [48] predicts an anticonvulsant outcome if four distinct portions of an epileptogenic neural network are stimulated with intermittent out-of-phase fixed-frequency bursts.

5. Temporally structured ES

Although temporal patterns of neuronal cell discharge have long been hypothesized to be an important part of how information is coded within the network, very few studies have attempted to use such temporal coding as a parameter for ES therapy [49]. The first work to consider altering interpulse intervals (IPIs) as a strategy to desynchronize epileptogenic neural networks was published in this

Please cite this article as: Medeiros DC, Moraes MFD, Focus on desynchronization rather than excitability: A new strategy for intraencephalic electrical stimulation, Epilepsy Behav (2013), http://dx.doi.org/10.1016/j.yebeh.2013.12.034

very same journal 3–4 years ago [50]. In this study, the authors tested the hypothesis that low-frequency ES (set at 4 Hz) would promote neuronal synchronization if IPIs remained constant but would inhibit abnormal coupling if ES was not periodic. The targeted structure chosen was the amygdaloid complex (AMY). Control groups with fixed IPI burst discharges and with no constraints towards the total size of each random 4-pulse "package" of ES were used to avoid misleading conclusions. Animals were submitted to constant i.v. PTZ infusion and latency to seizure threshold measured under the different ES protocols. As expected, periodic IPIs showed a proconvulsant effect, while nonperiodic IPIs (with "package" restriction) showed clear anticonvulsant properties; control groups did not differ from nonelectrically stimulated animals.

Other researchers have since then shown the effects of temporally coded ES on behavioral outcome. Quinkert et al. [51] used a logistic equation to design nonstandard patterns of ES and compared it with fixed-frequency (50 Hz) stimulation pertaining to how it would affect central nervous system arousal. The authors concluded that although several other ES parameters were maintained constant (i.e., pulse width, intensity, waveform, and overall number of stimuli per unit of time), the temporal reorganization of ES pulse presentation had a significant effect on several behavioral markers evaluated (e.g., fidgeting movements, ambulation, and an independent measure of whole body movement) as well as affecting EEG spectral energy distribution [52]. Accordingly, Mesquita et al. [37] showed – using fMRI technology – that periodic and random IPIs, applied to the same structure (i.e., AMY), had quite distinct activation patterns throughout the CNS. The authors devised an ES carbon-fiber electrode compatible with fMRI imaging and were able to detect significant increase in BOLD (blood oxygen level densitometry) signal in the thalamus and hippocampus – contralateral to stimulation – using periodic IPIs, while nonperiodic IPIs (random stimulation) evoked activity in the nucleus accumbens.

However, if a dynamic ictogenic process is artificially induced by continuous i.v. infusion of PTZ, the temporal arrangement of IPIs proved to interfere with circuitry connectivity and neural activity [37]. Using the same IPI patterns published by Cota et al. [50], sequential fMRI images recorded during continuous PTZ i.v. infusion showed increased temporal lobe activity ipsilateral to periodic IPI ES. Nonperiodic IPIs had the opposite effect, showing decreased activation of ipsilateral structures, thus compromising seizure propagation. Thus, the ES temporal coding modulates the underlying neural activity by facilitating or impairing seizure propagation, even if all other ES parameters (e.g., targeted structure, ES current, duration, and overall frequency) are maintained constant. Authors suggest that temporally coded ES has its dual effect by acting on circuitry coupling, consequently synchronizing or desynchronizing scattered microdomains, thus influencing seizure propagation. However, the differential effect of ES temporal coding on seizure outcome is very much dependent on the anatomical target chosen. The anterior nucleus of the thalamus, for example, has been shown to have no difference in PTZ seizure threshold modulation either by using fixed or random IPIs [53], both having a significant anticonvulsant effect. This nucleus has long been suggested as an adequate DBS target for anticonvulsant treatment [54–56], with ES parameters varying among different reports.

The combined results from the above experiments have influenced the design of new DBS equipment to include the flexibility of programmable IPI ES protocols. In an ingenious design, Ewing et al. [57] published a fully programmable, rechargeable, preclinical ES device that complied with the possibility of executing temporally coded ES patterns. These devices envision a future in which a feedback loop of closed circuit prediction–abortion epileptic treatment will be available, using very low frequency – temporally coded – ES patterns.

6. Conclusion

This review is an addendum to other reviews on the subject of DBS therapy in epilepsy, which focuses on a new perspective on ES parameter tampering: temporal pattern coding. The rationale is based on the desynchronization effect that temporally coded ES has on epileptogenic neural networks, rather than its effect on overall brain excitability. Rather than depressing neuronal activity, the new therapeutic approach aims to compromise the abnormal connectivity of microseizure domains, thus inhibiting the spread of ictogenic activity.

Acknowledgments

We are grateful to Brazilian agencies CNPq, FAPEMIG, CAPES, and PRPq/UFMG for financial support.

Conflict of interest

The authors declare that there are no conflicts of interest.

References

[1] Engel J. Epilepsy: global issues for the practicing neurologist. New York, N.Y.: Demos Medical Pub.; 2005
[2] French JA. Refractory epilepsy: clinical overview. Epilepsia 2007;48(Suppl. 1):3–7.
[3] Zeber JE, Copeland LA, Amuan M, Cramer JA, Pugh MJV. The role of comorbid psychiatric conditions in health status in epilepsy. Epilepsy Behav 2007;10:539–46.
[4] McNamara JO. Cellular and molecular basis of epilepsy. J Neurosci 1994;14:3413–25.
[5] Lennox WG. Science and seizures: new light on epilepsy and migraine. Third ed. New York: Harper & Brothers; 1941.
[6] Zhang ZJ, Valiante TA, Carlen PL. Transition to seizure: from "macro"- to "micro"-mysteries. Epilepsy Res 2011;97:290–9.
[7] Spencer SS. When should temporal-lobe epilepsy be treated surgically? Lancet Neurol 2002;1:375–82.
[8] Meeren HKM, Pijn JPM, Van Luijtelaar ELJM, Coenen AML, da Silva FHL. Cortical focus drives widespread corticothalamic networks during spontaneous absence seizures in rats. J Neurosci 2002;22:1480–95.
[9] Richardson MP. New observations may inform seizure models: very fast and very slow oscillations. Prog Biophys Mol Biol 2011;105:5–13.
[10] Aroniadou-Anderjaska V, Fritsch B, Qashu F, Braga MF. Pathology and pathophysiology of the amygdala in epileptogenesis and epilepsy. Epilepsy Res 2008;78:102–16.
[11] McCormick DA, Contreras D. On the cellular and network bases of epileptic seizures. Annu Rev Physiol 2001;63:815–46.
[12] Steriade M. Neuronal substrates of sleep and epilepsy. Cambridge: Cambridge University Press; 2003.
[13] Scharfman HE. The neurobiology of epilepsy. Curr Neurol Neurosci Rep 2007;7:348–54.
[14] Kudela P, Franaszczuk PJ, Bergey GK. Changing excitation and inhibition in simulated neural networks: effects on induced bursting behavior. Biol Cybern 2003;88:276–85.
[15] Uhlhaas PJ, Singer W. Neural synchrony in brain disorders: relevance for cognitive dysfunctions and pathophysiology. Neuron 2006;52:155–68.
[16] Niedermeyer E, Lopes da Silva FH. Introduction to the Neurophysiological Basis of the EEG and DC Potentials. In: Electroencephalography: basic principles, clinical applications, and related fields. 5th ed.; London: Lippincott Williams & Wilkins; 2005, pp. 15–26 .
[17] Buzsaki G, Horvath Z, Urioste R, Hetke J, Wise K. High-frequency network oscillation in the hippocampus. Science 1992;256:1025–7.
[18] Ylinen A, Bragin A, Nadasdy Z, Jando G, Szabo I, Sik A, et al. Sharp wave-associated high-frequency oscillation (200 Hz) in the intact hippocampus: network and intracellular mechanisms. J Neurosci 1995;15:30–46.
[19] Levesque M, Bortel A, Gotman J, Avoli M. High-frequency (80–500 Hz) oscillations and epileptogenesis in temporal lobe epilepsy. Neurobiol Dis 2011;42:231–41.
[20] Rosenow F, Luders H. Presurgical evaluation of epilepsy. Brain 2001;124:1683–700.
[21] Zijlmans M, Jiruska P, Zelmann R, Leijten FSS, Jefferys JGR, Gotman J. High-frequency oscillations as a new biomarker in epilepsy. Ann Neurol 2012;71:169–78.
[22] Womelsdorf T, Fries P, Mitra PP, Desimone R. Gamma-band synchronization in visual cortex predicts speed of change detection. Nature 2006;439:733–6.
[23] Varela F, Lachaux JP, Rodriguez E, Martinerie J. The brainweb: phase synchronization and large-scale integration. Nat Reviews 2001;2:229–39.
[24] Bressler SL, Coppola R, Nakamura R. Episodic multiregional cortical coherence at multiple frequencies during visual task-performance. Nature 1993;366:153–6.
[25] Lachaux JP, Rodriguez E, Martinerie J, Varela FJ. Measuring phase synchrony in brain signals. Hum Brain Mapp 1999;8:194–208.
[26] Zeitler M, Fries P, Gielen S. Assessing neuronal coherence with single-unit, multi-unit, and local field potentials. Neural Comput 2006;18:2256–81.
[27] Schevon CA, Ng SK, Cappell J, Goodman RR, McKhann Jr G, Waziri A, et al. Microphysiology of epileptiform activity in human neocortex. J Clin Neurophysiol 2008;25:321–30.
[28] Stead M, Bower M, Brinkmann BH, Lee K, Marsh WR, Meyer FB, et al. Microseizures and the spatiotemporal scales of human partial epilepsy. Brain 2010;133:2789–97.
[29] Jiruska P, Csicsvari J, Powell AD, Fox JE, Chang WC, Vreugdenhil M, et al. High-frequency network activity, global increase in neuronal activity, and synchrony expansion precede epileptic seizures in vitro. J Neurosci 2010;30:5690–701.

Please cite this article as: Medeiros DC, Moraes MFD, Focus on desynchronization rather than excitability: A new strategy for intraencephalic electrical stimulation, Epilepsy Behav (2013), http://dx.doi.org/10.1016/j.yebeh.2013.12.034

[30] Jiruska P, de Curtis M, Jefferys JGR, Schevon CA, Schiff SJ, Schindler K. Synchronization and desynchronization in epilepsy: controversies and hypotheses. J Physiol Lond 2013;591:787–97.
[31] Zijlmans M, Jacobs J, Kahn YU, Zelmann R, Dubeau F, Gotman J. Ictal and interictal high frequency oscillations in patients with focal epilepsy. Clin Neurophysiol 2011;122:664–71.
[32] Singer W, Gray CM. Visual feature integration and the temporal correlation hypothesis. Annu Rev Neurosci 1995;18:555–86.
[33] Jefferys JG, Menendez de la Prida L, Wendling F, Bragin A, Avoli M, Timofeev I, et al. Mechanisms of physiological and epileptic HFO generation. Prog Neurobiol 2012;98:250–64.
[34] Tehovnik EJ, Tolias AS, Sultan F, Slocum WM, Logothetis NK. Direct and indirect activation of cortical neurons by electrical microstimulation. J Neurophysiol 2006;96:512–21.
[35] Kuga N, Sasaki T, Takahara Y, Matsuki N, Ikegaya Y. Large-scale calcium waves traveling through astrocytic networks in vivo. J Neurosci 2011;31:2607–14.
[36] Canals S, Beyerlein M, Murayama Y, Logothetis NK. Electric stimulation fMRI of the perforant pathway to the rat hippocampus. Magn Reson Imaging 2008;26:978–86.
[37] Mesquita MBS, Medeiros DD, Cota VR, Richardson MP, Williams S, Moraes MFD. Distinct temporal patterns of electrical stimulation influence neural recruitment during PTZ infusion: an fMRI study. Prog Biophys Mol Biol 2011;105:109–18.
[38] Sasaki T, Matsuki N, Ikegaya Y. Metastability of active CA3 networks. J Neurosci 2007;27:517–28.
[39] Kalitzin SN, Velis DN, da Silva FHL. Stimulation-based anticipation and control of state transitions in the epileptic brain. Epilepsy Behav 2010;17:310–23.
[40] Medeiros DC, Oliveira LB, Mourao FA, Bastos CP, Cairasco NG, Pereira GS, et al. Temporal rearrangement of pre-ictal PTZ induced spike discharges by low frequency electrical stimulation to the amygdaloid complex. Brain Stimul 2013. http://dx.doi.org/10.1016/j.brs.2013.11.005 (in press).
[41] Feindel W. The contributions of Wilder Penfield to the functional anatomy of the human brain. Hum Neurobiol 1982;1:231–4.
[42] Binnie CD. Vagus nerve stimulation for epilepsy: a review. Seizure 2000;9:161–9.
[43] Fisher R, Salanova V, Witt T, Worth R, Henry T, Gross R, et al. Electrical stimulation of the anterior nucleus of thalamus for treatment of refractory epilepsy. Epilepsia 2010;51:899–908.
[44] Morrell MJ, Grp RSES. Responsive cortical stimulation for the treatment of medically intractable partial epilepsy. Neurology 2011;77:1295–304.
[45] Fridley J, Thomas JG, Navarro JC, Yoshor D. Brain stimulation for the treatment of epilepsy. Neurosurg Focus 2012;32.
[46] Loscher W, Fassbender CP, Nolting B. The role of technical, biological and pharmacological factors in the laboratory evaluation of anticonvulsant drugs. II. Maximal electroshock seizure models. Epilepsy Res 1991;8:79–94.
[47] Gwinn RP, Spencer DD. Fighting fire with fire: brain stimulation for the treatment of epilepsy. Clin Neurosci Res 2004;4:95–105.
[48] Tass PA. A model of desynchronizing deep brain stimulation with a demand-controlled coordinated reset of neural subpopulations. Biol Cybern 2003;89:81–8.
[49] Wasserman GS. Isomorphism, task dependence, and the multiple meaning theory of neural coding. Biol Signals 1992;1:117–42.
[50] Cota VR, Medeiros Dde C, Vilela MR, Doretto MC, Moraes MF. Distinct patterns of electrical stimulation of the basolateral amygdala influence pentylenetetrazole seizure outcome. Epilepsy Behav 2009;14(Suppl. 1):26–31.
[51] Quinkert AW, Schiff ND, Pfaff DW. Temporal patterning of pulses during deep brain stimulation affects central nervous system arousal. Behav Brain Res 2010;214:377–85.
[52] Quinkert AW, Pfaff DW. Temporal patterns of deep brain stimulation generated with a true random number generator and the logistic equation: effects on CNS arousal in mice. Behav Brain Res 2012;229:349–58.
[53] Medeiros DD, Cota VR, Vilela MRSD, Mourao FAG, Massensini AR, Moraes MFD. Anatomically dependent anticonvulsant properties of temporally-coded electrical stimulation. Epilepsy Behav 2012;23:294–7.
[54] Mirski MA, Rossell LA, Terry JB, Fisher RS. Anticonvulsant effect of anterior thalamic high frequency electrical stimulation in the rat. Epilepsy Res 1997;28:89–100.
[55] Takebayashi S, Hashizume K, Tanaka T, Hodozuka A. Anti-convulsant effect of electrical stimulation and lesioning of the anterior thalamic nucleus on kainic acid-induced focal limbic seizure in rats. Epilepsy Res 2007;74:163–70.
[56] Mirski MA, Ziai WC, Chiang J, Hinich M, Sherman D. Anticonvulsant serotonergic and deep brain stimulation in anterior thalamus. Seizure 2009;18:64–70.
[57] Ewing SG, Porr B, Riddell J, Winter C, Grace AA. SaBer DBS: a fully programmable, rechargeable, bilateral, charge-balanced preclinical microstimulator for long-term neural stimulation. J Neurosci Methods 2013;213:228–35.

Please cite this article as: Medeiros DC, Moraes MFD, Focus on desynchronization rather than excitability: A new strategy for intraencephalic electrical stimulation, Epilepsy Behav (2013), http://dx.doi.org/10.1016/j.yebeh.2013.12.034

Epilepsy & Behavior 23 (2012) 294–297

Contents lists available at SciVerse ScienceDirect

Epilepsy & Behavior

journal homepage: www.elsevier.com/locate/yebeh

Anatomically dependent anticonvulsant properties of temporally-coded electrical stimulation

Daniel de Castro Medeiros [a], Vinícius Rosa Cota [b], Maura Regina Silva da Páscoa Vilela [a], Flávio Afonso Gonçalves Mourão [a], André Ricardo Massensini [a], Márcio Flávio Dutra Moraes [a,*]

[a] Núcleo de Neurociências (NNC), Departamento de Fisiologia e Biofísica, Instituto de Ciências Biológicas, Universidade Federal de Minas Gerais, Minas Gerais, Brazil
[b] Laboratório de Bioengenharia, Departamento de Engenharia Biomédica, Universidade Federal de São João Del-Rei, São João Del Rey, Minas Gerais, Brazil

ARTICLE INFO

Article history:
Received 17 October 2011
Revised 9 January 2012
Accepted 10 January 2012
Available online 25 February 2012

Keywords:
Epilepsy
Deep brain stimulation
Amygdaloid complex
Thalamus
Temporal patterns

ABSTRACT

In the PTZ animal model of epilepsy, electrical stimulation applied to the amygdaloid complex may result in either pro-convulsive or anticonvulsant effect, depending on the temporal pattern used (i.e. periodic-PS and non-periodic-NPS electrical stimulation). Our hypothesis is that the anatomical target is a determinant factor for the differential effect of temporally-coded patterns on seizure outcome. The threshold dose of PTZ to elicit forelimb clonus and generalized tonic–clonic seizure behavior was measured. The effect of amygdaloid complex PS on forelimb clonus threshold showed a pro-convulsive effect while NPS was anticonvulsant. NPS also significantly increased generalized tonic–clonic threshold; while PS, although at lower threshold levels, did not present statistical significance. Thalamus stimulation did not affect forelimb clonus threshold and showed similar anticonvulsant profiles for both PS and NPS on generalized tonic–clonic threshold. In summary, the anatomical target is a determinant factor on whether temporally-coded ES differentially modulates seizure outcome.

1. Introduction

Epilepsy is characterized by recurrent and spontaneous seizures caused by hyperexcitable and hypersynchronous underlying neural networks [1]. Despite the great advances of drug development over the last decades [2], pharmacological treatment is still unable to satisfactorily control seizures in about one third to one fourth of epilepsy patients [3–5]. Intracranial electrical stimulation (ES) is emerging as a new alterative approach for the treatment of pharmacoresistant epilepsy [6].

Classically, ES is believed to work either by suppressing or inhibiting epileptogenic structures, analogous to surgical ablation (high frequency stimulation), or by activating or stimulating neural networks that would modulate seizure-like activity (low frequency stimulation) [7–9]. The careful choice of parameters such as frequency, intensity and anatomical positioning of electrodes were believed to govern the ES usage as a seizure-suppressing procedure. Nevertheless, previous results from our laboratory, using the PTZ animal model of epilepsy, showed that a fixed 4-stimuli-per-second ES, in the amygdaloid complex (AMG), could either facilitate or interfere with the behavioral manifestation of the seizure, depending on how the stimulus was temporally coded [10,11]. Thus, the frequency parameter alone cannot explain the effect of ES on the PTZ seizure outcome, opening a new venue of possibilities in order to enhance ES efficiency as a therapeutic tool against epilepsy.

However, it has not yet been evaluated if other structures, besides the AMG, may respond to time-coded electric stimulation, differentially modulating seizure activity depending on the pattern of ES used. Our hypothesis is that not every structure will be able to decode time-patterns of ES. One such alternative target to temporally-coded ES is the thalamus (TAL), already tested throughout the literature (periodic high-frequency ES only) and showing positive results in seizure suppression [12]. Although the TAL has extensive connections with forebrain and brainstem regions [13], which may explain why thalamic ES is used in the treatment of pharmacoresistant epilepsy, its function and neural architecture differ greatly from that of the AMG. The objective of this work is to test whether time-coded ES in the thalamus has the same effect as that observed for the AMG, either facilitating (periodic stimulation) or interfering (non-periodic stimulation) with the behavioral manifestation of the seizure in the PTZ animal model of epilepsy.

* Corresponding author at: Núcleo de Neurociências, Departamento de Fisiologia e Biofísica, Instituto de Ciências Biológicas, Universidade Federal de Minas Gerais, Av. Antônio Carlos, 6627, CEP 31270-901, Campus Pampulha, Belo Horizonte, MG, Brazil. Fax: +55 31 3409 2924.
E-mail addresses: mfdm@ufmg.br, mfdm@icb.ufmg.br (M.F.D. Moraes).

1525-5050/$ – see front matter © 2012 Elsevier Inc. All rights reserved.
doi:10.1016/j.yebeh.2012.01.004

2. Methods

2.1. Electrical stimulation

We designed and built an electrical stimulator composed of a constant-current isolation unit driven by the output of an MP3 player (model NWZ-B152 2GB — Sony). Each output ES signal was designed using Adobe Audition 1.0 and transformed into a 44.1-kHz, 16-bit, mono waveform, MP3 format compatible with the D/A hardware output. Although constrained at a fixed total frequency of 4 stimuli per second, two patterns of temporally-coded stimuli were used: 1) constant inter-pulse intervals (IPIs) of 250 ms (periodic stimulus, PS); 2) randomized IPI (non-periodic stimulus, NPS) (Fig. 1). Each single stimulus consisted of a 350-μA square wave pulse of 100-μs duration. The temporal patterns used were chosen based on previous reports from our laboratory [10,11].

2.2. Animals

Male Wistar rats (n = 44; weighing 250–300 g), supplied by the CEBIO-ICB-UFMG vivarium, were housed under controlled environmental conditions (22 ± 1 °C), with a 12:12-h light–dark cycle and free access to food and water. All experiments were executed under Protocol License no. 150/06 approved by the university's Ethical Committee for Animal Experimentation (CETEA–UFMG). Efforts were made to avoid any unnecessary distress to the animals, and the lowest possible number of animals was used. The CETEA directives are in compliance with NIH guidelines for the care and use of animals in research.

2.3. Surgical procedures

Bipolar electrodes, made of a twisted pair of stainless-steel teflon-coated wires (Model 791400, A-M Systems Inc., Carlsborg, WA, USA), were surgically implanted in the AMG (n = 24) and the TAL (n = 20). Animals were anesthetized by means of an i.p. injection of the mixture of ketamine (70 mg/kg — Pfizer, Karlsruhe, Germany) and xylazine (15 mg/kg — Bayer, Leverkusen, Germany) and positioned in a stereotaxic frame (Stoelting Co., Wood Dale, IL, USA). Coordinates for the anterior nucleus of the thalamus (AP = 1.3 mm, ML = 1.6 mm, referenced from the bregma suture, and 5.5 mm from dura mater) and amygdaloid complex (AP = 2.8 mm, ML = 5.0 and 7.2 from dura mater) were derived from the Paxinos and Watson's rat atlas [14]. The electrode was fixed to the bone with zinc cement and soldered to a telephone jack (Model RJ-11), which, in turn, was fixed onto the skull with dental acrylic. After surgery, animals received a prophylactic pentabiotic (2.5 mg/kg) treatment and were allowed to recover for 5 days before the experimental procedure. Groups were further subdivided according to the temporally-coded ES applied: no stimulus (AMG n = 12, TAL n = 9); PS (AMG n = 7, TAL n = 5) and NPS (AMG n = 5, TAL n = 6).

2.4. PTZ infusion

Before commencing the stimulation procedure, the caudal vein was cannulated for intravenous infusion of PTZ (10 mg/ml — Sigma) diluted in saline. The cannula was connected to an infusion pump set at the rate of 1 ml/min. Results were expressed as the PTZ threshold dose normalized by body weight (g/kg of animal) for forelimb clonus (FC) and generalized tonic–clonic (GTC) seizure onset. The choice of the former FC and GTC behavioral markers is based on the scoring scale proposed by Velisek et al. [15], in which FC would correspond to a fully developed minimal seizure (scale 3) while GTC would be a fully developed maximal seizure (scale 5). After stimulation, animals received an anesthetic overdose of urethane (140 mg/kg) before brain removal and histological procedures. Brains were sliced in order to confirm the electrode position. Animals with incorrect positioning of electrodes were not included in analysis.

Data are presented as means ± S.E.M. Statistical comparisons were made using one-way ANOVA and post-hoc Student–Newman–Keuls (SNK). The PTZ thresholds for both convulsive behavior markers, FC and GTC seizures, were compared according to the stimulus pattern (no-stimuli, PS and NPS). Values of $p<0.05$ were considered statistically significant.

3. Results

All animals displayed the typical convulsive behavior sequence of the PTZ model [15] 1) initial intensive grooming, sniffing, moving arrests; 2) followed by occasional isolated myoclonic jerks with ear and facial twitching; 3) clonus of the head muscles and forelimbs, and the presence of the righting reflex (the FC behavioral marker); 4) generalized clonus, without the tonic phase, and, finally; 5) the GTC that is usually preceded by a jump, followed by tonic falling and flexion or extension of forelimbs and hind limbs (maximum seizure).

Animals exposed to PS on AMG during PTZ infusion had significantly lower FC threshold ($FC_{PS} = 14.2 \pm 1.5$ mg/kg; $p<0.001$) when

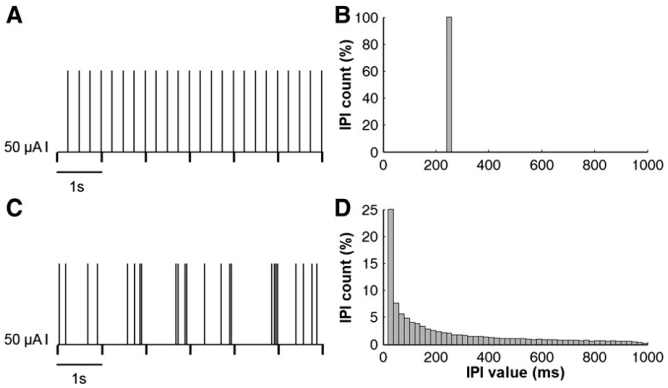

Fig. 1. Rats were stimulated with two different temporal patterns: (A) periodic (PS) and (C) non-periodic (NPS) electrical stimulation. The inter-pulse-intervals (IPI) for the PS and NPS are depicted respectively in histograms of occurrence B and D. Electrical stimulation, for both patterns, was characterized by a 350-μA, 100-μs duration and by four-stimuli-per-second pulse. Note that while PS has a fixed IPI (B) of 250 ms (4 Hz), NPS presents fairly randomized IPIs (see Cota et al. [10] for details).

compared to control ($FC_{control} = 22.8 \pm 1.2$ mg/kg) (Fig. 2A). In contrast, NPS displayed significantly higher threshold for both behavioral markers ($FC_{NPS} = 38.3 \pm 1.7$ mg/kg; $p<0.001$ and $GTC_{NPS} = 72.2 \pm 7.9$ mg/kg; $p<0.01$) (Figs. 2A and B) compared to controls ($FC_{control} = 22.8 \pm 1.2$ mg/kg and $GTC_{control} = 53.1 \pm 5.5$ mg/kg) (Figs. 2A and B). In addition, NPS and PS groups were significantly different for both FC ($p<0.001$) and GTC ($p<0.01$) [FC (Fig. 2A); one-way ANOVA: $F[2,21] = 50.21$, $p<0.0001$; GTC (Fig. 2B); one-way ANOVA: $F[2,21] = 3.78$, $p<0.0394$].

No significant effect was observed, for thalamic PS and NPS, on FC seizure threshold when compared to control. However, GTC threshold was significantly higher for both PS and NPS ($GTC_{PS} = 70.5 \pm 4.0$ mg/kg; $GTC_{NPS} = 70.3 \pm 3.9$ mg/kg) groups when compared to controls ($GTC_{control} = 49 \pm 2$ mg/kg) [FC (Fig. 3A); one-way ANOVA: $F[2,17] = 0.24$, $p = 0.78$; GTC (Fig. 3B); one-way ANOVA: $F[2,17] = 13.81$, $p = 0.0003$].

Although the mechanical lesion due to electrode insertion is easily visible in histology, there was no significant difference between AMG and TAL control groups (none of which was submitted to ES, but both were implanted with the same electrodes as the experimental groups). Thus, although this may be an issue for other studies, this particular work refrained from further discussion on the matter.

4. Discussion

The results confirm that distinct temporal patterns of ES, when applied to the AMG, differentially modulate seizure outcome in the PTZ continuous infusion model (i.e. PS had pro-convulsant properties while NPS was anticonvulsant). These results are in accordance with previous data from the literature [10], which suggest that PS would resonate with epileptogenic circuits, thus facilitating seizures outcome; while NPS would desynchronize circuits and interfere with neural recruitment necessary for the epileptic process. However, TAL ES did not significantly affect FC seizure threshold and had an anti-convulsant effect on GTC threshold for both temporally-coded ES patterns used (PS and NPS). In fact, the relevance of data presented here is significantly increased based upon the logical sequence of prior publications [10,11].

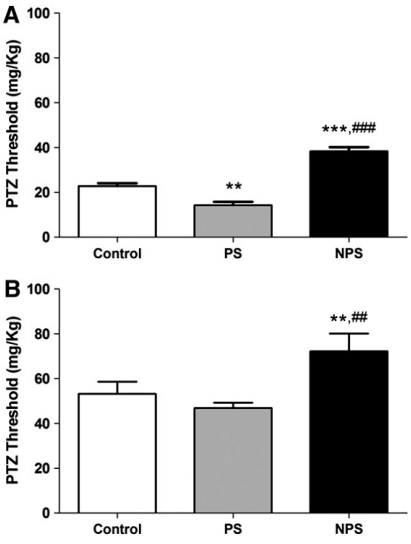

Fig. 2. PTZ threshold (normalized by body weight) for two convulsive behaviors: forelimb clonus (A) and generalized tonic–clonic seizures (B). Periodic stimulation (PS) and non-periodic stimulation (NPS) patterns were applied to the amygdaloid complex. Periodic stimulation (PS) decreased PTZ threshold for forelimb clonus (pro-convulsant effect). Non-periodic stimulation (NPS) increased PTZ threshold for both forelimb clonus and generalized tonic–clonic seizures when compared with all groups (anticonvulsant effect). $^{**}p<0.01$, $^{***}p<0.001$ periodic and non-periodic vs. control group, $^{\#\#}p<0.01$, $^{\#\#\#}p<0.001$ periodic vs. non-periodic in one-way ANOVA, post-hoc SNK. See the Results section for the numerical values of bars from this figure.

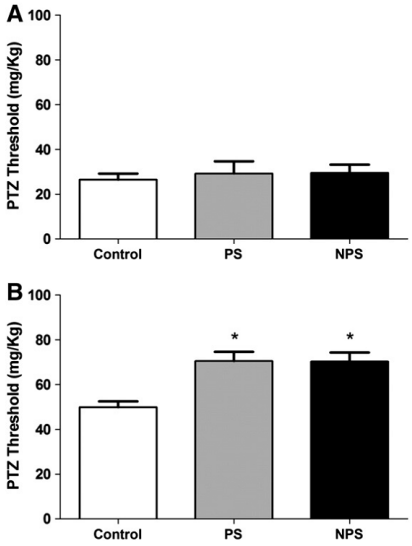

Fig. 3. PTZ threshold (normalized by body weight) for two convulsive behaviors: forelimb clonus (A) and generalized tonic–clonic seizures (B). Periodic stimulation (PS) and non-periodic stimulation (NPS) patterns were applied to the thalamus. No difference was observed between PS and NPS for forelimb clonus threshold. However, both the PS and NPS increased drug threshold for generalized tonic–clonic seizure when compared with control group (anticonvulsant effect). $^{*}p<0.05$, periodic and non-periodic vs. control group in one-way ANOVA, post-hoc SNK. See the Results section for the numerical values of bars from this figure.

Although PTZ creates a nonspecific condition of hyperexcitability, in part due to its GABAergic antagonist properties [16], evidence suggests that multiple neural circuits are gradually recruited into the ictogenic process as the drug is absorbed. In fact, low doses of PTZ (<40 mg/kg) typically evoke minimal seizures (i.e. myoclonic jerks, forelimb and head clonus [15]), which are classically correlated with limbic structures [17,18]; while higher doses of PTZ evoke maximal seizures (i.e. generalized tonic–clonic behavior), which are most likely correlated with brainstem activation [19]. The precedence of forebrain recruitment over brainstem substrates in the PTZ-induced seizures is suggestive of a higher threshold of the latter when compared to the former [19]. However, the view that these two substrates are completely independent seizure generators is not supported the literature [20,21]; in fact, the interactions between forebrain and brainstem seizure networks, under certain conditions, have an important overall modulation on seizure outcome. As an example, in an epileptic animal model of repetitive brainstem seizures, induced by high intensity sound stimulation [22], forebrain circuits are secondarily recruited after 13–17 audiogenic seizures. However, once recruited, forebrain circuits inhibit GTC seizures and generalized electrographic activity, maintaining only focal temporal lobe epileptiform discharges.

Our results show that ES has a clear modulatory effect in forebrain circuits only when applied to the AMG, based on FC onset data (Fig. 2). In addition, brainstem circuits seem to be affected by both AMG and TAL ES, however, possibly by two different mechanisms: a) in the case of AMG ES, forebrain synchronization/de-synchronization modulates brainstem circuits and b) the TAL ES directly interferes with brainstem neural recruitment without requiring forebrain.

The amygdaloid complex plays an important role in modulation and transfer of epileptiform activity in several animal models of temporal lobe epilepsy [23–26]. The AMG has monosynaptic afferents from and efferents to the parahippocampal areas (e.g., entorhinal cortex and subiculum) [27], providing the anatomical substrate for transfer and modulation of epileptiform activity. These connections provide an explanation for the pattern dependent effect of AMG-ES in FC threshold and increased GTC threshold [11]. One possible explanation as to why AMG PS did not significantly alter seizure threshold for GTC, since it did have a pro-convulsant effect in FC, is that forebrain modulation in epileptogenic brain-stem circuits would be primarily inhibitory [19]. Also, it is important to highlight that PS and NPS may have similar consequences in the underlying circuitry excitability but rather different effects on neural synchronization [11].

The thalamus provides the major inputs to cortex and primarily, but definitely not exclusively, working as a relay nucleus, which integrates and passes information from primary sensory modalities, basal ganglia, cerebellum, and the limbic system [28]. Due to its extensive connections, it is not surprising that the thalamus plays an important role in the abnormal synchronization between cortical and subcortical structures in tonic–clonic seizures [29]. Therefore, TAL ES, in contrast to AMG ES, seems to directly inhibit epileptogenic brainstem seizures, independently on the degree of synchronization imposed by PS/NPS, which is comprehensible, considering that this structure may relay information to the same output independently of the ES pattern used.

In summary, our results suggest that the amygdaloid complex is capable of decoding temporal arrangements of stimuli paradigm, which, in this case, may play an important role in desynchronizing epileptic seizures, especially forebrain seizure-like activity.

Acknowledgments

We are grateful to Brazilian agencies CNPq, INCeMaq (INCT CNPq), FAPEMIG, CAPES and PRPq/UFMG for financial support.

References

[1] Engel Jr J. Introduction to temporal lobe epilepsy. Epilepsy Res 1996;26:141–50.
[2] Loscher W, Schmidt D. New horizons in the development of antiepileptic drugs. Epilepsy Res 2002;50:3–16.
[3] French JA. Refractory epilepsy: clinical overview. Epilepsia 2007;48(Suppl. 1):3–7.
[4] Loscher W. Animal models of epilepsy for the development of antiepileptogenic and disease-modifying drugs. A comparison of the pharmacology of kindling and post-status epilepticus models of temporal lobe epilepsy. Epilepsy Res 2002;50:105–23.
[5] Wuttke TV, Lerche H. Novel anticonvulsant drugs targeting voltage-dependent ion channels. Expert Opin Investig Drugs 2006;15:1167–77.
[6] Lim SN, Lee ST, Tsai YT, et al. Long-term anterior thalamus stimulation for intractable epilepsy. Chang Gung Med J 2008;31:287–96.
[7] McIntyre CC, Grill WM. Finite element analysis of the current-density and electric field generated by metal microelectrodes. Ann Biomed Eng 2001;29:227–35.
[8] McIntyre CC, Savasta M, Kerkerian-Le Goff L, Vitek JL. Uncovering the mechanism(s) of action of deep brain stimulation: activation, inhibition, or both. Clin Neurophysiol 2004;115:1239–48.
[9] Volkmann J. Deep brain stimulation for the treatment of Parkinson's disease. J Clin Neurophysiol 2004;21:6–17.
[10] Cota VR, Medeiros DdeC, Vilela MR, Doretto MC, Moraes MF. Distinct patterns of electrical stimulation of the basolateral amygdala influence pentylenetetrazole seizure outcome. Epilepsy Behav 2009;14(Suppl. 1):26–31.
[11] Mesquita MB, Medeiros Dde C, Cota VR, Richardson MP, Williams S, Moraes MF. Distinct temporal patterns of electrical stimulation influence neural recruitment during PTZ infusion: an fMRI study. Prog Biophys Mol Biol 2011;105:109–18.
[12] Lim SN, Lee ST, Tsai YT, et al. Electrical stimulation of the anterior nucleus of the thalamus for intractable epilepsy: a long-term follow-up study. Epilepsia 2007;48:342–7.
[13] Jones EG. Thalamic organization and function after Cajal. Prog Brain Res 2002;136:333–57.
[14] Paxinos G, Watson C. The rat brain in stereotaxic coordinates. 4th ed. San Diego; London: Academic; 1998.
[15] Velisek L, Kubova H, Pohl M, Stankova L, Mares P, Schickerova R. Pentylenetetrazol-induced seizures in rats: an ontogenetic study. Naunyn Schmiedebergs Arch Pharmacol 1992;346:588–91.
[16] Macdonald RL, Barker JL. Pentylenetetrazol and penicillin are selective antagonists of GABA-mediated post-synaptic inhibition in cultured mammalian neurones. Nature 1977;267:720–1.
[17] Browning R, Maggio R, Sahibzada N, Gale K. Role of brainstem structures in seizures initiated from the deep prepiriform cortex of rats. Epilepsia 1993;34:393–407.
[18] Eells JB, Clough RW, Browning RA, Jobe PC. Comparative fos immunoreactivity in the brain after forebrain, brainstem, or combined seizures induced by electroshock, pentylenetetrazol, focally induced and audiogenic seizures in rats. Neuroscience 2004;123:279–92.
[19] Browning RA, Nelson DK. Modification of electroshock and pentylenetetrazol seizure patterns in rats after precollicular transections. Exp Neurol 1986;93:546–56.
[20] Marescaux C, Vergnes M, Kiesmann M, Depaulis A, Micheletti G, Warter JM. Kindling of audiogenic seizures in Wistar rats: an EEG study. Exp Neurol 1987;97:160–8.
[21] Garcia-Cairasco N, Wakamatsu H, Oliveira JA, Gomes EL, Del Bel EA, Mello LE. Neuroethological and morphological (Neo-Timm staining) correlates of limbic recruitment during the development of audiogenic kindling in seizure susceptible Wistar rats. Epilepsy Res 1996;26:177–92.
[22] Dutra Moraes MF, Galvis-Alonso OY, Garcia-Cairasco N. Audiogenic kindling in the Wistar rat: a potential model for recruitment of limbic structures. Epilepsy Res 2000;39:251–9.
[23] Akirav I, Richter-Levin G. Mechanisms of amygdala modulation of hippocampal plasticity. J Neurosci 2002;22:9912–21.
[24] Moraes MF, Chavali M, Mishra PK, Jobe PC, Garcia-Cairasco N. A comprehensive electrographic and behavioral analysis of generalized tonic–clonic seizures of GEPR-9s. Brain Res 2005;1033:1–12.
[25] Moraes MF, Mishra PK, Jobe PC, Garcia-Cairasco N. An electrographic analysis of the synchronous discharge patterns of GEPR-9s generalized seizures. Brain Res 2005;1046:1–9.
[26] Vouimba RM, Richter-Levin G. Physiological dissociation in hippocampal subregions in response to amygdala stimulation. Cereb Cortex 2005;15:1815–21.
[27] Racine R, Okujava V, Chipashvili S. Modification of seizure activity by electrical stimulation. 3. Mechanisms. Electroencephalogr Clin Neurophysiol 1972;32:295–9.
[28] Norden AD, Blumenfeld H. The role of subcortical structures in human epilepsy. Epilepsy Behav 2002;3:219–31.
[29] Zhong Y, Lu G, Zhang Z, Jiao Q, Li K, Liu Y. Altered regional synchronization in epileptic patients with generalized tonic-clonic seizures. Epilepsy Res 2011;97:83–91.

Progress in Biophysics and Molecular Biology 105 (2011) 109–118

Contents lists available at ScienceDirect

Progress in Biophysics and Molecular Biology

journal homepage: www.elsevier.com/locate/pbiomolbio

Original Research

Distinct temporal patterns of electrical stimulation influence neural recruitment during PTZ infusion: An fMRI study

Michel Bernanos Soares Mesquita [a,b], Daniel de Castro Medeiros [a], Vinícius Rosa Cota [a,c], Mark P. Richardson [b], Steven Williams [b], Márcio Flávio Dutra Moraes [a,b,*]

[a] Núcleo de Neurociências (NNC), Departamento de Fisiologia e Biofísica, ICB, UFMG, Brazil
[b] King's College London, London, UK
[c] Universidade Federal de São João Del Rei, Brazil

ARTICLE INFO

Article history:
Available online 31 October 2010

Keywords:
Basolateral amygdala
Pentylenetetrazole
Synchronization
Desynchronization
Electrical stimulation
Synfire chains

ABSTRACT

Our working hypothesis is that constant inter-pulse interval (IPI) electrical stimulation (ES) would resonate with endogenous epileptogenic reverberating circuits, favoring seizure, while random inter-interval ES protocol would promote desynchronization of such neural networks, interfering with the abnormal recruitment of neural structures. Male Wistar rats were stereotaxically implanted with a monopolar ES carbon-fiber electrode (minimizing fMRI artifact) in the amygdala. A 7T fMRI scanner was used to evaluate brain activity during ES, fixed four pulses per second ratio, using either a periodic IPI (ES-P) or random IPI (non-periodic ES-NP) stimulation paradigm. Appropriate imaging protocols were used to compare baseline BOLD (blood oxygen level dependent) MRI with scans during ES. A second series of experiments, both without stimuli and under the same ES paradigms, were evaluated during continuous infusion of pentylenetetrazole (PTZ, 4 mg/ml/min) through an i.v. catheter. Our results show that temporal lobe activation during ES-P or ES-NP did not present any statistical differences during ES. However, during PTZ infusion, PTZ-P facilitated recruitment of the temporal lobe ipsilateral to ES while PTZ-NP showed significantly less activation ipsilateral to ES and, in turn, less inter-hemispheric differences. Altogether, our results support the hypothesis of reverberating circuits being synchronized by ES-P and desynchronized by ES-NP. Time-coded low frequency stimulation may be an interesting alternative treatment for patients with refractory epilepsy.

1. Introduction

Epilepsy is a very common and serious primary brain disease, with an incidence of 24–53/100,000 and prevalence of 0.4–0.8% in developed countries (Hauser et al., 1998), characterized by recurrent and spontaneous seizures caused by hyperexcitable and hypersynchronous underlying neural networks (Engel, 1996). The suppression of seizures is the main therapeutic goal for neurologists treating people with epilepsy, even when lacking a better etiological understanding of the disease. Despite the great advances of drug development over the last decades (Loscher and Schmidt, 2002), pharmacological treatment is still unable to satisfactorily control seizures in about one third to one fourth of epilepsy patients (French, 2007; Loscher and Schmidt, 2002; Wuttke and Lerche, 2006). In addition, many of these patients, with refractory epilepsy, are not eligible for ablative surgery, which, in most cases, requires a readily identifiable epileptogenic focus (Centeno et al., 2006; Spencer, 2002; Wiebe et al., 2001). Thus, investigation of alternative methods of treatment, such as electrical stimulation (ES) of neural structures (Theodore and Fisher, 2004), is of great interest in current epileptology. ES may be applied peripherally [e.g. Vagus Nerve Stimulation – VNS (Ben-Menachem, 2002; Binnie, 2000; Valencia et al., 2001) or Trigeminal Nerve Stimulation – TNS (DeGiorgio et al., 2003; Fanselow et al., 2000)] or targeted to a variety of structures within the central nervous system [Deep Brain Stimulation – DBS (Benabid et al., 2002; Hodaie et al., 2002; Vonck et al., 2005), such as: the anterior nucleus of the thalamus (Hamani et al., 2004; Mirski et al., 1997), subthalamic nuclei (Benabid et al., 2002; Chabardes et al., 2002) or the epileptogenic focus itself (Vonck et al., 2002)]. Classically, ES is believed to work either by suppressing or inhibiting epileptogenic structures,

* Corresponding author at: Núcleo de Neurociências, Department of Physiology and Biophysics, Institute of Biological Sciences, Federal University of Minas Gerais, Av. Antonio Carlos, 6627, CEP 31270-901 Campus Pampulha, Belo Horizonte, MG, Brazil. Tel.: +55 31 3499 2930; fax: +55 31 3499 2924.
E-mail address: mfdm@icb.ufmg.br (M.F.D. Moraes).

0079-6107/$ – see front matter © 2010 Elsevier Ltd. All rights reserved.
doi:10.1016/j.pbiomolbio.2010.10.005

analogous to surgical ablation (McIntyre and Grill, 2001; McIntyre et al., 2004a; Volkmann, 2004), or by activating or stimulating neural networks that would modulate seizure-like activity. Nevertheless, this simplistic view does not explain the complex underlying mechanisms by which ES is effective (Theodore and Fisher, 2004) on suppressing seizures (McIntyre et al., 2004a; McIntyre et al., 2004b).

Elegant numerical simulations of neural network dynamics have guided epileptologists in better understanding the relationship between excitability and synchronicity (Kudela et al., 2003), leading to paradigm changing ideas on how to suppress the mass recruitment of neural substrates during ictogenesis. In a neural modeling study, Tass and Hauptmann (2007) showed that it would be theoretically possible to desynchronize neural masses with appropriate spatial–temporal ES protocols without the need for chronic high frequency (HF) stimulation, which could lead to undesirable complications (Freund, 2005; Kumar et al., 2003; Rodriguez-Oroz et al., 2005; Volkmann et al., 2004). The important change in paradigm of these new approaches, especially when comparing to anticonvulsant drug therapy, is to target the synchronization aspect of epileptogenic neural networks instead of their excitability. Our laboratory tested time-coded ES patterns, designed to either resonate or desynchronize epileptogenic reverberant circuits, in the PTZ animal model of epilepsy (Cota et al., 2009). In this work we showed that a fixed 4 stimuli per second ES could either facilitate or interfere with the behavioral manifestation of the seizure depending on how the stimulus was temporally coded. Such novel stimulation techniques may selectively desynchronize neuronal populations involved in epilepsy, thus being the biological validation of the "network desynchronization" therapeutic approach.

Although Cota et al. (2009) presented behavioral evidence to support the anticonvulsant effect of desynchronizing ES (dES), there is still no direct biological validation regarding how, and to what extent, ES interferes with neural mass recruitment during the transition to the ictal state. Understanding how abnormal activity propagates throughout the epileptic brain requires the acquisition and analysis of data containing anatomic, temporal and magnitude components. Electrophysiological measures could be used to determine seizure propagation (Durand, 1993; Gale, 1992; Moraes et al., 2005b; Snead, 1992; Timofeev and Steriade, 2004) however; this technique presents inherent insensitivity with respect to anatomic localization. Functional magnetic resonance imaging (fMRI) is much better suited to this purpose and has been applied to quantifying seizure propagation in the PTZ animal model of epilepsy (Keogh et al., 2005). Once the methodological problems regarding physical compatibility between intracranial ES and fMRI imaging were resolved, our objective was to provide biological evidence for theoretical modeling data suggesting that low frequency desynchronizing ES (non-periodic/random temporally coded stimuli, anti-resonant with epileptogenic oscillators) would disrupt PTZ seizure propagation while synchronizing ES (periodic stimuli resonant with epileptogenic oscillators) would promote or facilitate neural mass recruitment. By applying ES paradigms to only one side of the brain (amygdaloid complex in the temporal lobe), the contra-lateral hemisphere could be considered as a paired control.

2. Materials and methods

All experiments were done in accordance with United Kingdom's Animals (Scientific Procedures) Act 1986, under Home Office approval, with respective project and personal licenses, for researchers involved with procedures.

2.1. Electrical stimulation

We designed and built an electrical stimulator composed of a constant-current isolation unit (Digitimer DS3 Isolated Constant Current Stimulator) driven by a PC-programmable clocking system. C++ software was developed to program the stimulator with two patterns of temporally coded stimuli, all delivering a total of four pulses per second (to guarantee the same energy flow): 1) constant inter-pulse intervals (IPIs) of 250 ms (periodic stimulus, P); 2) randomized IPI (non-periodic stimulus, NP). Each single stimulus consisted of a 500 μA square wave pulse of 100 μs duration. The temporal patterns used were chosen based on previous report from our laboratory (Cota et al., 2009) that showed an optimal pro-convulsive effect for P-IPI and anti-convulsive action of the NP-IPI.

2.2. MRI compatible electrodes

The electrode used for stimulation had to be compatible with fMRI imaging. Three kinds of electrodes were tested, using a monopolar montage, in order to choose the one with least imaging artifact: stainless steel (model #791400, A-M Systems, California, USA), tungsten (California Fine Wire Company) and glass-coated carbon fiber. The construction of the carbon-fiber electrode is described in detail elsewhere (Moraes and Garcia-Cairasco, 1997). In summary, a bundle of 10–20 μm carbon-fibers is placed inside a glass micropipette while attached to a microelectrode puller (Glass 2BBL, World Precision Instruments, Inc., New Haven, CT). In addition, after pulling the pipette, a stereomicroscopic guide is used to heat the micropipette tip in order to melt the glass over the carbon fiber and, thus, firmly fixing it to the micropipette.

2.3. Animal preparation

Male Wistar rats were randomly assigned to two experimental groups: ES group (n = 7) and ES with PTZ (n = 21). All animals underwent a surgical procedure for implantation of a monopolar stimulation electrode in the amygdaloid complex. Animals were anesthetized via systemic i.p. urethane injection (1.5 g/kg at 1.5 g of urethane in a 10 ml saline solution) and locally with lidocaine chlorohydrate plus epinephrine (2%) and then positioned in a stereotaxic frame (Stoelting). Coordinates for the right basolateral amygdala (AP = 2.8 mm; ML = 5.0 mm referenced from the bregma suture and 7.2 mm from dura-mater) were derived from the Paxinos and Watson Atlas for Rats (Paxinos and Watson, 1998). The electrode, fixed in the skull with acrylic, was connected to the positive lead of the stimulator. The negative lead was connected to a carbon pad electrode attached to the left hind paw of the rat. After the surgical procedure, animals were positioned inside the MRI scanner while temperature, pulse oxymetry and respiratory frequency were monitored. A constant flow of air/oxygen (80/20%) was provided by means of connecting polyethylene tubing to the animal nose.

2.4. Groups

The ES group was designed to identify differences in activated areas due to the stimulation pattern itself. Thus, stimulation paradigms of 40 s of silence followed by 20 s of each kind of ES pattern were applied continuously until a total of 24 repetitions were made for each ES pattern. Due to interlaced distribution of ES patterns, each animal was its own control when comparing the effect of ES-P and ES-NP against silence (noES).

The ES with PTZ group was designed to verify how each ES pattern altered the propagation of epileptic substrates, abnormal neural mass recruitment, throughout PTZ i.v. infusion. Thus, during the surgical procedure, animals were cannulated through the tail

vein for continuous PTZ infusion. An infusion rate of 0.1 ml/min using a PTZ concentration of 40 mg/kg was optimally chosen to avoid significant changes in blood volume while promoting abnormal neural mass recruitment (seizure propagation) within an average period of 15 min. Animals were sacrificed with an anesthetic overdose before any behavioral ictal manifestation was evident. Animals from the ES with PTZ group were divided into three subgroups: without stimulation (PTZ-noES, $n = 7$), periodic stimulation (PTZ-P, $n = 7$) and non-periodic stimulation (PTZ-NP, $n = 7$).

2.5. Image acquisition

MR images were acquired using a 7.0 T horizontal small bore magnet (Varian, Palo Alto, CA, USA) and a custom built transmit-receive bird-cage RF coil with an inner diameter of 40 mm, linked to a LINUX-based control console running VnmrJ acquisition software (v2.3, Varian, Palo Alto CA, USA). Structural T_2-weighted images were acquired using a fast spin-echo multi-slice sequence (FSEMS), with the following scanning parameters: TR = 4000 ms; echo train length = 4; effective TE = 60 ms; 4 averages; FOV = 32 × 32 mm; matrix = 128 × 128 voxels; slice thickness = 1 mm; whole brain coverage with 15 axial slices (interleaved); total scan duration = 8:32 min. Functional images were acquired with a single shot gradient-echo echo-planar sequence (GE-EPI), with the following scanning parameters: TR = 2500 ms; TE = 14 ms; FOV = 32 × 32 mm; matrix = 64 × 64 voxels; slice thickness = 1 mm; whole brain coverage with 15 axial slices (interleaved); 1152 volumes were acquired in the ES experiments, with a total scan duration of 48 min; 400 volumes were acquired in the PTZ experiments, with a total scan duration of 16.6 min.

2.6. Image analysis

Pre-processing and statistical analyses were performed using the Jim image analysis package, Version 5.0 (Xinapse Systems Ltd., Northants, UK, www.xinapse.com; 2010) and SPM5 (http://www.fil.ion.ucl.ac.uk; 2010).

For each subject, fMRI time series were realigned using a least squares approach and a 6-parameter (rigid body) spatial transformation (SPM5), where each image was aligned to the first image of the time series. A brain mask was then created manually (Jim), in order the remove non-brain tissue from the images, and applied to all realigned images using a matlab® script. The realigned/masked images were then spatially normalized to a standard in-house template using a 12-parameter spatial transformation (SPM5). Finally, normalized images were Gaussian smoothed using a full-width and half-maximum 3D kernel of 0.75 × 0.75 × 1.5 mm (150% of the voxel size).

Pre-processed images were statistically analyzed using a voxel by voxel, mass-univariate approach based on a general linear model (GLM). This process estimates a GLM according to the experimental protocol (i.e. resting period and type of electrical stimulation, for the ES group and pre and post PTZ infusion in the PTZ group) convolved with a hemodynamic response function (HRF) followed by interrogation of results using contrast vectors to produce group statistical parametric maps (SPM5). Data from the ES study were high-pass-filtered in time, using a cut-off period of 180 s and conditioned for temporal autocorrelations (due to aliased biorhythms) using AR1 correction. Contrast images (between-condition contrast) from each subject were used to produce a random-effects group-level t-test analysis. Data from the PTZ study were analyzed using a group-level fixed-effect approach. Since the temporal evolution of PTZ-induced changes was relatively slow, time series were not convolved with a HRF, temporally filtered or conditioned for temporal autocorrelations. Group statistical parametric maps were overlaid to FSEMS anatomical images (co-registered to the standard template). All data are displayed with an uncorrected threshold of $p < 0.05$.

Finally, SPM results from the PTZ study were analyzed for activation laterality. Matlab® scripts, written in house, were used to determine the mean value of supra-threshold T values, from statistical parametric maps from each subject, for ipsi and contra-lateral hemisphere in each of the 15 slices acquired (T threshold corresponding to a $p < 0.001$; given by SPM5). Mean T values for ipsi and contra-lateral hemisphere of each individual slice, within each group, were compared with paired t-test (Prism 4.0c, GraphPad Software Inc).

3. Results

Fig. 1 depicts the image artifacts generated by the three electrodes (stainless steel, tungsten and carbon fiber), implanted in the right basolateral amygdala. We can observe significant loss of signal surrounding the steel and tungsten electrodes (dark areas in the right hemisphere – white arrows) rendering the images unsuitable for analysis. However, no noticeable image artifact is present in the images acquired with carbon-fiber electrodes. Fig. 1 also shows an example of the carbon-fiber electrode chosen for experimental procedures. The electrode depicted in Fig. 1 was used throughout the experiments, even when no stimulation was applied.

As expected, the ES group (with no PTZ) showed a statistically significant recruitment of the area surrounding electrode placement for both ES paradigms (Fig. 2A and B slices 0 and +10), which corresponds to the amygdaloid complex. In this experiment, stimulation paradigms (i.e. NP and P) were applied to the same animal, preceded by a control silent period (without stimulation), in order to allow paired statistics, see methods for details. Although we could observe a trend of fewer activated voxels in the ES-NP group, within a region of interest (ROI) involving the temporal lobe, paired t-test did not show significant difference between ES-NP and ES-P. In addition to the areas around the electrode, ES-P produced contra-lateral activation spreading along thalamic and hippocampal structures, whereas ES-NP activated more anterior/frontal structures, mainly nucleus accumbens. The effect of NP stimulation recruiting frontal areas (Fig. 2B, slice +60) reinforces the idea that the amygdaloid complex is able to differentiate temporally coded processes even when the same overall stimulating frequency is used (4 stimuli per second).

The ES with PTZ group showed a bi-hemispheric recruitment for the PTZ-noES animals, in agreement with previous reports found in literature (Keogh et al., 2005). In general, a similar activation/inactivation pattern was also observed in the groups submitted to ES (Fig. 3). Nevertheless, the PTZ-P showed a more pronounced activation of the side ipsilateral to electrode implantation (slices +30, +40, +50 and +60 of Fig. 3B) while PTZ-NP protected the ipsilateral hemisphere against abnormal recruitment (slices −20, −10, 0 and +10 of Fig. 3C). Fig. 3 also shows that PTZ-NP had less activated posterior areas when compared to either PTZ-noES or PTZ-P.

The mean value of T was calculated for the right and left hemispheres, for each animal from the parametric maps of each slice, in order to determine lateralization during the PTZ seizure progression. We can observe that the PTZ-NP abolishes the lateralization in all the slices, whereas PTZ-P significantly enhances lateralization in slices +30 and +40 (Fig. 4). The mean T analysis did not statistically confirm the diminished ipsilateral activation of slices −20, −10, 0 and +10 (Fig. 3C). The PTZ-noES showed significant ipsilateral lateralization in slices −20 and −10 (+0, although not significant, showed a similar tendency), these are areas close to electrode placement and could be explained by local lesion to the

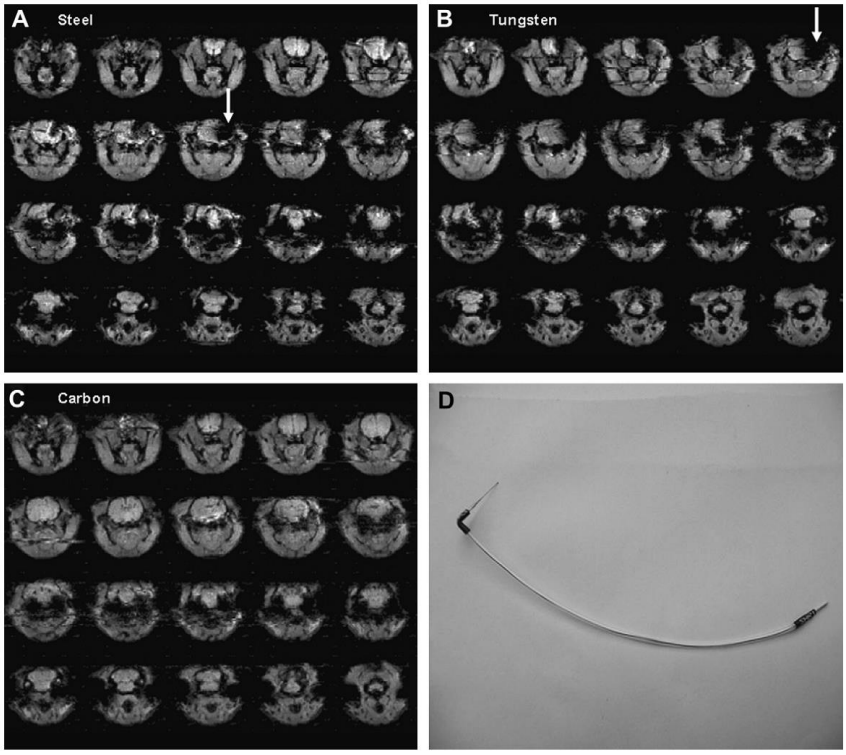

Fig. 1. Echo-planar images acquired with three different deep brain electrodes implanted in the right amygdaloid complex: A) stainless steel, B) tungsten and C) carbon fiber. An example of the electrode selected for experimental procedures is depicted in D. Arrows show the areas of image artifact. No image artifact was observed using the carbon-fiber electrodes.

blood brain barrier (BBB). Both PTZ-noES and PTZ-P showed contralateral lateralization for more posterior slices.

Fig. 5 depicts a voxel by voxel analysis of PTZ infused rats comparing PTZ-P (periodic stimulation) against PTZ-NP (non-periodic stimulation) in panel A, and PTZ-NP against PTZ-P in panel B. Fig. 5A clearly shows an increased ipsilateral activity, regarding electrode placement, when compared to Fig. 5B (slices varying from −20 to +20 are clearly less compromised in panel B). The same activation observed in Fig. 2B (slice +60) is evident throughout the whole frontal area of Fig. 5B. It is important to highlight that not only Figs. 2 and 5 come from different experiments, using different animals, but that Fig. 2 uses paired statistics while Fig. 5A and B is from respectively two different groups of animals continuously infused with PTZ. Thus, altogether, these results raise an interesting hypothesis that NP stimulation may not only play a direct desynchronizing effect in slices neighboring electrode placement (slices −20 to +20 from Fig. 5A when compared to Fig. 5B), but could also indirectly recruit frontal areas (Fig. 5B slices +40 to +70) that may contribute inhibiting seizure propagation. Nevertheless, the direct hypothesis (through desynchronizing effect) and indirect hypothesis (through activation of PTZ seizure-inhibitory frontal areas) are not exclusive.

In addition, when comparing SPM analysis of slices −20 to +20 from Figs. 3B and C, with 5A and B, the lateralization effect of suggested in Fig. 4 is even clearer. Fig. 5A presents pronounced activation (slices +10 to +40) the same regions of Fig. 3B, which neighbor electrode placement of PTZ-P animals. In contrast, for PTZ-NP maps, Figs. 3C and 5B show diminished activity in regions neighboring electrode placement (slices −20 to +30).

4. Discussion

The results show that distinct temporal patterns of ES, when applied to amygdala, differentially modulate neural mass recruitment in the animal model of PTZ continuous infusion. Our results not only confirm the behavioral counterpart published by our group in freely moving animals (Cota et al., 2009), but also support a more comprehensive theory of ictogenesis which takes into consideration not only hyperexcitability, but also and more importantly, hypersynchronization and reverberating neural networks.

Although testing hypothesis about functional imaging data sets is no easy task, the present work uses widely accepted statistical tools and correlates results from different experimental designs in order to address the main hypothesis of temporally coded stimuli effect on seizure outcome. In contrast with stimulus-induced response fMRI, where a time-locked stimulus is repeatedly presented to the subject in a known temporal pattern (similar to results in Fig. 2), resulting in more robust responses, pharmacological MRI

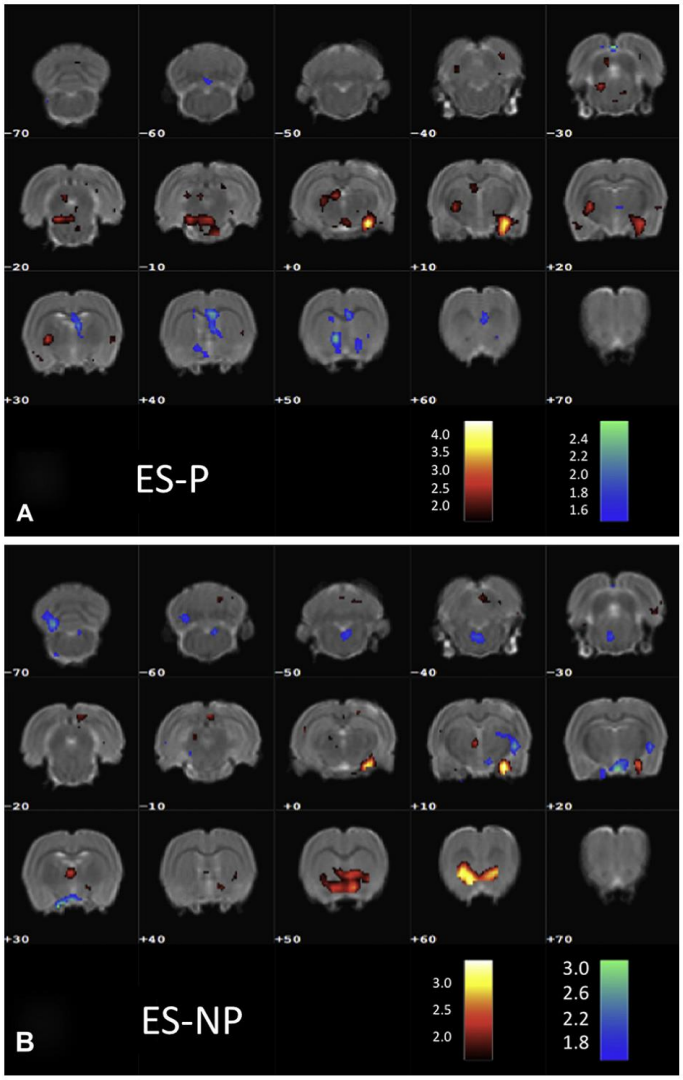

Fig. 2. Group statistical parametric maps of ES-P (A) and ES-NP (B) amygdaloid complex stimulation. Color coded t values vary from dark red to light yellow for statistically ($p < 0.05$) enhanced activation while light green to dark blue represent structure inhibition. We can observe similar activation (red/yellow blobs) in the amygdaloid complex for both stimuli paradigms (slices 0 to +20). However, ES-P produced contra-lateral activation spreading along thalamic and hippocampal structures whereas ES-NP activated more anterior/frontal structures, mainly nucleus accumbens.

shows much smaller BOLD changes, which are usually a single prolonged event, preventing signal averaging and frequently resulting in weak responses. In addition, these changes can be sometimes similar to normal scanner drifts (i.e. hardware and physiological), presenting further challenges since true signal might be embedded in normal drifts, being the case of PTZ infusion experiments (Figs. 3–5). Finally, the necessity of keeping the subjects under anaesthesia further contributes to physiological variability and, in consequence, to the instability of the BOLD signal (Pohlmann et al., 2007). However, the statistics used here are quite well accepted throughout literature for studies similar to the one presented (Ireland et al., 2005; Jones et al., 2005; Littlewood et al., 2006). Despite the higher risk of incurring in Type-II errors by using fixed-effects approach, several publications corroborated

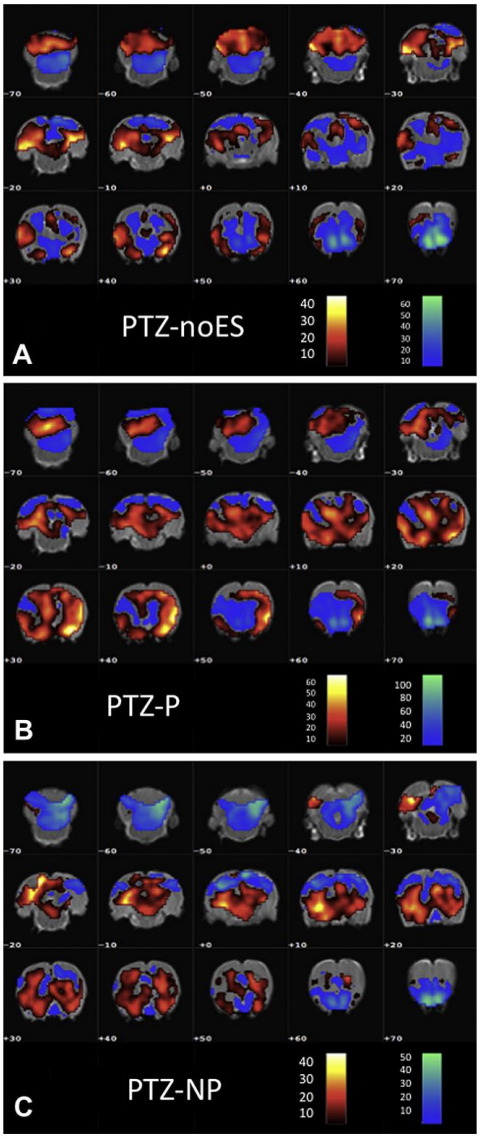

Fig. 3. Group statistical parametric maps of PTZ infused rats submitted to PTZ-noES (A – no estimulation), PTZ-P (B – periodic stimulation) or PTZ-NP (C – non-periodic stimulation). Color coded t values vary from dark red to light yellow for statistically ($p < 0.05$) enhanced activation while light green to dark blue represent structure inhibition. Slice sections varying from −7 mm to 7 mm, at a 1 mm interval, are shown for each stimulation paradigm. We can observe a similar activation pattern in all the groups. However, PTZ-P produces a more significant activation ipsilateral to the site of stimulation (right hemisphere slices +30 to +50), whereas PTZ-NP has a reduced activation pattern in slices ipsilateral to the site of stimulation (right hemisphere slices −20 to +20).

their BOLD results with other techniques such as 2-DG autoradiography (Littlewood et al., 2006; Pohlmann et al., 2007) and microdialysis (Littlewood et al., 2006) with good correlations.

Since PTZ is a GABAergic antagonist (Macdonald and Barker, 1977), it creates a non-specific condition of hyperexcitability necessary to induce seizures evoked by activating multiple reverberating neural circuits that are gradually recruited, and phase coupled, into the epileptogenic process. According to the theoretical work presented by Kudela et al. (2003), there should be an increased synchronization within circuits that have been excited and/or uninhibited. Although described in terms of bursting behavior of small neural network models, such theoretical work could explain why low doses of PTZ (<40/mg) typically evoke minimal seizures displaying myoclonic jerks, forelimb and head clonus and chewing (Velisek et al., 1992): fewer and more synchronized circuits are recruited. These behaviors are classically correlated with exacerbated activity of structures in the limbic system, including the amygdala and hippocampus (Eells et al., 2004), which represent a more restricted forebrain region that is more susceptible to PTZ action. In contrast, higher doses of the drug evoke minor seizures followed by major seizures with or without a tonic phase and generalized tonic–clonic behavior (Velisek et al., 1992), both correlated with activation of a broader brain territory that includes structures in hindbrain, midbrain and forebrain structures (Eells et al., 2004; Moraes et al., 2005b). These local and broader neural circuits are connected and synchronized during ictogenesis, as suggested by electrophysiological data (Moraes et al., 2005a), by means of physiological neuro-anatomical connections and a pathological hyperexcitable condition. From Fig. 3, it is clear that there is a bilateral recruitment of the PTZ-noES group; nevertheless, slices −20 and −10 (+0, although not significant, showed a similar tendency), even though PTZ was applied systemically, indicate ipsilateral lateralization. This apparent inconsistency could be explained by local lesion, in some rats, due to electrode placement. The damaged BBB would facilitate PTZ diffusion resulting in lateralized activation close to the electrode site. Electrical stimulation, although activating neural masses, would partially protect against BBB lesion thus explaining the non-lateralized T mean parameters, in the same slices, for the ES-P and ES-NP groups. In addition, our results show that an ES-P protocol favors ipsilateral abnormal brain connectivity (slices +30, +40, +50 and +60 of Fig. 3B and slices +30 and +40 of Fig. 4 – PTZ-P) and contra-lateral activation of posterior areas, most likely resultant from decussating fibers between forebrain–hindbrain connections. It is important to highlight that the dose of PTZ was invariable for all stimulation protocols and noES. In other words, by promoting synchronization and better coupling between different reverberating circuits, ES-P would recruit more neural masses and promote hyperexcitation. This would give rise to a myriad of stereotypical convulsive behaviors and cognitive deficits (Uhlhaas and Singer, 2006).

The fact that the mean T analysis (Fig. 4) did not statistically confirm the diminished ipsilateral activation of slices −20, −10, 0 and +10 (Fig. 3C) for the PTZ-NP group does not invalidate the anti-resonant hypothesis of NP stimulation. The lateralization analysis of Fig. 4 is much less anatomically specific than what is shown in Fig. 3, in effect, if smaller ROI were chosen, differences would become more evident. In addition, the lack of statistical difference, in terms of lateralization (Fig. 4 PTZ-NP), for more anterior slices is also suggestive of an anti-convulsive property of the NP stimulation paradigm. Thus, in order to better highlight the lateralizing effect of the stimulation paradigm during PTZ infusion, contrast Fig. 5A clearly shows an increased ipsilateral activity of periodic stimulation against non-periodic, regarding electrode placement, when compared to 5B NP against P (slices varying from −20 to +20 are clearly less compromised in panel B). Although

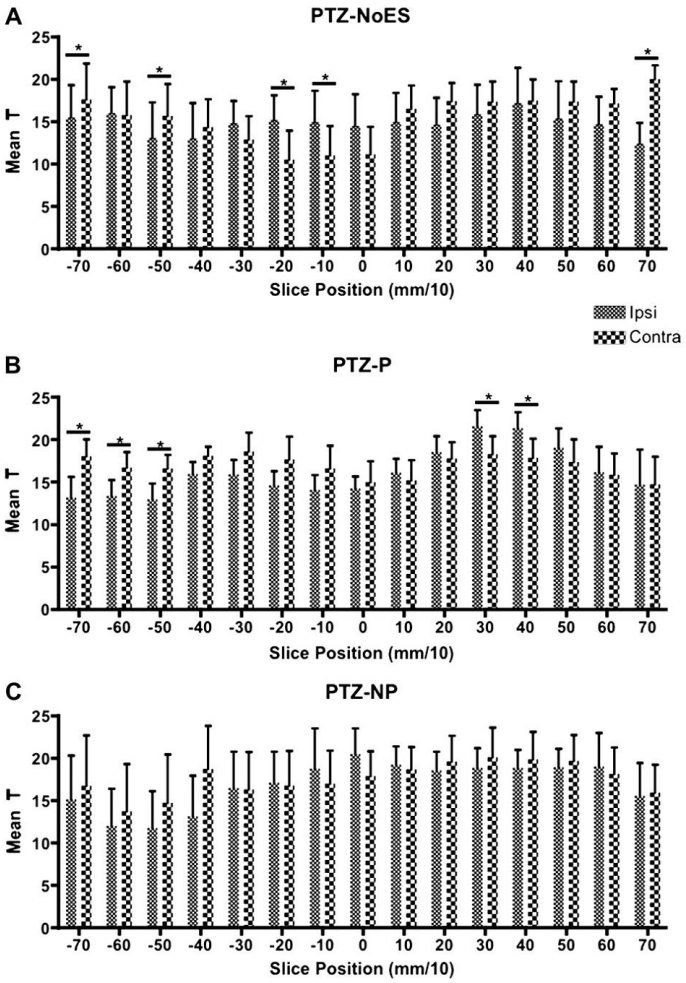

Fig. 4. In order to quantify lateralization of brain recruitment during seizure, the mean value of T for each hemisphere, from parametric maps of all recorded animals, was calculated for each anterior–posterior slice (−70 to +70 × 0.1 mm). The bar graphs show PTZ-noES (PTZ without electrical stimulus) in the top panel (A) while (B) and (C) show PTZ-P and PTZ-NP stimulation paradigms respectively (*represents $p < 0.05$; paired t-test between mean T values in the ipsi and contra-lateral hemispheres in each slice).

Figs. 2 and 5 come from different experiments, using different animals, the same activation observed in Fig. 2B (slice +60) is evident throughout the whole frontal area of Fig. 5B. Thus, it is possible that the anti-convulsive property of NP stimulation could be associated to both a direct desynchronization of temporal lobe structures (Figs. 3C and 5B slices −20 to 20), as discussed before, as well as an indirect activation of pre-frontal areas, know to inhibit temporal lobe substrates (McDonald et al., 1996). Nevertheless, the direct (through desynchronizing effect) and indirect (through activation of PTZ seizure-inhibitory frontal areas) hypothesis are not exclusive and could be interacting to produced an enhanced deactivation of slices −20 to +20 in Fig. 5B.

Using neural modeling, Tass and Hauptmann (2007) proposed that, depending on the stimulation protocol, a population of neurons could learn pathologically strong interactions (e.g. periodic stimulation) or, in contrast, desynchronizing stimulation, would promote the weakening of such abnormal synaptic interactions (multi-site non synchronous stimuli) and disrupt the epileptic process. Although there are some differences in terms of what is considered a temporally coded desynchronizing stimulus and the time scale of synaptic plasticity proposed, data presented here are, at least to some extent, a biological validation of theoretical mathematical modeling regarding the therapeutic properties of anti-resonant/desynchronizing low frequency ES for treating epilepsy.

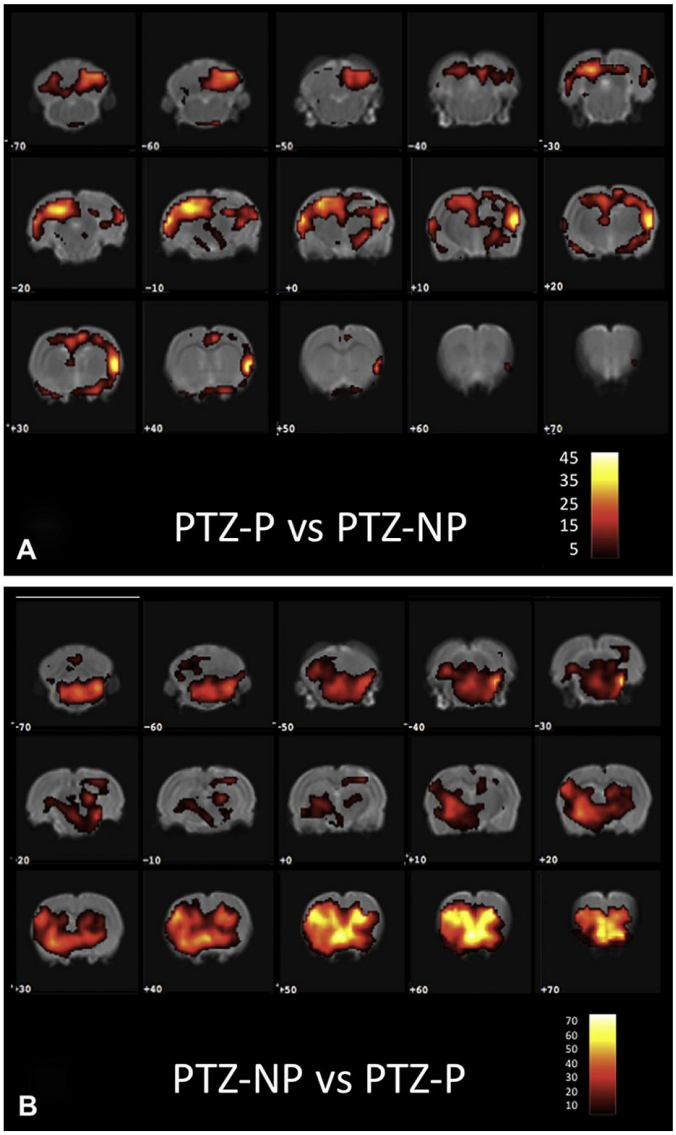

Fig. 5. Group statistical parametric maps of PTZ infused rats comparing PTZ-P (periodic stimulation) against PTZ-NP (non-periodic stimulation) in panel A, and PTZ-NP against PTZ-P in panel B. Color coded t values varying from dark red to light yellow represent voxels that present significantly enhanced activity when comparing the first group against the second. As explained in Figs. 2 and 3, slice sections vary from −7 mm to 7 mm at 1 mm intervals. Panel A clearly shows increased ipsilateral activity (i.e. electrode placement) when compared to panel B; in fact, slices varying from −20 to +20 are clearly less compromised in panel B.

The pro-convulsive effect of ES-P depicted in Fig. 3 has a much faster time scale (since the evolution of the entire recruitment happens within minutes) than that proposed by the before mentioned work (Tass and Hauptmann, 2007), which would be comparable to a "kindling like phenomenon". Nevertheless, adapting the theoretical modeling conclusions using short term synaptic changes would show how desynchronization in the course of the stimulation would be plausible thus explaining our results using ES-NP.

It is important to highlight that probably not all brain structures would respond to time-coded low frequency ES. The amygdaloid complex was chosen because of its role in the modulation and transfer of epileptiform activity in several animal models of temporal lobe epilepsy (Akirav and Richter-Levin, 2002; Moraes et al., 2005a,b; Vouimba and Richter-Levin, 2005). Supramaximal ES of the amygdala has been shown to produce hippocampal afterdischarge, whereas repetitive subthreshold ES induces plastic changes in the temporal lobe that culminate in epileptiform activity (Hirsch et al., 1997). The amygdaloid complex has monosynaptic afferents to and efferents from the parahippocampal areas (e.g., entorhinal cortex and subiculum) (Racine, 1972), providing the anatomical substrates for transfer and modulation of epileptic activity. In short, as the amygdala plays a key role in the synchronization process, acting as a modulator and a center for the transfer of epileptiform activity (Hirsch et al., 1997).

In summary, our understanding is that ES of the amygdala modulates seizure initiation and propagation through direct modulation of neural epileptiform activity in local as well as longer-range neural circuits. The periodic stimulation used in this study is in the frequency range of epileptiform activity, as revealed by electrophysiological studies (Moraes et al., 2005a) and, thus, may facilitate the synchronization of reverberant epileptiform networks in a positive resonant modulation. On the other hand, ES-NP promotes desynchronization and, thus, disrupts the positive feedback process of neural mass recruitment.

Our results use a new temporally coded form of ES that, along with the classical periodical stimulation, provide a biological validation of the effect of ES on neural desynchronizing and synchronizing activity, respectively. The impact of such findings on the treatment of epilepsies is even more promising if one considers that ES was kept within 4 stimuli per second. Such a strategy may overcome some unwanted collateral effects of classical HFS for the treatment of epilepsy, such as a higher energy transfer to brain tissue. However, much work must be done in order to better assess the synchronizing/desynchronizing effects of ES using multiple sites of stimulation and different animal models of epilepsy for biological validation.

Acknowledgements

We are grateful to CNPq, FAPEMIG, CAPES and PRPq/UFMG, for financial support. Márcio Flávio Dutra Moraes is recipient of CAPES and CNPq research fellowship. INCeMaq – National Institute of Science and Technology, also supported this work.

References

Akirav, I., Richter-Levin, G., 2002. Mechanisms of amygdala modulation of hippocampal plasticity. J. Neurosci. 22, 9912–9921.
Ben-Menachem, E., 2002. Vagus-nerve stimulation for the treatment of epilepsy. Lancet Neurol. 1, 477–482.
Benabid, A.L., Minotti, L., Koudsie, A., de Saint Martin, A., Hirsch, E., 2002. Antiepileptic effect of high-frequency stimulation of the subthalamic nucleus (corpus luysi) in a case of medically intractable epilepsy caused by focal dysplasia: a 30-month follow-up: technical case report. Neurosurgery 50, 1385–1391. discussion 1391–1392.
Binnie, C.D., 2000. Vagus nerve stimulation for epilepsy: a review. Seizure 9, 161–169.
Centeno, R.S., Yacubian, E.M., Sakamoto, A.C., Ferraz, A.F., Junior, H.C., Cavalheiro, S., 2006. Pre-surgical evaluation and surgical treatment in children with extra-temporal epilepsy. Childs Nerv. Syst. 22, 945–959.
Chabardes, S., Kahane, P., Minotti, L., Koudsie, A., Hirsch, E., Benabid, A.L., 2002. Deep brain stimulation in epilepsy with particular reference to the subthalamic nucleus. Epileptic Disord. 4 (Suppl. 3), S83–S93.
Cota, V.R., Medeiros Dde, C., Vilela, M.R., Doretto, M.C., Moraes, M.F., 2009. Distinct patterns of electrical stimulation of the basolateral amygdala influence pentylenetetrazole seizure outcome. Epilepsy Behav. 14 (Suppl. 1), 26–31.
DeGiorgio, C.M., Shewmon, D.A., Whitehurst, T., 2003. Trigeminal nerve stimulation for epilepsy. Neurology 61, 421–422.
Durand, D., 1993. Ictal patterns in experimental models of epilepsy. J. Clin. Neurophysiol. 10, 281–297.
Eells, J.B., Clough, R.W., Browning, R.A., Jobe, P.C., 2004. Comparative fos immunoreactivity in the brain after forebrain, brainstem, or combined seizures induced by electroshock, pentylenetetrazol, focally induced and audiogenic seizures in rats. Neuroscience 123, 279–292.
Engel Jr., J., 1996. Introduction to temporal lobe epilepsy. Epilepsy Res. 26, 141–150.
Fanselow, E.E., Reid, A.P., Nicolelis, M.A., 2000. Reduction of pentylenetetrazole-induced seizure activity in awake rats by seizure-triggered trigeminal nerve stimulation. J. Neurosci. 20, 8160–8168.
French, J.A., 2007. Refractory epilepsy: clinical overview. Epilepsia 48 (Suppl. 1), 3–7.
Freund, H.J., 2005. Long-term effects of deep brain stimulation in Parkinson's disease. Brain 128, 2222–2223.
Gale, K., 1992. Subcortical structures and pathways involved in convulsive seizure generation. J. Clin. Neurophysiol. 9, 264–277.
Hamani, C., Ewerton, F.I., Bonilha, S.M., Ballester, G., Mello, L.E., Lozano, A.M., 2004. Bilateral anterior thalamic nucleus lesions and high-frequency stimulation are protective against pilocarpine-induced seizures and status epilepticus. Neurosurgery 54, 191–195. discussion 195–197.
Hauser, W.A., Rich, S.S., Lee, J.R., Annegers, J.F., Anderson, V.E., 1998. Risk of recurrent seizures after two unprovoked seizures. N. Engl. J. Med. 338, 429–434.
Hirsch, E., Danober, L., Simler, S., Pereira de Vasconcelos, A., Maton, B., Nehlig, A., Marescaux, C., Vergnes, M., 1997. The amygdala is critical for seizure propagation from brainstem to forebrain. Neuroscience 77, 975–984.
Hodaie, M., Wennberg, R.A., Dostrovsky, J.O., Lozano, A.M., 2002. Chronic anterior thalamus stimulation for intractable epilepsy. Epilepsia 43, 603–608.
Ireland, M.D., Lowe, A.S., Reavill, C., James, M.F., Leslie, R.A., Williams, S.C., 2005. Mapping the effects of the selective dopamine D2/D3 receptor agonist quinelorane using pharmacological magnetic resonance imaging. Neuroscience 133, 315–326.
Jones, N., O'Neill, M.J., Tricklebank, M., Libri, V., Williams, S.C., 2005. Examining the neural targets of the AMPA receptor potentiator LY404187 in the rat brain using pharmacological magnetic resonance imaging. Psychopharmacology (Berl.) 180, 743–751.
Keogh, B.P., Cordes, D., Stanberry, L., Figler, B.D., Robbins, C.A., Tempel, B.L., Green, C.G., Emmi, A., Maravilla, K.M., Schwartzkroin, P.A., 2005. BOLD-fMRI of PTZ-induced seizures in rats. Epilepsy Res. 66, 75–90.
Kudela, P., Franaszczuk, P.J., Bergey, G.K., 2003. Changing excitation and inhibition in simulated neural networks: effects on induced bursting behavior. Biol. Cybern. 88, 276–285.
Kumar, R., Lozano, A.M., Sime, E., Lang, A.E., 2003. Long-term follow-up of thalamic deep brain stimulation for essential and parkinsonian tremor. Neurology 61, 1601–1604.
Littlewood, C.L., Jones, N., O'Neill, M.J., Mitchell, S.N., Tricklebank, M., Williams, S.C., 2006. Mapping the central effects of ketamine in the rat using pharmacological MRI. Psychopharmacology (Berl.) 186, 64–81.
Loscher, W., Schmidt, D., 2002. New horizons in the development of antiepileptic drugs. Epilepsy Res. 50, 3–16.
Macdonald, R.L., Barker, J.L., 1977. Pentylenetetrazol and penicillin are selective antagonists of GABA-mediated post-synaptic inhibition in cultured mammalian neurones. Nature 267, 720–721.
McDonald, A.J., Mascagni, F., Guo, L., 1996. Projections of the medial and lateral prefrontal cortices to the amygdala: a Phaseolus vulgaris leucoagglutinin study in the rat. Neuroscience 71, 55–75.
McIntyre, C.C., Grill, W.M., 2001. Finite element analysis of the current-density and electric field generated by metal microelectrodes. Ann. Biomed. Eng. 29, 227–235.
McIntyre, C.C., Savasta, M., Kerkerian-Le Goff, L., Vitek, J.L., 2004a. Uncovering the mechanism(s) of action of deep brain stimulation: activation, inhibition, or both. Clin. Neurophysiol. 115, 1239–1248.
McIntyre, C.C., Savasta, M., Walter, B.L., Vitek, J.L., 2004b. How does deep brain stimulation work? Present understanding and future questions. J. Clin. Neurophysiol. 21, 40–50.
Mirski, M.A., Rossell, L.A., Terry, J.B., Fisher, R.S., 1997. Anticonvulsant effect of anterior thalamic high frequency electrical stimulation in the rat. Epilepsy Res. 28, 89–100.
Moraes, M.F., Chavali, M., Mishra, P.K., Jobe, P.C., Garcia-Cairasco, N., 2005a. A comprehensive electrographic and behavioral analysis of generalized tonic–clonic seizures of GEPR-9s. Brain Res. 1033, 1–12.
Moraes, M.F., Garcia-Cairasco, N., 1997. Glass pipette-carbon fiber microelectrodes for evoked potential recordings. Braz. J. Med. Biol. Res. 30, 1319–1324.
Moraes, M.F., Mishra, P.K., Jobe, P.C., Garcia-Cairasco, N., 2005b. An electrographic analysis of the synchronous discharge patterns of GEPR-9s generalized seizures. Brain Res. 1046, 1–9.
Paxinos, G., Watson, C., 1998. The Rat Brain in Stereotaxic Coordinates. Academic, San Diego, London, pp. xxvi, 236 pp.
Pohlmann, A., Barjat, H., Tilling, L.C., James, M.F., 2007. Pharmacological fMRI – challenges in analysing drug-induced single-event BOLD responses. Conf. Proc. IEEE Eng. Med. Biol. Soc. 2007, 3411–3416.
Racine, R.J., 1972. Modification of seizure activity by electrical stimulation. I. After-discharge threshold. Electroencephalogr. Clin. Neurophysiol. 32, 269–279.
Rodriguez-Oroz, M.C., Obeso, J.A., Lang, A.E., Houeto, J.L., Pollak, P., Rehncrona, S., Kulisevsky, J., Albanese, A., Volkmann, J., Hariz, M.I., Quinn, N.P., Speelman, J.D., Guridi, J., Zamarbide, I., Gironell, A., Molet, J., Pascual-Sedano, B., Pidoux, B., Bonnet, A.M., Agid, Y., Xie, J., Benabid, A.L., Lozano, A.M., Saint-Cyr, J., Romito, L., Contarino, M.F., Scerrati, M., Fraix, V., Van Blercom, N., 2005. Bilateral deep brain stimulation in Parkinson's disease: a multicentre study with 4 years follow-up. Brain 128, 2240–2249.

Snead 3rd, O.C., 1992. Pharmacological models of generalized absence seizures in rodents. J. Neural. Transm. (Suppl. 35), 7–19.
Spencer, S.S., 2002. When should temporal-lobe epilepsy be treated surgically? Lancet Neurol 1, 375–382.
Tass, P.A., Hauptmann, C., 2007. Therapeutic modulation of synaptic connectivity with desynchronizing brain stimulation. Int. J. Psychophysiol. 64, 53–61.
Theodore, W.H., Fisher, R.S., 2004. Brain stimulation for epilepsy. Lancet Neurol. 3, 111–118.
Timofeev, I., Steriade, M., 2004. Neocortical seizures: initiation, development and cessation. Neuroscience 123, 299–336.
Uhlhaas, P.J., Singer, W., 2006. Neural synchrony in brain disorders: relevance for cognitive dysfunctions and pathophysiology. Neuron 52, 155–168.
Valencia, I., Holder, D.L., Helmers, S.L., Madsen, J.R., Riviello Jr., J.J., 2001. Vagus nerve stimulation in pediatric epilepsy: a review. Pediatr. Neurol. 25, 368–376.
Velisek, L., Kubova, H., Pohl, M., Stankova, L., Mares, P., Schickerova, R., 1992. Pentylenetetrazol-induced seizures in rats: an ontogenetic study. Naunyn Schmiedebergs Arch. Pharmacol. 346, 588–591.
Volkmann, J., 2004. Deep brain stimulation for the treatment of Parkinson's disease. J. Clin. Neurophysiol. 21, 6–17.
Volkmann, J., Allert, N., Voges, J., Sturm, V., Schnitzler, A., Freund, H.J., 2004. Long-term results of bilateral pallidal stimulation in Parkinson's disease. Ann. Neurol. 55, 871–875.
Vonck, K., Boon, P., Achten, E., De Reuck, J., Caemaert, J., 2002. Long-term amygdalohippocampal stimulation for refractory temporal lobe epilepsy. Ann. Neurol. 52, 556–565.
Vonck, K., Boon, P., Claeys, P., Dedeurwaerdere, S., Achten, R., Van Roost, D., 2005. Long-term deep brain stimulation for refractory temporal lobe epilepsy. Epilepsia 46 (Suppl. 5), 98–99.
Vouimba, R.M., Richter-Levin, G., 2005. Physiological dissociation in hippocampal subregions in response to amygdala stimulation. Cereb. Cortex 15, 1815–1821.
Wiebe, S., Blume, W.T., Girvin, J.P., Eliasziw, M., 2001. A randomized, controlled trial of surgery for temporal-lobe epilepsy. N. Engl. J. Med. 345, 311–318.
Wuttke, T.V., Lerche, H., 2006. Novel anticonvulsant drugs targeting voltage-dependent ion channels. Expert Opin. Investig. Drugs 15, 1167–1177.

Artigos publicados durante o mestrado relacionado com a tese

Epilepsy & Behavior 14 (2009) 26–31

Contents lists available at ScienceDirect

Epilepsy & Behavior

journal homepage: www.elsevier.com/locate/yebeh

Distinct patterns of electrical stimulation of the basolateral amygdala influence pentylenetetrazole seizure outcome

Vinícius Rosa Cota [a,b], Daniel de Castro Medeiros [b], Maura Regina Silva da Páscoa Vilela [b], Maria Carolina Doretto [b], Márcio Flávio Dutra Moraes [b,*]

[a] Instituto Internacional de Neurociências de Natal Edmond e Lily Safra, Natal-RN, Brazil
[b] Núcleo de Neurociências (NNC), Departamento de Fisiologia e Biofísica, ICB, UFMG, Av. Antonio Carlos, 6627 CEP 31270-901 Campus Pampulha, Belo Horizonte-MG, Brazil

ARTICLE INFO

Article history:
Received 7 August 2008
Revised 4 September 2008
Accepted 5 September 2008

Keywords:
Basolateral amygdala
Pentylenetetrazole
Synchronization
Desynchronization
Electrical stimulation
Seizure suppression
Behavior modulation
Synfire chains

ABSTRACT

Our working hypothesis is that constant interpulse interval (IPI) electrical stimulation would resonate with endogenous epileptogenic reverberating circuits, inducing seizures, whereas a random interinterval electrical stimulation protocol would promote desynchronization of such neural networks, producing an anticonvulsant effect. Male Wistar rats were stereotaxically implanted with a bipolar electrical stimulation electrode in the amygdala. Pentylenetetrazole (10 mg/ml/min) was continuously infused through an intravenous catheter to induce seizures while four different patterns of temporally coded electrical stimulation were applied: periodic stimulation (PS), pseudo-randomized IPI stimulation (LH), restrictively randomized IPI stimulation (IH), and bursts of 20-ms IPIs (burst). PS decreased the pentylenetetrazole threshold to forelimb clonus, whereas IH increased the threshold to forelimb clonus and to generalized tonic–clonic seizures. We hypothesize that PS facilitates forelimb clonus by reverberating with epileptogenic circuits in the limbic system, whereas IH delays forelimb clonus and generalized tonic–clonic seizures by desynchronizing the epileptic neural networks in the forebrain–midbrain–hindbrain circuits.

1. Introduction

In about one-fourth of persons with epilepsy, seizures are not satisfactorily controlled with pharmacological treatment [1–3]. In addition, many of these patients with refractory epilepsy are not eligible for ablative surgery, which, in most cases, requires a readily identifiable epileptogenic focus [4–6]. A more recent alternative available for these patients is electrical stimulation (ES) of the nervous system [7]. ES may be applied peripherally in structures such as the vagus nerve (vagus nerve stimulation) [8–10] and the trigeminal nerve (trigeminal nerve stimulation) [11,12] or targeted to a variety of structures in the central nervous system (deep brain stimulation) [13–15], most predominantly the anterior nucleus of the thalamus [16,17], the subthalamic nuclei [18,19], and the epileptogenic focus itself [20]. Classically, continuous or intermittent high-frequency ES (high-frequency stimulation) is the overall adopted pattern for an anticonvulsant effect, whereas low-frequency ES (low-frequency stimulation) is generally believed to be proconvulsant [7].

Although targeting of different neural substrates with ES has proved to be an effective approach to controlling seizures [7], the underlying mechanisms of seizure suppression are still poorly understood [21,22]. Classically, there are two main philosophies regarding neural substrate excitability to explain the clinical benefits of ES in epilepsy: (1) ES works by suppressing or inhibiting epileptogenic structures, which is analogous to the functional ablation performed by neurosurgery; or (2) ES works by activating or stimulating neural networks that would modulate seizure-like activity. In fact, it has been reported that changing either ES parameters (e.g., amplitude, frequency, and wave morphology) or the structure targeted may influence the effect of ES on seizure control, in some cases even resulting in seizure potentiation [23]. This work addresses a different paradigm, in which ES may also play a critical role in neural synchronization depending on the temporal pattern used (i.e., pulses not distributed evenly in time), even though overall frequency of stimulation, amplitude, and electrode placement are maintained constant. In particular, the use of temporally coded/low-frequency ES may bring significant improvement in the undesired side effects of ES of neural structures.

The existence of epileptogenic neural networks that gradually synchronize by means of oscillatory reverberating circuits has been suggested in animal models of epilepsy, for example, the Genetic Epilepsy Prone Rat (GEPR). Moraes et al. [24] proposed that the EEG spike morphology signature found in the GEPR-9 seizure is the result of sequential and recurrent involvement of

* Corresponding author. Fax: +55 31 3499 2924.
E-mail address: mfdm@icb.ufmg.br (M.F.D. Moraes).

1525-5050/$ - see front matter © 2008 Elsevier Inc. All rights reserved.
doi:10.1016/j.yebeh.2008.09.006

forebrain–midbrain–hindbrain neural substrates. Moreover, in the GEPR tonic–clonic seizure, the interspike interval increases linearly after each spike [25], which would corroborate the theory of a reverberating circuit that would gradually compromise neural communication between elements in the loop due to either metabolic or neurochemical stress. Accordingly, the reverberating neural networks that oscillate and generate epileptiform activity would be modulated either by setting any element of the reverberating loop in a refractory state or by desynchronizing the sequential involvement of such elements. Our working hypothesis is that an ES protocol consisting of fixed-frequency ES that would resonate with endogenous epileptogenic reverberating circuits would induce seizures, whereas a nonperiodic (e.g., random) ES protocol would promote desynchronization of such neural networks, thus behaving as an anticonvulsant.

In the present report, the basolateral amygdala was chosen as the ES target using the pentylenetetrazole (PTZ) animal model of epilepsy. The amygdaloid complex was chosen because of its role in the modulation and transfer of epileptiform activity in several animal models of temporal lobe epilepsy [26–29]. Supramaximal ES of the amygdala has been shown to produce hippocampal afterdischarge, whereas repetitive subthreshold ES induces plastic changes in the temporal lobe that culminate in epileptiform activity [30]. The amygdaloid complex has monosynaptic afferents to and efferents from the parahippocampal areas (e.g., entorhinal cortex and subiculum) [31], providing the anatomical substrates for transfer and modulation of epileptic activity. In this work, we tested the hypothesis that low-frequency ES (four stimuli per second) of the basolateral amygdala would differentially modulate seizure outcome in PTZ-treated animals if applied at either (1) constant intervals or (2) randomly spaced intervals.

2. Methods

All experiments were done in accordance with the Ethical Committee for Animal Experimentation (Comitê de Ética em Experimentação Animal—CETEA) of the Federal University of Minas Gerais (Universidade Federal de Minas Gerais—UFMG), and Procedures for animal care were previously approved by this organization under Protocol 150/06.

We designed and built an electrical stimulator composed of a constant-current isolation unit driven by a PC-programmable clocking system. C++ software was developed to program the stimulator with four patterns of temporally coded stimuli, all delivering a total of four pulses per second (to guarantee the same energy flow): (1) constant interpulse intervals (IPIs) of 250 ms (periodic); (2) bursts with 20-ms IPIs (burst); (3) pseudo-randomized IPIs (linear decay histogram [LH stimulation]); and (4) restrictively randomized IPIs (inverse decay histogram [IH stimulation]). These temporal patterns are depicted in Fig. 1 along with their corresponding average histograms. The LH pattern was obtained by sorting four time stamps in a 1-s interval out of a uniform distribution using an internal library function. The IH pattern was obtained using the same built-in function with the following algorithm: (A) sort an interval *T1* in the range 20–940 ms, wait *T1,* and fire pulse; (B) sort an interval *T2* in the range *T1* + 20 ms to 960 ms, wait *T2,* and repeat pulse; (C) repeat B twice until four pulses are fired and wait to complete the second. A minimum biologically plausible separation of 20 ms between pulses was observed in all patterns. Pulses were square, positive monophasic waves of 100-μs duration with amplitudes varying from 100 to 350 μA.

A total of 74 male Wistar rats from Centro de Bioterismo (CEBIO) of UFMG were randomly assigned to each stimulus group on the day of the experiment (periodic $n = 19$, burst $n = 6$, LH $n = 9$, IH $n = 14$) and also to an extra nonstimulated control group (control $n = 26$); adjustments were made to maintain a minimum number of animals in each group. Mean weight did not differ significantly between groups (control: 306 ± 11 g, periodic: 292 ± 12 g, burst: 245 ± 12 g, LH: 253 ± 13 g, and IH: 313 ± 13 g, one-way ANOVA). All animals underwent a surgical procedure for implantation of a bipolar stimulation electrode. Electrodes were made of a twisted pair of stainless-steel (0.005 in.), Teflon-coated wires (Model 791400, A-M Systems Inc., Carlsborg, WA, USA). Animals were anesthetized via systemic sodium thiopental injection (40 mg/kg) and locally with lidocaine clorohydrate plus epinephrine (2%) and then positioned in a stereotaxic frame (Stoelting Co., Wood Dale, IL, USA). Coordinates for the right basolateral amygdala (AP = 2.8 mm, ML = 5.0 mm referenced from the bregma suture and 7.2 mm from dura mater) were derived from the Paxinos and Watson's atlas for rats [32]. Animals were pretreated with pentabiotics (19 mg/kg) and flunixin (2.5 mg/kg). After correct positioning, the electrode was fixed to the skull with zinc cement and soldered to a telephone jack (Model RJ-45 6x6), which was fixed onto the skull with dental acrylic. A 5- to 7-day post-operative recovery period was observed before stimulation began. On the day before the experiment, animals received very low frequency (0.25 Hz) ES of increasing current amplitude to determine the stimulus threshold, defined as the lowest amplitude of current capable of evoking observable and distinguishable twitching behavior. On the day of the experiment, animals were caudally cannulated for intravenous infusion of PTZ (Sigma) diluted in saline at a concentration of 10 mg/ml. The cannula was connected to an infusion pump set at the rate of 1 ml/min. The ES was initiated 10 s before beginning the infusion. The latencies to onset of forelimb clonus and tonic–clonic seizures were determined and were correlated with the injected PTZ dose. All experiments were recorded on VHS tape for behavioral analysis. After stimulation, brains were electrically lesioned (0.5 mA for 2 s) and immediately removed, sliced, and stained with neutral red (2%) for histological confirmation of electrode position. Animals that survived 60 min after the end of the experiment ($n = 4$) were anesthetized with urethane (140 mg/kg) and transcardially perfused with formaldehyde (4%) before brain removal and histology procedures. Animals with incorrect positioning of electrodes were not included in our analysis. PTZ dose data were normalized by body weight (PTZ threshold), and the results were analyzed with one-way ANOVA and assessed post hoc with the Tukey multiple comparison test. Survival ratio and occurrence of uncommon PTZ-induced behaviors, such as facial clonus, rearing and falling, and whole-body tonus, were assessed with contingency tables and Fisher's exact test. Data were considered to be statistically significant at $P < 0.05$.

3. Results

All animals, except for the saline-injected control group, displayed the convulsive behavior sequence typical of the PTZ model. This consisted of a first myoclonic jerk, followed by forelimb clonus (FC), generalized clonus, and generalized tonic–clonic seizures (GTCSs) [33]. Some seizure-related behavior was confused with the twitching reaction to ES; thus, only the occurrence of forelimb clonus and tonic-clonic seizures could be adequately quantified.

Distinct patterns of ES differentially modulated the latency to FC ($P < 0.0001$, one-way ANOVA) and GTCSs ($P < 0.0001$, one-way ANOVA), as shown in Figs. 2A and B, respectively. The PTZ threshold for FC was significantly reduced by periodic stimulation when compared with control ($P < 0.05$, post hoc Tukey test) and IH stimulation ($P < 0.001$, post hoc Tukey test). Neither burst nor LH

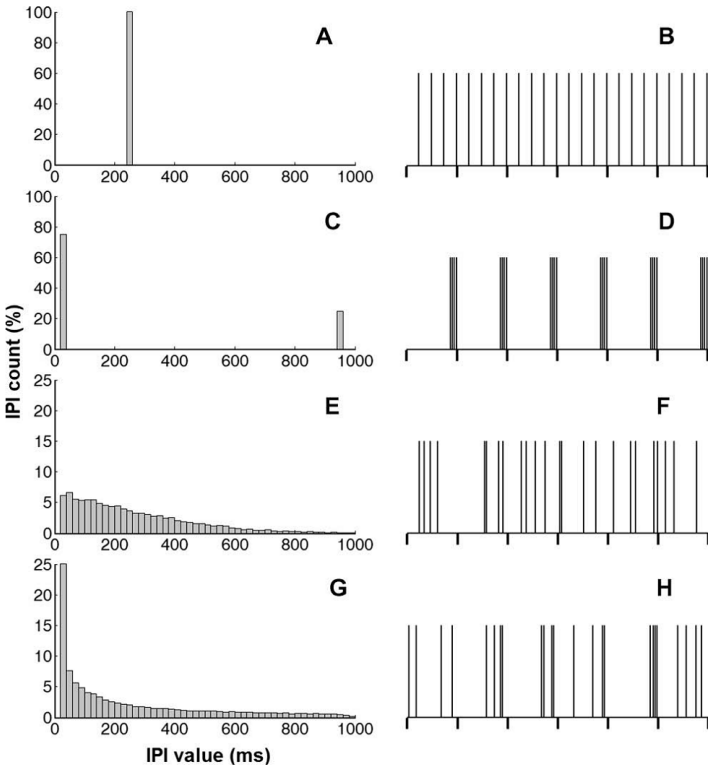

Fig. 1. Rats were stimulated with four different temporal patterns depicted here in descending order of rows: periodic (A, B), burst (C, D), LH (E, F), and IH (G, H). Left: IPI histograms. Right: typical realization of each pattern. The thick vertical lines below the *x* axis in the right panels mark the consecutive 1-s time windows considered for randomizing IPIs. Note there are always four pulses between each pair of these marks, guaranteeing the same mean energy flow for all patterns.

stimulation changed the FC PTZ threshold. Nevertheless, IH stimulation significantly increased threshold to FC when compared with all groups ($P < 0.05$ against control and burst, $P < 0.01$ against LH, and $P < 0.001$ against periodic, post hoc Tukey tests). Moreover, IH stimulation robustly increased (by almost twofold) the PTZ threshold to GTCSs when compared with all other groups ($P < 0.001$ against all groups, post hoc Tukey test). Periodic stimulation and other patterns had no overt effects on GTCSs when compared in a pairwise manner.

Rearing behavior, very uncommon in PTZ models [33], was observed in the periodic and IH groups (Table 1) when compared with the control group, with statistical significance ($P < 0.01$ and $P < 0.05$, respectively, Fisher's exact test). Finally, three animals in the IH group, one in the periodic group, and none in the other groups survived. Survival rate of the IH group was statistically greater than that for other groups pooled together, as assessed in Table 2 ($P < 0.05$, Fisher's exact test).

There were no statistically relevant correlations among weight, current, behavior threshold, and behavior occurrence in any groups (data not shown).

4. Discussion

The results clearly indicate that distinct temporal patterns of ES, when applied to the amygdala, differentially modulate PTZ-induced seizure behavior in a rodent model. The effects observed in this study could be predicted by a comprehensive theory of ictogenesis which takes in consideration not only hyperexcitability, but also, and more importantly, hypersynchronism and reverberating neural networks. In this sense, all three mechanisms must be kept in mind to adequately explain the results described.

As PTZ is a GABAergic antagonist [34], it creates a nonspecific condition of hyperexcitability necessary to induce seizures evoked by multiple reverberating neural circuits that are gradually recruited into the epileptogenic process as the drug is absorbed. In fact, low doses of PTZ (<40/mg) typically evoke minimal seizures displaying myoclonic jerks, forelimb and head clonus, and chewing [33]. These behaviors are classically correlated with exacerbated activity of structures in the limbic system, including the amygdala and hippocampus [35], which represent a more restricted forebrain region. In contrast, higher doses of the drug evoke minor seizures followed by major seizures with or without a tonic phase and generalized tonic–clonic behavior [33], both correlated with activation of a broader brain territory that includes structures in the hindbrain, midbrain, and forebrain [24,35]. These local and broader neural circuits are connected and synchronized during ictogenesis, as suggested by electrophysiological data [25], by means of physiological neuroanatomical connections and a pathological hyperexcitable condition. This gives rise to a myriad of stereotypical convulsive behaviors and cognitive deficits [36]. Finally, some

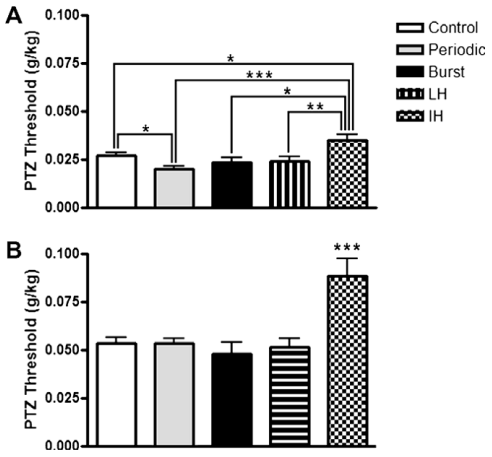

Fig. 2. PTZ threshold for two convulsive behaviors—forelimb clonus (A) and generalized tonic–clonic seizures (B)—according to stimulus pattern. IH stimulation increased drug threshold for both forelimb clonus and generalized tonic–clonic seizures when compared with all groups (both $P < 0.0001$, one way ANOVA; $^{*}P < 0.05$, $^{**}P < 0.01$, $^{***}P < 0.001$, all post hoc Tukey). Moreover, periodic stimulation decreased drug threshold for forelimb clonus ($P < 0.05$, post hoc Tukey).

Table 1
Contingency table for occurrence of rearing behavior

	With rearing	Without rearing
Control	0	26
Periodic[a]	6	13
Burst	0	6
LH	0	9
IH[b]	4	10

[a,b] Periodic and IH stimulated groups manifested more rearing behavior compared with the control group ([a]$P < 0.01$ and [b]$P < 0.05$, respectively, Fischer's exact test).

Table 2
Contingency table for survival ratio[a]

	Survived	Died
IH stimulus	3	11
Others	1	59

[a] All other groups (periodic, burst, LH, and control) have been pooled together under "Others."

structures, such as the amygdala play a key role in this synchronization process, acting as a modulator and a center for the transfer of epileptiform activity [29].

Our understanding is that ES of the amygdala modulates convulsive behavior through direct modulation of neural epileptiform activity in local as well as broader neural circuits, in a manner similar to that by which the structure acts during normal activity. The periodic stimulation used in this study is in the frequency range of epileptiform activity, as revealed by electrophysiological studies [25] and, thus, may facilitate forelimb clonus by adding energy to the limbic system in a resonating fashion. In contrast, we hypothesize that IH stimulation impairs reverberation of the limbic system (local) and forebrain–midbrain–hindbrain (broader) circuits through an antiresonating effect in each of them and also through blockage of synchronizing mechanisms among them. The effect results in the increase in PTZ threshold to forelimb clonus and generalized tonic–clonic seizures observed here.

Interestingly, rearing is a very uncommon behavior in the PTZ model and is said to be masked inside the GTCSs that would predominate in the motor expression [35]. Nevertheless, periodic stimulation increases its occurrence probably due to a facilitation process capable of unmasking it from GTCSs. By the same token, the increased rearing caused by IH stimulation is probably due to an unmasking process of delaying GTCSs. One could hypothesize that if rearing was normally observed in the PTZ model, periodic stimulation would decrease its threshold, and IH would have no effects. A direct consequence of this reasoning is to design analogous experiments using different animal models of epilepsy that display limbic seizures (e.g., audiogenic kindling of WARs, amygdala electrical kindling, acute and spontaneous pilocarpine-induced seizures).

The difference in seizure threshold between LH and IH is not easily understood, and further manipulations of the temporal pattern of stimulation may help clarify the basis for this phenomenon. Although they have a distribution over a wide range of IPI values, the histograms of LH and IH have very distinct shapes. The LH histogram can be fit ($R^2 = 0.98$) by a linear equation of inclination close to $-1/100$, whereas IH is fit ($R^2 = 0.98$) by a power equation of exponent close to -1 (Figs. 3A and B, respectively). A first consequence of these different shapes is that each of them accumulates IPI occurrences in distinct ranges. Two differences are worth noting. First, LH has a higher count of IPI in the range 220–280 ms (Fig. 3C) than does IH. As mentioned before, this is in the range of epileptiform activity frequency of discharge, and thus, IPIs in this range are probably resonating and convulsant, as suggested by the periodic group. Additionally, IH has a considerably higher count of IPIs within the range 20–100 ms than does LH (Fig. 3D). One could assume that this means IH has a higher content of high-frequency stimulation, thus corroborating previous work, mainly on deep-brain stimulation, which would have anticonvulsant properties. However, this is not true, once high-frequency stimulation is delivered at frequencies over 100 Hz [7,21,35] to produce its inhibitory effects. Also, burst stimulation in this study, which is composed mainly of brief periods of high-frequency stimulation, was not effective in suppressing seizures. The authors propose an alternative hypothesis that relies on the recognition of different temporal codes of pulses or cortical motifs, also called *cortical songs* [37], by specialized neuronal circuits arranged, for example, as the synfire chains [38]. The existence of such circuits is strongly suggested by experimental studies [39–41]; a series of biologically plausible proposals have been described [42–45] and their features have been modeled and studied in silico [38,46–48]. According to these studies, pattern recognition circuits would reverberate when neuronal inputs have a specific well-defined temporal structure [38], and two or more of these circuits may synchronously couple when sharing the same temporal pattern of activity [49]. Finally, cortical motifs have strict timing constraints, and their constitutive pulses must be grouped within a certain time limit. Although there is no consensus on a value, some authors suggest that the whisking frequency (10 Hz or 100-ms period) is a restrictive time window for somatosensory processing [39]. In this sense, our understanding is that IH randomly activates multiple distinct circuits by "sending" randomized cortical motifs through efferents of the amygdala at a much faster rate than does LH, because it has a higher count of short IPIs in the range 20–100 ms. This would severely impair neural synchronization of local circuits, once they are activated by distinct patterns, preventing them from being coupled. It would also impair the transfer of epileptiform activity to broader circuits once the amygdala would fire in a pattern that may be not synchronized.

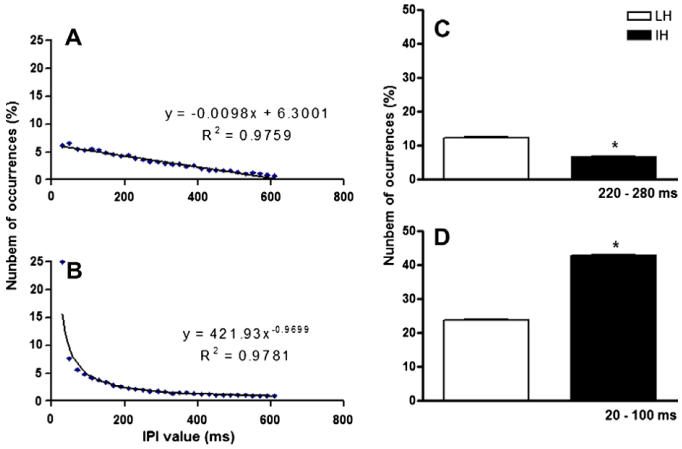

Fig. 3. Curve fitting for the mean histogram ($n = 8$ simulated histograms) of the two randomized stimulus patterns. The LH mean histogram is fit by a linear equation of inclination close to −1/100 (A), and the IH mean histogram is fit by a power curve of exponential close to −1 (B), both with high correlation factors ($R^2 = 0.9759$ and $R^2 = 0.9781$, respectively). This causes IH to have a lower IPI count in the epileptogenic range 220–280 ms (C) ($P < 0.0001$, Student's t test) and a higher IPI count in the range 20–100 ms (D) ($P < 0.0001$, Student's t test) compared with LH.

In short, a reasonable hypothesis for the difference between the two stimulation patterns is based on the proportions of resonating and antiresonating power present in each of them. The proportions of antiresonating and resonating power of LH stimulation patterns would not be high enough, probably close to one in a proper scale, canceling each other out. In contrast, the IH pattern would have a proportion such that the antiresonating power would overcome resonating power by far. This would make IH a seizure-suppressing stimulus, whereas LH would have no effect. A possible way to correlate antiresonating power with a randomized pattern construction algorithm would be to apply different limits around fixed 4-Hz time stamps (0, 250, 500, and 750 ms) for randomization of pulses and analyzing their effects in seizure suppression.

Our results suggest that desynchronizing neural activity by neurostimulation is an alternative to be considered in the treatment of epileptic disorders in clinical practice. A next logical step would be to run clinical trials of human deep-brain stimulation activated in LH and IH patterns. Such a strategy may overcome some unwanted collateral effects of classic high-frequency stimulation for the treatment of human epilepsy, such as a higher energy transfer to brain tissue. However, much work must be done in animal models to better assess the synchronizing/desynchronizing effects of ES. Moreover, behavior modulation through random patterns and other temporal codes of stimulation may provide fruitful insights into the mechanisms of seizure genesis, propagation, and termination.

Conflict of interest statement

The authors state that no other people or organization have inappropriately influenced this work. Therefore, there is no pertinent claim of a conflict of interest.

Acknowledgments

We are grateful to Gioconda Alves de Assumpção for technical assistance and to CNPq, FAPEMIG, CAPES, and PRPq /UFMG for financial support. Márcio Flávio Dutra Moraes and Maria Carolina Doretto are recipients of CNPq research fellowships.

References

[1] French JA. Refractory epilepsy: clinical overview. Epilepsia 2007;48(Suppl. 1):3–7.
[2] Löscher W, Schmidt D. New horizons in the development of antiepileptic drugs. Epilepsy Res 2002;50:3–16.
[3] Wuttke TV, Lerche H. Novel anticonvulsant drugs targeting voltage-dependent ion channels. Expert Opin Invest Drugs 2006;15:1167–77.
[4] Centeno R, Yacubian E, Sakamoto E, Ferraz A, Carrete Junior H, Cavalheiro S. Pre-surgical evaluation and surgical treatment in children with extratemporal epilepsy. Child's Nerv Syst 2006;22:945–59.
[5] Wiebe S, Blume WT, Girvin JP, Eliasziw M. For the Effectiveness and Efficiency of Surgery for Temporal Lobe Epilepsy Study Group. A randomized, controlled trial of surgery for temporal-lobe epilepsy. N Engl J Med 2001;345:311–8.
[6] Spencer SS. When should temporal-lobe epilepsy be treated surgically? Lancet Neurol 2002;1:375–82.
[7] Theodore WH, Fisher RS. Brain stimulation for epilepsy. Lancet Neurol 2004;3:111–8.
[8] Ben Menachem E. Vagus-nerve stimulation for the treatment of epilepsy. Lancet Neurol 2002;1:477–82.
[9] Binnie CD. Vagus nerve stimulation for epilepsy: a review. Seizure 2000;9:161–9.
[10] Valencia I, Holder DL, Helmers SL, Madsen JR, Riviello J. Vagus nerve stimulation in pediatric epilepsy: a review. Pediatr Neurol 2001;25: 368–76.
[11] DeGiorgio CM, Shewmon DA, Whitehurst T. Trigeminal nerve stimulation for epilepsy. Neurology 2003;61:421–2.
[12] Fanselow EE, Reid AP, Nicolelis MAL. Reduction of pentylenetetrazole-induced seizure activity in awake rats by seizure-triggered trigeminal nerve stimulation. J Neurosci 2000;20:8160–8.
[13] Benabid AL, Minotti LMD, Koudsie AMD, Saint Martin AMD, Hirsch EMD. Antiepileptic effect of high-frequency stimulation of the subthalamic nucleus (corpus luysi) in a case of medically intractable epilepsy caused by focal dysplasia: a 30-month follow-up [technical case report]. Neurosurgery 2002;50:1385–92.
[14] Hodaie M, Wennberg RA, Dostrovsky JO, Lozano AM. Chronic anterior thalamus stimulation for intractable epilepsy. Epilepsia 2002;43:603–8.
[15] Vonck K, Boon P, Claeys P, Dedeurwaerdere S, Achten R, Van Roost D. Long-term deep brain stimulation for refractory temporal lobe epilepsy. Epilepsia 2005;46(Suppl. 5):98–9.
[16] Hamani C, Ewerton FIS, Bonilha SM, Ballester G, Mello LE, Lozano AM. Bilateral anterior thalamic nucleus lesions and high frequency stimulation are protective against pilocarpine-induced seizures and status epilepticus. Neurosurgery 2004;54:191–7.

[17] Mirski MA, Rossell LA, Terry JB, Fisher RS. Anticonvulsant effect of anterior thalamic high frequency electrical stimulation in the rat. Epilepsy Res 1997;28:89–100.
[18] Chabardès S, Kahane P, Minotti L, Koudsie A, Hirsch E, Benabid A. Deep brain stimulation in epilepsy with particular reference to the subthalamic nucleus. Epileptic Disord 2002;4:83–93.
[19] Benabid A, Minotti L, Koudsie A, Saint Martin A, Hirsch E. Antiepileptic effect of high-frequency stimulation of the subthalamic nucleus (corpus luysi) in a case of medically intractable epilepsy caused by focal dysplasia: a 30-month follow-up [technical case report]. Neurosurgery 2002;50:1385–91.
[20] Vonck K, Boon P, Achten E, De Reuck J, Caemaert J. Long-term amygdalohippocampal stimulation for refractory temporal lobe epilepsy. Ann Neurol 2002;52:556–65.
[21] McIntyre CC, Savasta M, Walter BL, Vitek JL. How does deep brain stimulation work? Present understanding and future questions. J Clin Neurophysiol 2004;21:40–50.
[22] McIntyre CC, Savasta M, Kerkerian-Le Goff L, Vitek JL. Uncovering the mechanism(s) of action of deep brain stimulation: activation, inhibition, or both. Clin Neurophysiol 2004;115:1239–48.
[23] Rizzone M, Lanotte M, Bergamasco B, et al. Deep brain stimulation of the subthalamic nucleus in Parkinson's disease: effects of variation in stimulation parameters. J Neurol Neurosurg Psychiatry 2001;71:215–9.
[24] Moraes MFD, Mishra PK, Jobe PC, Garcia-Cairasco N. An electrographic analysis of the synchronous discharge patterns of GEPR-9s generalized seizures. Brain Res 2005;1046:1–9.
[25] Moraes MFD, Chavali M, Mishra PK, Jobe PC, Garcia-Cairasco N. A comprehensive electrographic and behavioral analysis of generalized tonic–clonic seizures of GEPR-9s. Brain Res 2005;1033:1–12.
[26] Vouimba RM, Richter-Levin G. Physiological dissociation in hippocampal subregions in response to amygdala stimulation. Cereb Cortex 2005;15:1815–21.
[27] Akirav I, Richter-Levin G. Mechanisms of amygdala modulation of hippocampal plasticity. J Neurosci 2002;22:9912–21.
[28] Moraes MFD, Galvis-Alonso OY, Garcia-Cairasco N. Audiogenic kindling in the Wistar rat: a potential model for recruitment of limbic structures. Epilepsy Res 2000;39:251–9.
[29] Hirsch E, Danober L, Simler S, et al. The amygdala is critical for seizure propagation from brainstem to forebrain. Neuroscience 1997;77:975–84.
[30] Racine RJ. Modification of seizure activity by electrical stimulation: I. After-discharge threshold. Electroencephalogr Clin Neurophysiol 1972;32:269–79.
[31] Knowles WD. Normal anatomy and neurophysiology of the hippocampal formation. J Clin Neurophysiol 1992;9:252–63.
[32] Paxinos G, Watson C. The rat brain in stereotaxic coordinates. San Diego: Academic Press; 1998.
[33] Velisek L, Kubova H, Pohl M, Stankova L, Mares P, Schikerova R. Pentylenetetrazol-induced seizures in rats: an ontogenetic study. Naunyn-Schmiedeberg's Arch Pharmacol 1992;346:588–91.
[34] MacDonald RL, Barker JL. Pentylenetetrazol and penicillin are selective antagonists of GABA-mediated post-synaptic inhibition in cultured mammalian neurones. Nature 1977;267:720–1.
[35] Eells JB, Clough RW, Browning RA, Jobe PC. Comparative fos immunoreactivity in the brain after forebrain, brainstem, or combined seizures induced by electroshock, pentylenetetrazol, focally induced and audiogenic seizures in rats. Neuroscience 2004;123:279–92.
[36] Uhlhaas PJ, Singer W. Neural synchrony in brain disorders: relevance for cognitive dysfunctions and pathophysiology. Neuron 2006;52:155–68.
[37] Ikegaya Y, Aaron G, Cossart R, et al. Synfire chains and cortical songs: temporal modules of cortical activity. Science 2004;304:559–64.
[38] Jin DZ. Spiking neural network for recognizing spatiotemporal sequences of spikes. Phys Rev E 2004;69:21905–13.
[39] Ehud A, Sebastian H, Miriam Z. Decoding temporally encoded sensory input by cortical oscillations and thalamic phase comparators. Proc Natl Acad Sci USA 1997;94:11633–8.
[40] Hopfield JJ, Carlos DB. What is a moment? Transient synchrony as a collective mechanism for spatiotemporal integration. Proc Natl Acad Sci USA 2001;98:1282–7.
[41] Rauschecker JP, Tian B, Hauser M. Processing of complex sounds in the macaque nonprimary auditory cortex. Science 1995;268:111–4.
[42] Buonomano DV, Merzenich MM. Temporal information transformed into a spatial code by a neural network with realistic properties. Science 1995;267:1028–30.
[43] deCharms RC, Blake DT, Merzenich MM. Optimizing sound features for cortical neurons. Science 1998;280:1439–44.
[44] Hansel D, Mato G. Existence and stability of persistent states in large neuronal networks. Phys Rev Lett 2001;86:4175.
[45] Shimegi S, Akasaki T, Ichikawa T, Sato H. Physiological and anatomical organization of multiwhisker response interactions in the barrel cortex of rats. J Neurosci 2000;20:6241–8.
[46] Hayon G, Abeles M, Lehmann D. A model for representing the dynamics of a system of synfire chains. J Comput Neurosci 2005;18:41–53.
[47] Abeles M, Hayon G, Lehmann D. Modeling compositionality by dynamic binding of synfire chains. J Comput Neurosci 2004;17:179–201.
[48] Tank DW, Hopfield J. Neural computation by concentrating information in time. Proc Natl Acad Sci USA 1987;84:1896–900.
[49] Womelsdorf T, Schoffelen JM, Oostenveld R, et al. Modulation of neuronal interactions through neuronal synchronization. Science 2007;316:1609–12.